An investigation into the feasibility of improving the sustainability of a biogas fueled electricity generator by capturing CO_2 exhaust emissions using photosynthetic green microalgae

by

Merritt Kennedy

A thesis submitted in partial fulfillment

of the requirements for the degree of

Master of Applied Science (M.A.Sc.) in Natural Resources Engineering

The Faculty of Graduate Studies

Laurentian University

Sudbury, Ontario, Canada

THESIS DEFENCE COMMITTEE/COMITÉ DE SOUTENANCE DE THÈSE
Laurentian Université/Université Laurentienne
Faculty of Graduate Studies/Faculté des études supérieures

Title of Thesis Titre de la thèse	An investigation into the feasibility of improving the sustainability of a biogas fueled electricity generator by capturing CO_2 exhaust emissions using photosynthetic green microalgae	
Name of Candidate Nom du candidat	Kennedy, Merritt	
Degree Diplôme	Master of Science	
Department/Program Département/Programme	Natural Resources Engineering	Date of Defence Date de la soutenance October 28, 2020

APPROVED/APPROUVÉ

Thesis Examiners/Examinateurs de thèse:

Dr. John Ashley Scott
(Co-Supervisor/Co-directeur(trice) de thèse)

Dr. Cory Laamanen
(Co-Supervisor/Co-directeur(trice) de thèse)

Dr. Nathan Basiliko
(Committee member/Membre du comité)

Approved for the Faculty of Graduate Studies
Approuvé pour la Faculté des études supérieures
Dr. Lace Marie Brogden
Madame Lace Marie Brogden
Acting Dean, Faculty of Graduate Studies
Doyenne intérimaire, Faculté des études supérieures

Dr. Nikolai DeMartini
(External Examiner/Examinateur externe)

ACCESSIBILITY CLAUSE AND PERMISSION TO USE

Abstract

Municipal solid waste landfills release a methane rich biogas, which can be combusted in stand-alone electricity generators. This work, which measured the exhausted off-gas from a biogas fed generator, which at an average of 526˚C was 5,556 Nm^3/hour and contained 11% CO_2. It is hypothesized that this off-gas could be captured and used as a year-round carbon source for photosynthetic microalgae. A pilot plant concept is modeled to be built at later date for a feasibility CO_2 capture study. The proposed pilot plant consists of ten 1 m^3 tanks (1 seed tank, 3 sets of biological triplicates) and would take 0.34% of the total off-gas. The model produced indicated that it could be operated above 15˚C and 30˚C year-round and has the potential to produce 2.7 kg $_{\text{dry weight microalgae}}$ m^{-3} day^{-1} of lipid-rich microalgae for research and market analysis purposes.

Keywords

Electricity generator, landfill biogas, off-gas, carbon dioxide (CO_2), microalgae, lipids

Acknowledgments

First, I would like to express my sincerest appreciation to my supervisor, Dr. Ashley Scott and my co-supervisor Dr. Corey Laamanen. Thank you for the constant support, guidance, knowledge and patience throughout my research. You have both helped me achieve my goal and couldn't have done it without you! I would also like to thank Dr. Nathan Basiliko, a member of my advisory committee from Laurentian University. Thank you for taking the time and insight.

A huge thank you to my loving parents for the constant encouragement and support throughout my thesis journey. Thank you for all the laughs and keeping me grounded, this would not have been achieved without your love. Thank you to my two little sisters and little brother. A special thank you to my boyfriend and his parents for the support, encouragement and love. I would also like to thank my grandparents for listening to my thoughts throughout my research and always being interested in my work.

To all my friends, thank you for your encouragement and many smiles throughout this process.

This thesis would not have been possible without the industrial partnership with ConvenGen/GSU Business Development Team, the Sudbury landfill electricity generator and Mitacs Accelerate internship.

Table of Contents

List of Tables

List of Figures

Nomenclature

Symbol	Description
A	Surface area (top) of bioreactor (m^2)
A_w	Area of bioreactor walls and bottom (m^2)
C_{Bowen}	Bowen Coefficient (61.3 Nm^{-2} $^{\circ}C^{-1}$)
C_D	Drag force coefficient
$C_{p,G}$	Specific heat capacity of off-gas (J kg^{-1} $^{\circ}C^{-1}$)
$C_{p,L}$	Specific heat capacity of liquid (J kg^{-1} $^{\circ}C^{-1}$)
D_b	Bubble diameter (m)
D_o	Orifice diameter (m)
e_G	Vapor pressure in ambient air (mmHg)
e_s	Saturation vapor pressure of air at the bioreactor temperature (mmHg)
E_b	Energy contribution from gas bubbles (W)
ϵ	Gas hold up (dimensionless)
F_D	Drag force (N)
f	Frequency of bubble formation (s^{-1})
Fr	Froude number
h	Heat transfer coefficient (W m^{-2} $^{\circ}C^{-1}$)
H_G	Total solar radiation (W m^{-2})
k	Thermal conductivity (W m^{-1} $^{\circ}C^{-1}$)
n	Orifices per unit area (m^{-2})
p_{atm}	Density of standard atmosphere (kg m^{-3})
p_L	Density of water (kg m^{-3})
p_G	Density of off-gas (kg m^{-3})
Q_O	Gas flow rate per orifice (m^3 s^{-1})
Q_F	Generator off-gas flow rate (total) (m^3 s^{-1})
R_{Bowen}	Bowen coefficient
Re	Reynolds number
S_t	Solar radiation (W m^{-2})

T	Temperature (˚C)
u_b	Steady ascent velocity (m s^{-1})
q	Heat flux (W)
z	Thickness (m)
Z	Water depth of bioreactor (m)
V	Volumetric flow rate (m^3 s^{-1})
α_L	Absorptivity of the liquid (dimensionless)
ξ	Reflectivity (dimensionless)
τ	Transmissivity (dimensionless)
ϵ	Gas holdup (dimensionless)
Subscripts	
a	Ambient
air	Air
b	Bubble
Cond	Conduction
Conv	Convection
Evap	Evaporation
OG	Off-gas
G	Gas above bioreactor surface
HE	Heat exchanger
i	Inlet
ins	Insulating material
L	Liquid (water)
o	Orifice
out	Off-gas outlet
solar	Solar input
w	Wall
x	Capture efficiency of the heat exchanger

Chapter 1

1 Introduction

This introductory chapter provides general background information about the research and outlines the objectives of this dissertation.

1.1 Background

The greenhouse gas effect is a natural way that our planet keeps the temperature in a suitable living range. Without the greenhouse gas effect the earth would be around -18˚C and not suitable for life as we know it (Kweku et al., 2018) (Zulfequar Ahmad Khan, 2017). However, with the increasing concentrations of greenhouse gases, this temperature maintenance equilibrium is no longer maintained (Al-Ghussain, 2019). The substantial release of anthropogenic greenhouse gases has led to climate change, which is seen in the increase of the global average temperature, rise in sea level, deviation in the characteristics of seasons and change in rainfall patterns (El Zein, 2015), (Zulfequar Ahmad Khan, 2017).

These greenhouse gases, that trap excess heat into the atmosphere, include carbon dioxide (CO_2), methane (CH_4), nitrous oxide (N_2O) and fluorinated gases (HFCs, PFCs, SF_6 and NF_3) (Environment and Climate Change Canada, 2019). Mitigation of greenhouse gas emissions through the utilization of biogases as a renewable energy source has gained significant interest. Biogas applications include combustion in boilers, electricity generators and/or combined heat and power, and upgrading to a high-BTU fuel that can be injected into the natural gas grid.

Landfills emit a CH_4 rich biogas that can be captured and repurposed in the aforementioned technologies. Producing electricity from the combustion of CH_4 rich biogas has been widely used all over the world and reduces greenhouse gas (GHG) emissions being released to the environment. After combustion, the reciprocating engines exhaust is laden with a less potent greenhouse gas, CO_2, so to further improve environmental performance work is needed to mitigate the levels of CO_2 released by these systems.

The use of green photosynthetic microalgae to reduce CO_2 emissions to the atmosphere has significant potential to mitigate CO_2 emissions, as these microalgae can utilize CO_2 rich off-gas as a carbon source and can produce large yields of bioproducts, such as lipids, of significant commercial value. High lipid yields can be converted into biodiesel or indeed used as a promising source of nutraceuticals, such as omega-3 fatty acids. However, there are limitations on microalgal production, with one significant one being cultivation temperature – which is typically required to be between 15˚C and 30˚C (Chisti, 2007).

This thesis has designed a novel pilot plant for carbon capture by microalgae from small-scale generator's CO_2-laden off-gas. The model takes into account the CO_2 percentage in the off-gas, as well as the temperature and the gas quantity to be efficiently sparged into bioreactors, as well as regional atmospheric data. As an additional model output, it also predicts the amount of potential algal biomass as well as lipid yield.

1.2 Thesis Objectives

There are two objectives of this dissertation, with a focus on repurposing CO_2 from a small-scale industrial off-gas source in the form of a biogas fueled electricity generator. First, to determine

the year-round quantity and concentration of CO_2 emissions from the off-gas of a landfill biogas generator and, second, to model a pilot plant system that can capture and repurpose the CO_2 in the off-gas to improve environmental impact. The CO_2 rich off-gas will be used to stimulate the growth of photosynthetic microalgae, in bioreactors, that can produce high value-added biocompounds.

Unfortunately, due to Covid-19 restrictions, the modeled pilot plant was not able to be constructed and tested onsite.

The thesis is presented such that Chapter 2 is a literature review, which provides background information and context for the thesis. It includes descriptions of different landfill gas utilization technologies and the emissions reductions associated with each technology. Chapter 3 includes collected site-specific data on landfill biogas and generator performance and emissions. Chapter 4 provides an adapted model for a pilot plant that captures CO_2 and sparges it into bioreactors. The pilot plant consists of ten 1 m^3 bioreactors for biological experiments to optimize the environmental performance of the generator, with the goal of scaling up to larger tanks. This chapter includes the required heat needed to maintain suitable cultivation conditions for microalgae in the bioreactors, as well as the potential production levels of algal biomass and lipids.

Chapter 2

2 Reducing the greenhouse gas impact of landfill emissions through energy creation

This chapter is a review of landfill biogas emissions and different waste-to-energy options to reduce these harmful greenhouse gas emissions.

Abstract

Landfill biogas emissions contribute significantly to overall greenhouse gas (GHG) emissions worldwide and municipal solid waste (MSW) in landfills is a major contributor to the emissions, namely through the production of methane. This review outlines the parameters that affect the production of landfill biogas including climate, and composition as well as age of MSW. Landfill biogas capture, treatment and utilization options are discussed – including flaring, direct use, electricity generation and alternative fuel. The treatment and utilization options are compared to the untreated option, in terms of overall GHG emissions.

Keywords

Landfill biogas, municipal solid waste, waste-to-energy, flaring, direct use, electricity, alternative fuel, utilization, greenhouse gas, methane, carbon dioxide

2.1 Introduction

While the agricultural and the energy and oil production sectors remain the most significant contributors to worldwide anthropogenic greenhouse gas emissions, an often overlooked and more easily managed emission source is landfills. Worldwide solid waste disposal emits 5% of anthropogenic greenhouse gas (GHG) emissions (C. Zhang et al., 2019), due largely to landfill biogases which account for 30% of total anthropogenic methane (CH_4) emissions (Purmessur & Surroop, 2019). Five key anthropogenic sources of greenhouse gases include agriculture, oil and gas operations, landfills, coal, and wastewater, which together emit 68% of all CH_4 emissions (Chai et al., 2016). This makes landfills the third largest anthropogenic CH_4 emissions source (Chai et al., 2016). Global methane emissions from landfills were calculated as 846.7 MMT $CO_{2\ eq}$ in 2010 and emissions from landfills are expected to rise to 905 MMT $CO_{2\ eq}$ by 2020 (USEPA, 2012). The global warming potentials of methane and carbon dioxide are 25 and 1, respectively (Government of Canada, 2019b).

Global annual waste generation in 2016 was 2.22 billion tonnes and is expected to increase by 70% to 3.75 billion tonnes by 2050 (Kaza et al., 2018). Global solid waste in 2016 generated an estimated 1.76 billion tonnes of $CO_{2\ eq}$, and without any improvement in worldwide capture and utilization of GHGs, annual emissions are projected to increase to 2.87 billion tonnes by 2050 (Kaza et al., 2018). For comparison, in 2014, Canada generated 37 million tonnes of MSW, of which 60% originated from non-residential sources (Government of Canada, 2017). In 2016, Canadian landfills generated about 17 Mt $CO_{2\ eq}$ from MSW (Environment and Climate Change Canada, 2019). Comparing the global CH_4 emission from landfilling, Canada emits 1.9% of these emissions. In 2014, United States generated 258 million tonnes of MSW and only 136

million tonnes were discarded in landfills (Lee et al., 2017). In 2016, 107.7 Mt $CO_{2\ eq}$ were generated from MSW (USEPA, 2018a) and comparing this value with the global CH_4 emissions from landfills, United States emitted 12% of the global total.

In most countries MSW management operations have been established through institutions with responsibility of policy development and regulating the waste sector but vary between countries (USEPA, 2012). In Canada, regulations stipulate mandatory collection of landfill biogas is required for new or expanding sites with a total waste disposal capacity greater than 1.5 million m^3, or smaller sites near populated areas (Government of Ontario, 2019). In Canada, the amount of CH_4 generated by landfills has steadily increased primarily due to a larger population, the increase has been offset by the increase in use of capture technologies of landfill biogas (Environment and Climate Change Canada, 2019). In 2017 43% of biogas generated at landfills was recovered from capture technologies, compared to the 19% in 1990 (Environment and Climate Change Canada, 2019).

2.2 Types of landfills

MSW generated around the world does not have a constant composition and quantity, so when determining the emission levels and the appropriate handling and management techniques it is critical to know how these variables affect biogas production (Abdel-Shafy & Mansour, 2018). The composition, calorific value and moisture content of the MSW are three major variables in predicting the amount of gaseous emissions produced. The volume produced can then be used to determine the necessary type of landfill, and if the site is suitable for a solid waste to energy (WTE) conversion facility (Abdel-Shafy & Mansour, 2018).

2.2.1 Dump

Dumps are the most inefficient MSW treatment system, as there are no engineered plans – so no beneficial treatment is utilized. All kinds of waste are disposed of in one area, waste is not compacted, no preventive measures for gaseous or leachate emissions are taken and the waste is not covered (making gas capture impractical) (Manfredi et al., 2009). A majority of developing countries don't have the financial resources for more advanced techniques and dump their MSW without proper control – resulting in air, soil and water pollution near these municipalities (Abdel-Shafy & Mansour, 2018). As such, dumps will produce landfill biogas at levels dictated by the solid waste characteristics (discussed in section 3) without reduction.

2.2.2 Conventional landfill

The conventional landfill is designed to implement collection and management of the leachate and biogas generated in the landfill (Manfredi et al., 2009). Conventional landfills, however, do very little with regards to optimizing degradation rate and generation of leachate, instead opting to implement technical measures to collect and manage the emissions (Manfredi, 2009). Commonly, the handling of leachate utilizes installed liners on the bottom and sides of the landfill to allow for leachate collection and treatment prior to discharge to surface waterbodies (Manfredi et al., 2009).

Conventional landfills also typically include a biogas handling system, consisting of a collection system, gas treatment and potentially a top cover, to mitigate the emissions of uncollected biogas (Manfredi et al., 2009). The most common treatment option is the combustion of landfill biogas

emissions, and this is typically achieved through flaring (which reduces the global warming potential of emissions by converting CH_4 to CO_2), although a similar reduction can also be achieved through a passive oxidation of methane in top covers (Manfredi et al., 2009).

2.2.3 Engineered landfill

Engineered landfill technologies have been developed to adopt active measures, such as adding leachate, water and air, to enhance the degradation process of MSW compared to traditional landfills. This enhanced degradation translates to an increased rate of biogas generation, which subsequently makes it easier to both estimate the emissions and develop efficient biogas collection systems. This increased emission flow rate, and corresponding shorter lifespan, increases the potential for biogas utilization to produce electricity or combined heat and power generation (Manfredi et al., 2009). Additional advantages compared to conventional landfills, which were outlined by (Grossule et al., 2018)(Reinhart & Barlaz, 2010), are:

- Environmental impacts are reduced due to control of landfill emissions and improved leachate quality
- Post-closure care timeframe of the landfill is generally shortened due to increased stabilization rates, thus reducing aftercare costs and turnover times for the landfill
- Refuse settlement and density are increased

Engineered landfills can be subcategorized as: bioreactors, flushing-bioreactors and semi-aerobic landfills, each with unique characteristics (Manfredi et al., 2009).

2.2.3.1 Bioreactors

Bioreactor landfills are designed to have a continuous supply of moisture and nutrients, which enhances the microbial anaerobic environment. This is accomplished by collecting and recirculating the leachate through the waste mass, to maintain the moisture level at capacity for the landfill (Manfredi et al., 2009). A bioreactor landfill is proven to enhance the waste decomposition rate and increase the gaseous emissions (Nwaokorie et al., 2018).

2.2.3.2 Flushing bioreactors

Flushing bioreactor landfills mix large amounts of water and leachate together to flush out soluble waste fragments and accelerate the waste stabilization processes (Grossule et al., 2018) (Manfredi et al., 2009). Flushing large amounts of water through the bioreactor has several benefits, including accelerating waste stabilization, removing contaminants, such as metals and inorganic contaminates (chloride, nitrogen, phenols), eliminating soluble contaminates early in the landfill life and reducing the production of ammonia in the landfill (Reinhart et al., 2002).

2.2.3.3 Semi-aerobic landfills

Semi-aerobic landfills, take a different approach, utilizing a combination of anaerobic and aerobic degradation processes. Initially aerobic processes deplete oxygen levels in the landfill, at which point the anaerobic process is utilized. This anaerobic digestion continues until the methane yield inside the landfill biogas becomes too low to justify utilization, which usually translates to a minimum of 10-15 Nm^3 CH_4/tonne wet low organic waste (typically 5-10 years of degradation). At this point, the system is aerated to reintroduce aerobic processes through air injections (Manfredi et al., 2009). Simultaneously, gas venting is strategically positioned in the

landfill to increase oxygen levels and improve the aerobic environment (Matsufuji, 2007). For the remaining lifespan of the waste aerobic stabilization is utilized, preventing methane generation (Manfredi et al., 2009).

2.3 Landfill biogas production

There are four active phases within the landfill dictating landfill biogas production (Table 1). Anaerobic conditions are developed within a year (United States Environmental Protection Agency, 2018) and the resulting landfill biogas is approximately 45-60% methane (CH_4), and 40-55% percent carbon dioxide (CO_2). It can also contain small quantities of nitrogen, oxygen, sulfide and ammonia (Government of Canada, 2017); Danthurebandara et al., 2012), as well as trace non-methane organic compounds, such as benzene, xylene and butane (Jaramillo & Matthews, 2005). Generation of landfill biogas can last for up to 30 years after the landfill closes (Jaramillo & Matthews, 2005).

Table 1: The four different phases involved in landfill biogas (Lombardi et al., 2006; Khalil et al., 2014)

Phase	Definition	Description of Phase
One	Aerobic decomposition	Aerobic bacteria break down organic waste and deplete oxygen levels. These bacteria break down carbohydrates, fats and proteins, producing a CO_2 rich landfill biogas.
Two	Acidogenesis	The establishment of anaerobic conditions in which bacteria reduce organic wastes to long chain carbon compounds, as well as acids and alcohols, leasing to production of CO_2, CH_4 and trace amounts of ammonia and hydrogen sulphide.
Three	Acetogenesis	Anaerobic oxidation of the acids and alcohols produced in Phase 2 to create acetate, as well as lowering the pH of the system.
Four	Methanogenesis	Anaerobic conversion of acetate into CO_2 and CH_4. This phase can be subdivided as there are two different groups of methanogens – one that converts acetate directly into methane and a second that combines hydrogen and CO_2 to create methane.

While the bacteria driven processes taking place are similar across sites, the composition of MSW will vary from one municipality to another, and significantly from one country to another (Abdel-Shafy & Mansour, 2018). This is of importance as MSW composition effects the volume of methane being generated, as a function of the biogenic carbon content of the waste (Manfredi et al., 2009). The biogenic carbon content for different materials commonly found in MSW is detailed in Table 2 along decomposition rates.

Table 2: Average biogenic carbon content for universal average materials found in landfills (Manfredi et al., 2009) and (Lombardi et al., 2006)

Material Fraction	**Biogenic Carbon Content (kg C tons^{-1} (wet fraction))**	**Decomposition Rate**
Household waste (all fractions)	160-200	Rapid (less than 5 years)
Kitchen organics	100-120	Rapid (less than 5 years)
Newspaper	360-440	Rapid (less than 5 years)
Office paper	300-360	Rapid (less than 5 years)
Cardboard	300-380	Rapid (less than 5 years)
Wood	400-450	Slow (up to 50 years)
Plastic	0	Slow (up to 50 years)
Glass	0	Slow (up to 50 years)
Metal	0	Slow (up to 50 years)
Predominantly mineral waste	15-25	Slow (up to 50 years)

From the biogenic carbon content, landfill biogas generation and emissions are commonly predicted with first order decay models (Nwaokorie et al., 2018). These models are used to quantify the amount of biogas generation being released during the landfill lifespan (Vu et al., 2017). Biodegradable organic material can be divided into two classifications, based on the rate of decomposition - either rapid (three months to 5 years) or slow (up to 50 years or more) (Lombardi et al., 2006).

2.3.1 Conditions that effect landfill biogas

The characteristics of the waste and the local environment affect the rate and composition of landfill biogas produced (Berger et al., 2001). The calculation of biogas production is complicated, as waste composition in landfills varies both spatially and temporally. Additionally, the necessary biological processes are affected by the age of refuse, moisture content, temperature, pH and oxygen concentrations of the landfill, which all contribute to the amount of CH_4 produced (Nwaokorie et al., 2018; C. Zhang et al., 2019). The composition of the waste is the most important factor in predicting the volume of landfill biogas produced (Mohsen & Abbassi, 2020).

The decay rates reported in warmer and wetter climates are higher in literature, suggesting a correlation between climatic conditions and waste decay rate in first order decay models (Vu et al., 2017). While controlled conditions in laboratory landfill simulators, including pH, moisture content and nutrient addition, give higher biogas production rates compared to actual landfills, which do not try to regulate the conditions at optimal levels (Chiemchaisri et al., 2007). So it is important to account for these non-ideal conditions when scaling up laboratory data. The parameters are summarized in Table 3.

Table 3: Different affects parameters have on the landfill biogas (adapted from Berger et al., 2001)

Parameter	Affect
Waste Composition	• Higher organic waste content, the more landfill biogas that is produced through bacterial decomposition (positive) • More chemicals disposed of in landfills, the higher non-methane volatile organic compounds (NMOC's) and other gases will be produced (positive) • High salt concentration inhibit methane producing bacteria (negative)
Age of Refuse	• Buried waste less than 10 years old produces more landfill biogas through bacterial decomposition, volatilization and chemical reactions than does older waste (positive) • Peak biogas production is 5-7 years after waste is buried (positive) • Different portions of the landfill may not produce the same amount of landfill biogas depending when waste was placed and buried (negative)
Moisture Content	• Increased moisture content in a landfill encourages bacterial decomposition and transports nutrients and bacteria to all areas within the landfill – optimal moisture content is 40% wet weight of waste for max biogas production (positive) • Moisture also promotes chemical reactions that produce biogas (positive) • Heavy rainfall/permeable landfill covers produce higher biogas production (positive)
Temperature	• Temperature rise increases bacterial activity which results in increased biogas production (positive) • Capped landfill usually maintains stable temperature which maximizes biogas production (positive) • Colder temps inhibit bacterial activity (negative)
Presence of oxygen and nutrients in the landfill	• Oxygen inhibits methane production, the more oxygen in the landfill the longer the aerobic bacteria can decompose in Phase 1 (negative) • Certain nutrients can boost the growth of bacteria thus increasing landfill biogas, whereas some nutrients such as salt hinder the production of landfill biogas (Purmessur & Surroop, 2019).
pH	• pH influences the degradation in microbial activity. A pH level in the range of 5-8 is required (Goswami et al., 2016)

2.3.2 Climate and landfill covers

A study conducted by Goldsmith *et al.* (2012) stated that the production of methane emissions is a function of both climate and cover type. The different scenarios they examined include no

cover, temporary soil cover, intermediate soil cover and final or synthetic covers. The different climates were humid subtropical, humid continental, Mediterranean and semiarid which range from 2.7-207 g_{CH4} m^{-2} $day^{-1}$and Table 4 summarizes the effect that climate and landfill cover have on CH_4 production.

Table 4: Effect of climate and landfill cover type on CH_4 production [gCH_4 m-2 day-1] (adapted from Goldsmith et al., 2012)

Region	**Cover Type**			
	None	**Temporary soil**	**Intermediate soil**	**Final/Synthetic**
Humid subtropical	207	127	102	32
Humid continental (cool summers)	135		40	26
Mediterranean			11	6
Semiarid	85	11	3.7	2.7

The daily or intermediate covers are typically made of soil, but can also use wood chips or compost, as long as it is controlling the nuisance of insects, rodents, birds, litter and odour, as well as allowing vehicle access on the site and providing an acceptable site appearance (Government of Ontario, 2019). If a final cover is used for closure of a landfill site, it should be compatible with any gas control regulations and its characteristics will depend on the type of waste and the design objective for the cover (Government of Ontario, 2019). Final covers are designed to seal the landfill from the environment and typically are made of either clay or plastic in order to be impermeable to the biogas (Chai et al., 2016). The determination of the final cover

type depends on available materials and associated costs, landfill moisture conditions, climate leachate management costs and biogas collection objectives (World Bank Group, 2019).

Changes in climate conditions greatly influence the rate of decay in MSW and cause changes in collection efficiency of landfill biogas. Atmospheric pressure had significant effects on landfill biogas, where increasing barometric pressure (warming climate) enhances the flow rate of the landfill biogas and vice versa (Leone, 2007). For example, without a synthetic cover in wet tropical climates the decay rate is much faster (due to high temperatures and rainfall), this reduces the collection efficiency by releasing landfill biogas into the atmosphere faster than it can be collected increasing overall GHG emissions by 19% (Lee et al., 2017). While a closed, synthetically capped landfill in a humid, continental, warm summer climate, with a landfill biogas collection system in place, measured mostly background levels of methane (emitted to atmosphere) and produced an average emission rate of 0.09 $gCH_4\ m^{-2}\ day^{-1}$ (Goldsmith et al., 2012).

In the summer, the higher temperatures enhance the microbial metabolic activity, resulting in an increase of landfill biogas transfer rate inside the waste mass, and higher landfill biogas production. While in winter, lower temperatures not only slow metabolic activity but also tend to break up soil aggregates, reducing solubility of CH_4 and CO_2, and as a result more CH_4 and CO_2 escape from cracks in the soil aggregate (C. Zhang et al., 2019).

2.3.3 Landfill biogas collection

When a section of the landfill is closed off to additional waste placement, landfill biogas collection can typically begin (Environmental Protection Agency, 2017). Landfill biogas collection is either by vertical or horizontal wells (Fei et al., 2019). Vertical wells are drilled into

the waste and wellheads are connected to lateral piping that transports the biogas to a collection header using a blower or vacuum induction system (Environmental Protection Agency, 2017). Vertical wells are used more frequently due to lower costs of installation and their versatility in various sizes of landfills, as they can be used in a variety of engineered landfills (Fei et al., 2019).

A engineered landfill disposal method is used to control MSW, where the waste is deposited in thin layers and promptly compacted by heavy machinery, several layers are placed and compacted on top of each other to form a refuse cell (Curley, 2018). At the end of each day a refuse cell is covered with a layer of soil to prevent odours and windblown debris (Curley, 2018).

Horizontal wells are laid in trenches and are more useful for deeper landfills and in areas of active filling (Environmental Protection Agency, 2017). While horizontal wells can have a higher landfill biogas collection rate, they have a significantly increased cost and are only appropriate for larger landfills (Fei et al., 2019).

Within the biogas collection system there is a potential for condensation to form when the biogas from the landfill becomes warm at initial collection and cools down as it travels through the collection system. Condensation needs to be removed so that it does not restrict the landfill biogas collection system and disrupt any energy recovery processes (Environmental Protection Agency, 2017). A blower is necessary in the collection system to pull the biogas from the collection wells into the collection header and direct the biogas downstream to any treatment and energy recovery systems (Environmental Protection Agency, 2017).

2.4 Landfill biogas models

CH_4 emissions in landfill biogas from MSW can be estimated by Equation 1 (Fei et al., 2019), by including the total MSW generation from the landfill and the appropriate default values for calculation (Froiland Jensen & Pipatti, 2001).

$$\mathbf{CH_{4,emissions}} = (\mathbf{MSW_T} \times \mathbf{MSW_F} \times \mathbf{MCF} \times \mathbf{DOC} \times \mathbf{DOC_F} \times \mathbf{F} \times \frac{\mathbf{16}}{\mathbf{12}} - \mathbf{R})\ (\mathbf{1} - \mathbf{OX}) \quad \text{Equation 1}$$

Where,

$CH_{4,emissions}$ = Total generation of methane from municipal solid waste [Gg/yr]

MSW_T = Total MSW generation amount [Gg]

MSW_F = MSW fraction disposed in landfills

MCF = Methane correction factor, fraction decomposed aerobically in the year of deposition (default value 0.6 but ranges from 0.4 for shallow, unmanaged sites to 1.0 for managed sites)

DOC = Fraction of degradable organic carbon in the year of deposition

DOC_F = Volume fraction of DOC that can decompose (default value 0.77)

F = Volume fraction of CH_4 in generated landfill biogas (default value 0.5)

R = Fraction of CH_4 recovered

OX = Oxidation factor, fraction of waste that is oxidized (default value 0)

In comparison, to better account for the change in biogas production over time, the United States Environmental Protection Agency developed the LandGEM Model (Equation 2) (Purmessur & Surroop, 2019).

$$\mathbf{Q_{CH_4}} = \sum_{\mathbf{i=1}}^{\mathbf{n}} \sum_{\mathbf{j=0.1}}^{\mathbf{1}} \mathbf{k_i}\, \mathbf{L_0}\, \frac{\mathbf{M_I}}{\mathbf{10}} \mathbf{e}^{-\mathbf{kt_{ij}}} \qquad \text{Equation 2}$$

Q_{CH_4} = Annual methane generation in the year of calculation [Gg/yr]

n = Years after initial disposal [yr]

i = 1-year time increment

j = 0.1-year time increment

k_i = Methane generation rate of year i [year^{-1}]

L_0 = Methane generation potential capacity of year i [m^3/Mg]

M_i = Mass of waste accepted in the ith year [Mg]

t_{ij} = Age of the jth section of waste mass M_i accepted in the ith year

The Environmental Protection Agency created default values for k and L_0, simplifying the model, and as such are not changed during simulation (Purmessur & Surroop, 2019). This raises a problem due to the fact that waste composition, moisture and climatic conditions change over time. The methane generation rate in year i (k) is a function of refuse moisture content, availability of the nutrients for methanogens, pH and temperature where the suggested value is 0.05 but can range from 0.003-0.21 year^{-1} (USEPA, 1990) (Nwachukwu & Diya, 2013). The

higher the value of k is how fast the methane generation rate increases and subsequently decreases over time (USEPA, 1990).

The methane generation potential capacity of year i (L_o) is dependent on the type of refuse present in the landfill, the higher the biogenic carbon content the higher the value of L_o, the default value is 170 m^3/Mg but can range from 6.3-270 m^3/Mg (USEPA, 1990) (Nwachukwu & Diya, 2013). As such, relationships have been developed for calculating the methane generated due to decomposition of the landfill waste (Equation 3) (Purmessur & Surroop, 2019).

$$\mathbf{L_o = MCF \times DOC \times DOC_f \times F \times \frac{16}{12}} \qquad \text{Equation 3}$$

L_o=Methane generation potential

MCF= Methane correction factor

DOC= Fraction of degradable organic carbon in the year of deposition

DOC_f= Volume fraction of DOC that can decompose

F = Volume fraction of CH_4 in generated landfill biogas

$\frac{16}{12}$ = Molecular weight ratio of methane and carbon

The dissimilated organic fraction (DOC_f) is the portion of the DOC that is converted into biogas. The estimation is dependent on temperature in the anaerobic zone (˚C) of the landfill and based on a theoretical model, DOC_f= 0.014T +0.28 (Aguilar-Virgen et al., 2014).

2.5 Energy from landfill biogas

Several simple equations have been developed to examine the potential of converting landfill biogas to energy, specifically examining the potential production, thermal energy and electrical energy production potential. The landfill biogas utilization potential for conversion into energy products can be calculated according to Equation 4 (Fei et al., 2019):

$$\mathbf{U_p = CH_{4emission} \times C_e \times L_s \times E_e} \quad \text{Equation 4}$$

Where:

U_p = Landfill biogas utilization potential [Gg]

$CH_{4emission}$ = Landfill biogas methane generation potential [Gg]

C_e = Landfill biogas collection efficiency, fraction of landfill biogas that can be collected under current technology conditions

L_s = Landfill scale parameter, the fraction of landfills that could promote landfill biogas utilization, estimated at 70% for 2020

E_e = Energy conversion efficiency, the fractional conversion of landfill biogas into energy products under current technology conditions (Landfill biogas to electricity= 2.24 kWh/m^3landfill biogas and landfill biogas to natural gas= 0.517m^3/m^3 landfill biogas)

While the total thermal energy that can be produced from landfill biogas can be calculated using Equation 5 (Purmessur & Surroop, 2019).

$$\mathbf{E_{th} = \dot{m}_{CH4} \times LHV_{CH4} \times R} \quad \text{Equation 5}$$

Where:

E_{th} = Thermal energy [megawatt (MW)]

$\dot{m}_{CH4}$ = Flow rate of methane from the landfill [m^3/h]

LHV_{CH4} = Lower heating value of methane [35.8 MJ/m^3]

R = Fractional recovery of landfill biogas [unitless]

Lastly, the total electric energy that can be determined using Equation 6 (Purmessur & Surroop, 2019).

$$\mathbf{E_e = \dot{m}_{CH4} \times LVH_{CH4} \times R \times \eta_e} \quad \text{Equation 6}$$

Where:

E_e = Electrical energy [kWh]

η_e = Electric efficiency of the engine [unitless]

Landfill energy projects can both generate revenue and create jobs in the local community (USEPA, 2018b). The operation of landfill biogas collection begins with extracting biogas from landfills using wells and blowers (or a vacuum system). The extraction system directs the collected biogas to a central point, where it can be processed and treated depending upon the ultimate use for the biogas. Options include flaring (to convert CH_4 to CO_2, and reduce the global warming potential of the landfill) or beneficially using landfill biogas to produce energy (USEPA, 2018b). Landfill biogas energy projects can be used to produce natural gas, electrical

energy, Combination of Heat and Power (CHP), or can directly use the biogas to replace other heating methods. Figure 1 displays the options possible for landfill biogas treatment.

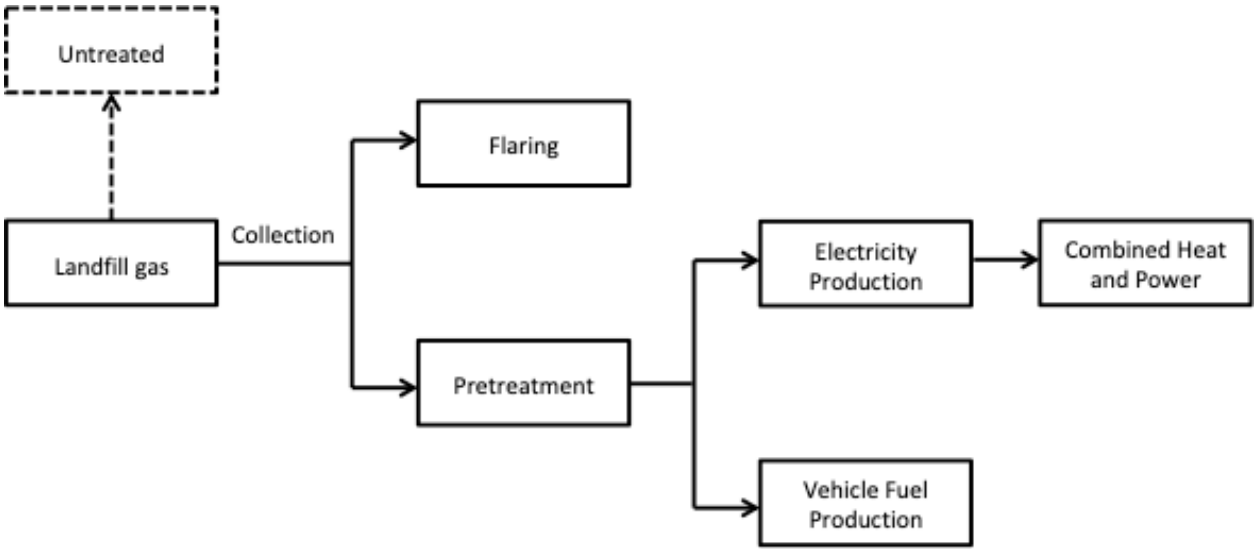

Figure 1: Diagram of options for landfill biogas (adapted from United States Environmental Protection Agency, 2018)

2.5.1 Options for landfill biogas treatment and utilization

MSW can be used to produce energy through the utilization of a number of technologies, such as conversion of landfill biogas to produce electricity, combined heat and power (Colpan et al., 2010), transport fuel (Murphy & McKeogh, 2004), or direct use options. Converting landfill biogas to energy creates a two-fold decrease in GHG emissions, reducing the impact from landfills and providing a renewable energy source (Lee et al., 2017). These operations are commonly termed as Waste-to-Energy (WTE) operations.

When no preventive measures are put in place for landfill emissions, it is required to treat emissions and further look at WTE options (Aracil et al., 2018). Flaring, combustion of collected biogas to reduce environmental impact without additional benefit, is the simplest treatment option and is used when the rate of landfill biogas emissions is too low to facilitate a WTE system. A biological cover, or bio-cover, can also be used when emissions are high, to mitigate CH_4 emissions through oxidation (Aghdam et al., 2018).

While biogas can be utilized through combustion to produce electricity, there is also potential for cogeneration and biofuel. When determining the best treatment method of MSW, the biogas collection efficiency is an important consideration, where the goal is to maximize CH_4 collection efficiency (Aghdam et al., 2018).

$$\mathbf{GRE}\ (\%) = \left(\frac{\mathbf{CH_4\ recovered}}{\mathbf{CH_4\ generated}}\right)\mathbf{x\ 100} \qquad \text{Equation 7}$$

$$\mathbf{CH_{4\ generated}} = \mathbf{CH_{4\ emitted}} + \mathbf{CH_{4\ oxidized}} + \mathbf{CH_{4\ recovered}} + \mathbf{CH_{4\ migrated}} + \Delta\mathbf{CH_{4\ storage}} \qquad \text{Equation 8}$$

Where GRE is the gas recovery efficiency (%), and CH_4 generated is a sum of several different components – shown in Equation 7 and 8 (Aghdam et al., 2018).

Pre-treatment of landfill biogas is required before any energy recovery system – to remove excess moisture, particulates and other impurities (Environmental Protection Agency, 2017). The type of treatment used depends on the biogas characteristics, type of energy recovery system, concentration of gas purity needed for use of energy recovery and country regulations (Environmental Protection Agency, 2017).

While the modelling of different WTE schemes is complicated by the variability of landfill biogas production as, in addition to the aforementioned climatic effects, the rate of biogas products varies significantly depending on the carbon content in the landfilled waste (Lee et al., 2017). For example, 1 ton of MSW can range from 40 to 250 m^3 of landfill biogas produced (Lou & Nair, 2009). GHG emissions also vary based on the amount of carbon sequestered in landfills, carbon from the decomposition of waste, CO_2 from combusted CH_4, CO_2 from CH_4 oxidation and any CH_4 emitted to the atmosphere (Lee et al., 2017).

2.5.2 Flaring

Flaring is an operation that burns landfill biogas which reduces odor, safety concerns and methane emissions (Jaramillo & Matthews, 2005). Despite this lack of energy recovery, it can be the best option available, depending on many site factors, including size and economic sufficiency. If a site is too small to support an infrastructure that produces further benefit or more positive uses are cost-prohibitive, the landfill biogas will be flared, as it is 97% effective at destroying non-methane organic compounds and converts CH_4 into CO_2 (Chai et al., 2016).

Flaring removes CH_4 (which has a global warming potential (GWP) of 25) and produces CO_2 (GWP of 1) at a 1:1 stoichiometric ratio. In the United States, the Environmental Protection Agency has established a New Source Performance Standard and Emission Guidelines for Municipal Solid Waste Landfills, which requires that large landfills (classified as landfills that emit more than 50 Mg/year of non-methane volatile organic compounds) must collect and combust their emissions (Jaramillo & Matthews, 2005).

Flaring is also a designed component for energy recovery systems, where it is used when landfill biogas emission are needed to be controlled during start-up and any downtime for maintenance

or to control any biogas that exceeds the energy conversion equipment (Environmental Protection Agency, 2017).

For example, a landfill in Italy, produces 1365 kg of $CO_{2\ eq}$ per 1 ton of MSW landfilled. By comparison, if utilizing flaring, the specific emission rate is reduced by more than half, to 577 kg of $CO_{2\ eq}$ per ton of MSW (Lombardi et al., 2006).

2.5.3 Landfill biogas for waste-to-energy

While flaring reduces CH_4 emissions, it is also a high energy feed (Gewald et al., 2012) for combustion to produce electricity (Lee et al., 2017). Therefore, instead of flaring, landfills of sufficient size can generate electricity to supplement regional electricity supply (Lee et al., 2017). Flaring or using landfill biogas to generate electricity will both generate the same amount of direct CO_2 emissions, but using it to generate electricity can help offset regional GHG emissions (Lee et al., 2017).

Other landfill biogas to energy projects include generating electricity with combined heat and power, direct use of biogas and converting biogas to natural gas or transport fuel. Common across all methods for utilizing landfill biogas to produce energy are four major benefits: (1) direct reduction of GHG emissions; (2) air pollution reduction by offsetting the utilization of non-renewable resources; (3) health and safety benefits; and (4) economic benefits (Purmessur & Surroop, 2019). These benefits are outlined in Table 5.

Table 5: Benefits of landfill biogas to energy projects (adapted from Purmessur & Surroop, 2019)

	Benefit
Direct reduction of GHG emissions	• 60%-90% of methane released in a landfill is captured to produce electricity based on different systems design and efficiency
Air pollution reduction	• Reduction of air pollution by offsetting utilization of non-renewable resources • Displacing or replacing fossil fuels that are used to produce electricity
Health and safety	• Collecting and channeling the landfill biogas to the energy conversion system, reduces biogas in atmosphere which also reduces the risk of explosions happening
Economic benefits	• Revenue is generated from sales of electricity • Design, operation and erection of the energy recovery facility can create new employment

2.5.3.1 Landfill biogas for direct use

Landfill biogas is considered a medium heating fuel (Rajaram et al., 2011), due to it being roughly 50% methane, that can be used in many different applications and industrial processes. The heating value of landfill biogas is between 16,785-20,495 kJ/m^3 compared to natural gas at 35,406 kJ/m^3 (Bade Shrestha & Narayanan, 2008). Directly using landfill biogas can offset the use of other fuels, such as natural gas, coal and fuel oil. Alternatively landfill biogas as an energy source has been used to evaporate H_2O and combust the volatile organic compounds in the landfill leachate, which reduces the need for expensive treatment and disposal of leachate (Dudek et al., 2010). If there is a nearby customer, then the biogas can be piped and used as a

replacement or supplementary fuel (Karakurt et al., 2012). Typically, distances less than 8-16 km are considered for economically feasible (Dudek et al., 2010).

The simplest and most cost effective method of directly using the landfill biogas is as a fuel for boilers or industrial processes (Dudek et al., 2010) (Niemczewska, 2012). However, there is no economical way to store biogas, so once collected immediate usage is required (Niemczewska, 2012).

Infrared heaters can also utilize landfill biogas, where the biogas is burned to heat a radiating surface that emits infrared energy (Dudek et al., 2010). Surfaces inside the building can release heat into the internal atmosphere and raise the temperature of the building, such as in garages and workshops (Dudek et al., 2010). It has been estimated that 51 m^3 of landfill biogas/hr is needed to heat a floor space of 600 m^2 (Dudek et al., 2010).

Another option is leachate evaporation, which requires heat to thermally treat the waste leachate from the landfill (R. Zhao et al., 2017). Landfill biogas is collected and directly used as an energy source evaporate H_2O and combust the volatile organic compounds in the leachate (Dudek et al., 2010).

2.5.3.2 Landfill biogas for electricity production and combined heat and power plants

Generating electricity from landfill biogas combustion is regarded as a positive alternative to simple flaring (Jaramillo & Matthews, 2005). By using landfill biogas waste-to-energy projects (WTE) that capture and combust the landfill biogas to generate electricity, the requirement to burn fossil fuels can be decreased (Jaramillo & Matthews, 2005). Commonly the landfill biogas,

generated from the anaerobic degradation of the organic fraction of MSW, can be combusted to produce electricity, combined heat and power. As well, used in gas and steam turbines (Ayodele et al., 2020) or transport fuel, such as CH_4 enriched biogas (explained in next section) (Murphy & McKeogh, 2004).

All of the WTE options have a lower capital cost than incineration and thus have smaller charges for quantity of waste received at landfill (Murphy & McKeogh, 2004). The usage of landfill biogas to create electricity (between 550-600 m^3/MWh of biogas for electricity generation (Yechiel & Shevah, 2016)) will displace the need for other regional electrical generation methods, thus reducing regional GHG emissions (Broun & Sattler, 2016).

Most commonly, reciprocating internal combustion engines are used for generating electricity from landfill biogas, due to compatibility of power production (1-3 megawatts per hour) and economic feasibility (Bove & Lunghi, 2006) (Tsatsarelis et al., 2006). Landfill biogas requires pre-treatment to reduce the sulphur and chlorine content to a maximum level of 550 to 60 ppm, respectively (Lombardi et al., 2006), to minimize production of undesirable by-products. Pretreated landfill biogas is dried and compressed to ensure efficient removal of contaminants before being fed to the reciprocating engine (Yechiel & Shevah, 2016). Landfill biogas is combusted with excess oxygen and the reciprocating internal combustion engine turns a generator and produces electricity (Jaramillo & Matthews, 2005). The reciprocating combustion engine typically has an electrical efficiency of 30-40% (Darrow et al., 2015). Used with CHP the engine can have an efficiency as high as 80% (Gupta et al., 2012).

Reciprocating combustion engines are also used for combined heat and power (CHP) systems, where the electricity is produced and a proportion of waste heat from the electrical generation

system is captured and used on-site (Holm-Nielsen et al., 2009). Thus, by definition, more energy is utilized beneficially and the efficiency of the system is increased when utilizing combined heat and power systems in landfills (Purmessur & Surroop, 2019). This is emphasized by the U.S. Department of Energy's claims that for a 1.1 MW electric capacity (which without any heat capture produces 1062 lbs of CO_2 emissions/MWh) with the addition of a thermal credit (calculated as the avoided fuel usage that would be used in an 80% efficiency boiler) there are 491 lbs of CO_2 emissions/MWh. This translates to a decrease in CO_2 emissions of 53.8% through capturing waste heat (U.S Department of Energy, 2019). Reciprocating engines have generally a 33% electrical efficiency and emissions from these operation are low, one example system, consumes around 10 970 kJ/kWh of fuel and emits 56.6 μg/kJ and 56.6 μg/kJ for NO_x and CO, respectively (Bove & Lunghi, 2006).

Gas and steam turbines are the second most utilized technology for electricity production (Bove & Lunghi, 2006), where landfill biogas is combusted and the energy generated is used to heat compressed air. This air expands and is used to spin the turbine and generate electricity using an attached generator (Jaramillo & Matthews, 2005). However, these operations are rarely utilized as it is more economically efficient to produce electricity utilizing the internal combustion engine (Jaramillo & Matthews, 2005). The advantage of gas and steam turbines is that despite their lower overall performance, they produce lower emissions compared to reciprocating combustion engines. The electrical efficiency of the turbines are typically 28%, compared to 33% for reciprocating combustion engines, which translates into using approximately 12 872 kJ/kWh of fuel generated (increase of 17.3%), but emitting 15 μ/kJ and 19 μ/kJ for NO_x and CO, respectively (reductions of 74.8% and 67.6%, respectively) (Bove & Lunghi, 2006). Additionally, other concerns limit the use of gas and steam turbines, such as low performance

(especially at reduced loads), high capital cost and a sensitivity to landfill biogas supply and ambient air temperatures (Tsatsarelis et al., 2006).

The annual operation of a typical 3 MW WTE electricity project reduces GHG emissions by approximately 17, 640 tonnes of CO_2, offsetting the consumption of almost 15 million gallons of gasoline or the equivalent of powering 1,900 homes (USEPA, 2008). Another study done by Broun & Sattler (2016), concluded that by using landfill biogas for electrical production conventional and bioreactor landfills reduced emissions of $CO_{2\ eq}$ per metric ton of landfilled MSW by 668 and 803 kg, respectively. While Yechiel and Sheval (2016) state that for every 1 ton of MSW, 0.78 MW of electricity could be generated, producing 6500-10000 MWh of electricity per year, relating this to powering 1500-2200 households in Europe (Yechiel & Shevah, 2016). Natividad Pérez-Camacho et al. (2019) stated that by utilizing biogas for electricity generation saves typically 300 kg of $CO_{2\ eq}$/MWh of electricity generated into the grid.

2.5.3.3 Landfill biogas to alternative fuel

Landfill biogas can decarbonize natural gas production and be sent to the natural gas grid (pipeline quality fuel such as biomethane or renewable natural gas) or used as vehicle fuel (such as in the form of compressed natural gas (Hoo et al., 2018) (Cucchiella et al., 2018)). Typical pipeline fuels are either medium or high-BTU (1000 BTU/f^3), and while landfill biogas can be blended with either, to be added to a high-BTU fuel (which can be sold to natural gas suppliers or used in a more diverse set of equipment) the biogas must be upgraded, which involves separating CH_4 from CO_2 (USEPA, 2008).

Upgrading the landfill biogas to produce high-BTU fuel (effectively biomethane) is done by removing impurities and CO_2 present in the landfill biogas to increase the amount of CH_4 to

make it comparable to natural gas (Natividad Pérez-Camacho et al., 2019). Typical landfill biogas consists of CH_4, CO_2, H_2S and siloxane. The latter two components must be removed, as they are highly corrosive to engines and cause erosion and blockages, respectively (Hoo et al., 2018).

Upgrading the landfill biogas can be done using many different techniques, such as chemical absorption, biological absorption, pressure swing absorption, water scrubbing and cryogenic technology (Hoo et al., 2018), once upgraded it can be compressed to the necessary pressure. By upgrading landfill biogas into biomethane it has a significantly increased number of possibilities for utilization, such as utilization as a fuel source to be injected into the natural gas grid (most common, directly displacing the fossil fuel-based natural gas supply) (Natividad Pérez-Camacho et al., 2019), used as sustainable biomethane in vehicles (Paolini et al., 2018) or integrating it with other biochemical conversion pathways for the production of biohydrogen or biohythane (Natividad Pérez-Camacho et al., 2019). However, upgrading landfill biogas into a high-BTU fuel has a very high cost and profitability depends on whether the landfill gas can economically offer large amounts of high-BTU fuel to offset the investment and operation costs (Tsatsarelis et al., 2006).

Creating vehicle fuel requires the lowest gate fee, but it is only able to utilize 50% of the landfill biogas for scrubbing, to convert into a CH_4-enriched fuel, making it a less favorable option for reducing emissions (Murphy & McKeogh, 2004). The remaining landfill biogas can be flared to reduce the environmental impact of the operation. A number of vehicle fuels can be produced depending on the need, including compressed natural gas, liquefied natural gas or methanol, where CO_2 and trace impurities are removed to produce a fuel that is at least 90% CH_4 (USEPA, 2008).

Biogas upgrading to biomethane and injecting into the gas grid for heating saves 191 kg $CO_{2\ eq}$/ MWh of energy generated by the biomethane (Natividad Pérez-Camacho et al., 2019). While utilizing the biogas as a petrol or diesel replacement results in the largest reduction of GHG, 524 and 477 kg of $CO_{2\ eq}$/ MWh of energy, respectively(Natividad Pérez-Camacho et al., 2019).

2.6 Comparison of landfill biogas utilization technologies and reduction of CO_2 emissions

Landfill biogas emissions are impacted by the location of the landfill, the carbon content of the waste and age of the landfill. The four main different options for landfill biogas utilization include (1) flaring, (2) beneficially using the landfill biogas with direct use, (3) electricity generation (with or without combined heat and power) and (4) creating alternative fuel to be injected into the grid. All of these technologies reduce the amount of $CO_{2\ eq}$ released to the atmosphere, compared to untreated landfill biogas release.

Due to the changing biogas emissions released by landfills, the results of CO_{2eq} emissions reduction for different landfills using the same technology for biogas treatment will vary. Typically, 1 million tonnes of municipal solid waste (MSW) will emit 12,233 m^3 of landfill biogas/day (Pierson, 2013). This will generally produce 0.78 MW of electricity (Pierson, 2013).

This translates into 4.92 m^3 of landfill biogas per year per 1 tonne of MSW, as shown by:

$$12{,}233\ \frac{\frac{m^3}{day}}{1\ \text{million tons of MSW}} \times 365\ \frac{day}{year}$$

$$= 4,465,045 \ \frac{\frac{\mathrm{m}^3}{\mathrm{year}}}{1 \text{ million tons of MSW}} \times \frac{1 \ ton}{0.907 \ tonnes}$$

$$= 4.92 \ \frac{\frac{\mathrm{m}^3}{\mathrm{year}}}{1 \text{ tonnes of MSW}}$$

To compare the impact of these technologies, an approximate standard of landfill biogas being an equal mixture of carbon dioxide and methane (50% CO_2 and 50% CH_4) will be utilized in the following sections. The mass of CH_4 in the gas is 4385 kg of CH_4 day^{-1} for 1 million tons of MSW. As such, the production of methane per meter cubed of MSW, per day, is 4.385 g_{CH4} m^{-3}_{MSW} day^{-1}, which represents the basis for both the majority of landfill gas impact and the potential for utilization. As methane represents a potential energy source but also, according to the Intergovernmental Panel on Climate Change (IPCC), has 25 times the global warming potential (GWP) compared to carbon dioxide (Brander, 2012), this factor will also be utilized to compare emissions on the basis of CO_2 equivalence.

All calculations in the following sections use normal meters cubed as their basis for comparing the impact of different landfill gas utilization technologies.

2.6.1 Untreated

In the base scenario, if landfill biogas is untreated and released to atmosphere, then:

$$\mathrm{CO_{2eq}} = \left(\frac{12\ 233\ \mathrm{Nm^3\ biogas/day}}{1 \text{ million tons of MSW}}\right)\left(\frac{0.5\ \mathrm{Nm^3\ CO_2}}{1\ \mathrm{Nm^3} \text{ of biogas}}\right) + \left(\frac{12\ 233\ \mathrm{Nm^3 biogas/day}}{1 \text{ million tons of MSW}}\right)\left(\frac{0.5\ \mathrm{Nm^3\ CH_4}}{1\ \mathrm{Nm^3} \text{ of biogas}}\right)\left(\frac{25\ \mathrm{CO_{2eq}}}{1\ \mathrm{CH_4}}\right)$$

$$CO_{2eq} = 6116.5 \ \frac{Nm^3\ CO_{2\ eq}/day}{1\ million\ tons\ MSW} + \ 152,912.5 \ \frac{Nm^3\ CO_{2\ eq}/day}{1\ million\ tons\ MSW}$$

$$CO_{2eq} = 159,029 \ \frac{Nm^3\ CO_{2\ eq}/day}{1\ million\ tons\ MSW} \times \frac{1\ ton}{0.907\ tonnes}$$

$$CO_{2eq} = 175\ 335 \ \frac{Nm^3\ CO_{2\ eq}/day}{1\ million\ tonnes\ MSW}$$

2.6.2 Flared

As a first treatment option, the landfill biogas is captured and flared to reduce emissions, where the perfect combustion of 1 kg of CH_4 produces 2.75 kg CO_2 (stoichiometrically 1:1). It is assumed that combustion is complete and all CH_4 is combusted into CO_2.

$$CO_{2eq} = 12,233 \ \frac{Nm^3 of\ biogas\ /day}{1\ milliom\ tons\ of\ MSW} \times \left(\frac{1\ m^3\ CO_2}{1\ m^3\ of\ biogas}\right)$$

$$CO_{2eq} = 12,233 \ \frac{Nm^3\ CO_{2\ eq}\ /day}{1\ million\ tons\ of\ MSW} \times \frac{1\ ton}{0.907\ tonnes}$$

$$CO_{2eq} = 13\ 487 \ \frac{Nm^3\ CO_{2\ eq}\ /day}{1\ million\ tonnes\ of\ MSW}$$

2.6.3 Direct Use

If the landfill biogas is positively used in a boiler for heat production, with the following assumptions and data:

- A natural gas heater would be used if landfill gas is not utilized
- All landfill biogas can be utilized

- The heating value of landfill biogas is used conservatively as 16,765 kJ/Nm^3 (range: 16,765 – 20,495 kJ/Nm^3)
- The heating value of natural gas is 35,406 kJ/Nm^3
- The density of natural gas is 0.8 kg/Nm^3 under standard conditions

Reduction in natural gas used

$$= \text{emissions of landfill waste per day} \times \frac{\text{Heating value of landfill biogas}}{\text{Heating value of natrual gas}}$$

$$= 12,233 \ \frac{\frac{\text{Nm}^3}{\text{day}}}{1 \text{ million tons of MSW}} \times \left(\frac{16{,}765 \ \frac{\text{KJ}}{\text{m}^3}}{35{,}406 \ \frac{\text{KJ}}{\text{m}^3}} \right)$$

$$= 5792 \ \frac{\frac{\text{Nm}^3}{\text{day}}}{1 \text{ million tons of MSW}} \times \frac{1 \ ton}{0.907 \ tonnes}$$

$$= 6584 \ \frac{\frac{\text{Nm}^3}{\text{day}}}{1 \text{ million tonnes of MSW}}$$

Therefore, 6584 Nm^3/day of natural gas combustion is reduced by directly utilizing the landfill biogas. Then, as the combustion process is the same as flaring, the reduction in CO_2 associated with the reduced combustion of natural gas can be reduced from the daily emissions.

$$\text{CO}_{2\text{ eq}} = \ 12{,}233 \frac{\frac{\text{Nm}^3\text{CO}_{2\text{ eq}}}{\text{day}}}{1 \text{ million tons of MSW}} - 5792 \ \frac{\text{Nm}^3}{\text{day}} (\rho_{\text{NG}}) \left(\frac{1 \text{ m}^3 \text{ CO}_2}{1 \text{ m}^3 \text{ CH}_4} \right)$$

$$\text{CO}_{2\text{ eq}} = \ 12{,}233 \frac{\frac{\text{Nm}^3\text{CO}_{2\text{ eq}}}{\text{day}}}{1 \text{ million tons of MSW}} - 5792 \ \frac{\text{Nm}^3}{\text{day}} \left(0.8 \ \frac{\text{kg}}{\text{m}^3} \right) \left(\frac{1 \text{ m}^3 \text{ CO}_2}{1 \text{ m}^3 \text{ CH}_4} \right)$$

$$CO_{2\ eq} = 9709\ \frac{\frac{Nm^3 CO_{2eq}}{day}}{1\ \text{million tons of MSW}} \times \frac{1\ ton}{0.907\ tonnes}$$

$$CO_{2\ eq} = 10\ 704\ \frac{\frac{Nm^3 CO_{2eq}}{day}}{1\ \text{million tonnes of MSW}}$$

Therefore, by using a boiler the emissions release per one million tonnes of MSW is 10, 704 Nm^3 $CO_{2\ eq}$/day.

2.6.4 Electricity

If the landfill biogas is combusted and positively used for electricity generation, in addition to the benefit of flaring, there is no need to use that electricity from another source – parallel to the reduction of natural gas utilized if the landfill biogas combustion is directly utilized in a boiler. However, since electricity is the product being replaced, the associated environmental impact is highly regional. For comparison, an average electricity production in Ontario, Canada is used. Specifically, in 2018, Ontario produced 63 tonnes CO_{2eq}/GWh and the generator associated with the landfill generates 0.78 MWh of electricity per 1 million tonnes of MSW.

$$\frac{63\ \text{tonnes}\ CO_{2\ eq}}{\text{GWh}} = \frac{X\ \text{tons}\ CO_{2\ eq}}{0.78\ \text{MWh} \times \frac{1\ \text{GWh}}{1000\ \text{MWh}}}$$

$$X = 0.04914\ \text{tonnes}\ CO_{2\ eq}$$

Therefore, 0.04914tonnes $CO_{2\ eq}$/GWh is what the electricity generator that produces 0.78 MWh.

Determining the further reduction of emissions from electricity generation, in addition to those achieved by biogas combustion:

$$\mathrm{CO_{2\,eq}} = 12{,}233\ \frac{\frac{N\mathrm{m^3\ CO_{2\,eq}}}{\mathrm{day}}}{1\ \text{million tons of MSW}} - 1.07\ \frac{\text{tons of } \mathrm{CO_{2\,eq}}}{\mathrm{GW day}\ 1\ \text{million tons of MSW}}$$

$$\mathrm{x}\left(0.78\ \frac{\mathrm{GW}}{\mathrm{h}}\right)\left(\frac{24\ \mathrm{h}}{1\ \mathrm{day}}\right)\left(\frac{556.2\ \mathrm{m^3 CO_2}}{1\ \text{ton of } \mathrm{CO_2}}\right)$$

$$\mathrm{CO_{2\,eq}} = 1092\ \frac{\frac{\mathrm{Nm^3\ CO_{2\,eq}}}{\mathrm{day}}}{1\ \text{million tons of MSW}} \times \frac{1\ ton}{0.907\ tonnes}$$

$$\mathrm{CO_{2\,eq}} = 1203\ \frac{\frac{\mathrm{Nm^3\ CO_{2\,eq}}}{\mathrm{day}}}{1\ \text{million tonnes of MSW}}$$

While this calculation was done in Ontario, it can be seen that across Canada and across the globe, the distribution of energy generation varies widely from locations (as shown in Table 7), utilizing the lifecycle GHG emissions of these electricity sources (Table 6) – the equivalent values for outside of Ontario can be calculated (Table 7).

Table 6: Lifecycle GHG emissions (mean average) of different electrical generation techniques (McIntyre et al., 2011)

Generation Method	**Tonnes CO_{2eq}/GWh**
Nuclear	29
Coal	888
Hydroelectric	26
Wind	26
Natural Gas	499
Solar	85
Biomass	45
Oil	733

Table 7: Percentage of electricity emissions and CO_2 emissions from various sectors and regions around the world (Australian Government, 2019; Burger, 2017; Government of Canada, 2019a; McIntyre et al., 2011)

		Fraction of each electricity sector				
Emissions	**Tonnes CO_{2eq}/ GWh**	**Ontario**	**Alberta**	**Canada**	**Germany**	**Queensland**
Nuclear	29	0.6		0.15	0.053	0.76
Coal	888		0.45	0.09	0.15	0.76
Hydroelectric	26	0.26	0.03	0.6	0.013	0.0093
Wind	26	0.07	0.05	0.04	0.082	0.0004
Natural Gas	499	0.05	0.45	0.09	0.03	0.16
Solar	85	0.01	0		0.34	0.041
Biomass	45	0.01	0.03	0.02	0.33	0.020
Oil	733	0	0		0	0.014
Total GWh		152,000	82,400	650,200	1,352,500	70, 747
Total emissions CO_{2eq} (tonnes)/ GWh		52.2	628	147	198	767
Total $CO_{2\ eq}$ emissions (tonnes)		7,938,960	51,712,592	95,397,344	268,210,300	54,101,368

The Government of Canada states that the electricity generation in Canada is 80% non-emitting which include hydro for 58.8%, nuclear for 14.6%, wind for 4.7%, biomass for 2% and solar for 0.5%, but the remaining 20% is from oil and diesel, natural gas, and coal (Government of Canada, 2019a). These all generate significant emissions from electricity production. Coal accounts for 67.8%, natural gas 28.9 % and oil and diesel at 3.2% of Canada's emissions from

electricity generation (Government of Canada, 2019a). The only significant fossil fuel in Ontario for source of electricity is natural gas, accounting for 8.2% of electricity generated in 2016, and the Canadian mean is 140g GHG/kWh (Government of Canada, 2019a). Whereas the Ontario Power Generation stated that 525 g CO_{2eq} /kWh was produced from natural gas (Ontario Power Generation Inc, 2016). And another source from Sustainable Buildings Canada claims the emission factor in 2013 (latest non-preliminary result) is 506 g CO_{2eq}/kWh, although this does not account for unallocated energy (transmission line losses, metering differences and other losses) (Singleton et al., 2017).

2.6.5 Alternative fuel

If landfill biogas is cleaned to produce biomethane, and that the enriched biogas is utilized as natural gas either injected in to the natural gas grid or used as transport fuel. The following assumptions have been made for this calculation:

- Due to the cleaning process of converting landfill biogas into pure biomethane, only 50% of the gas is able to be utilized
- Assuming 100% capture efficiency of the treated methane
- 1 kg CO_2 is equivalent to the volume of 0.546 Nm^3

$$\mathrm{CO_{2\,eq}} = 12{,}233\ \frac{\frac{\mathrm{Nm^3\ CO_{2\,eq}}}{\mathrm{day}}}{1\ \text{million tons of MSW}} - 3058\ \frac{\mathrm{Nm^3}}{\mathrm{day}} \times 0.717\ \frac{\mathrm{kg\ CH_4}}{1\ \mathrm{m^3}} \times 2.75\ \frac{\mathrm{kg\ CO_2}}{\mathrm{kg\ CH_4}} \times$$

$$\mathrm{CO_{2\,eq}} = 8941\ \frac{\frac{\mathrm{Nm^3\ CO_{2\,eq}}}{\mathrm{day}}}{1\ \text{million tons of MSW}} \times \frac{1\ ton}{0.907\ tonnes}$$

$$CO_{2\,eq} = 9858\ \frac{\frac{Nm^3\ CO_{2\,eq}}{day}}{1\ \text{million tonnes of MSW}}$$

Typical passenger vehicle emits about 4.6 metric tons of CO_2 per year assuming 35 km/gallon and 18 507 miles/year, where a gallon of gasoline emits 8887 g of CO_2/gallon = 2400 g CO_2/L. OPG states that natural gas releases 525 g CO_2 eq/ kWh and transportation releases 58.7 Mt CO_2 eq. (Ontario Power Generation Inc, 2016).

The emissions associated with renewable natural gas will be carbon neutral because it does not contribute to the net CO_2 into the atmosphere, so it eliminates the amount of CO_2 technically in the atmosphere by releasing biogenic CO_2

2.6.6 Summary of landfill biogas treatment and utilization with related $CO_{2\,eq}$ emissions released

Table 8 below shows the comparison of the various treatment methods for GHG's from landfills emissions, including the associated CO_2 emissions released.

Table 8: Summary of CO_2 emissions released with the associated treatment

Treatment	**$CO_{2\ eq}$ emissions released** $\left(\frac{\frac{Nm^3\ of\ CO_{2\ eq}}{day}}{1\ million\ tonnes\ MSW}\right)$	**Beneficially using landfill biogas**	**Percentage reduction (%, compared to untreated)**
Untreated	175 335	No	--
Flaring	13 487	No	92.3%
Direct Use (Boiler)	10 704	Yes	93.8%
Electricity (Ontario, Canada)	1203	Yes	99.3%
Alternative fuel	9858	Yes	94.4%

2.7 Conclusion

Municipal solid waste landfills contribute to GHG emissions globally, largely as a significant source of CH_4 anthropogenic emissions. While the quantity and composition of the landfill biogas is affected by multiple parameters, including the composition of the waste and climatic factors, there are common methods to reduce the impact of these systems. These treatment options include flaring, which has become a mandatory regulation in many countries as a minimum to reduce GHG emissions. However, while flaring is effective at reducing most of the CH_4 emissions, the biogas is not beneficially captured and used to its highest capacity. As such multiple beneficial utilization treatments have been developed, which include direct use of landfill biogas, generation of electricity, combined heat and power systems and enhancing gases

for use as alternative fuels. The comparison of landfill biogas utilization determined which treatment reduced the most CO_2 emissions per 1 million tons of landfilled MSW per day. No treatment, flaring, direct use (boiler), alternative fuel, and electricity were the order for most CO_2 emissions released to the atmosphere to the least amount of emissions released to the atmosphere with 175 335, 13 487, 10 704, 9858, 1202 m^3 of CO_2/day/1 million tonnes of landfill MSW, respectively. With identifying the emissions reduced, it is clear that there can still be more effort on reducing emissions from landfill biogas.

Direct use of landfill biogas is an effective way to reduce emissions and provides economic incentives. However, there are significant economic distance limitations, which limit distances from the source to 8-16 km. Depending on how large the landfill site is, this limitation determines how much biogas can be used directly. While in terms of electricity generation, reciprocating engines are the most commonly used technology for electric energy production having the lowest economic risk, higher efficiencies and is well matched with the size of most landfills. Using landfill biogas as vehicle fuel or high-BTU fuel, is gaining interest, but both come with a high investment and operating cost, and literature is unclear on if there are other limitations dictating why they aren't commonly used. Site-specific research needs to be done to determine more about the exhaust gas from reciprocating engines to generate electricity, with the potential for combined heat and power, as they are the most common and reduce the most emissions. More research needs to be done on alternative fuel production, to determine if it can be optimized and become the best option in the future.

Chapter 3

3 Stand-alone electricity generator emissions data

This chapter discusses the landfill biogas generation, electricity generator performance and off-gas production, and the opportunity for off-gas CO_2 sequestration by microalgae growth.

3.1 Background

In Sudbury, Ontario (Canada) a municipal solid waste landfill houses a biogas powered electricity generator – a system found also at other landfills. The process of electricity generation begins with collecting the biogas, which can be accomplished using either or a combination of vertical or horizontal wells in the landfill. The Sudbury landfill uses a horizontal collection system, with perforated piping that collects the landfill biogas and transports it through to a landfill biogas header pipe, non-perforated, to the landfill biogas collection facility (Cook & Educator, 2015). This biogas is then treated to remove moisture, particles and impurities before being sent to the reciprocating engine for electrical generation. When the electricity generator is not running, a flare is used to burn the landfill biogas and reduce CH_4 emissions being released directly into the atmosphere (Cook & Educator, 2015), as it is a significantly more potent greenhouse gas than the CO_2 produced in combustion.

The reciprocating gas engine is made by Caterpillar Inc. (engine model: G3520C) with a maximum electrical efficiency of 40%, which has been used for over 26 years in similar applications. The system is designed to treat impure fuel (such as landfill biogas) and clean it for safe use in the engine. It treats the biogas for water vapor, halides, siloxanes and sulphur compounds which are corrosive to metal and can damage the engine (Lee et al., 2014).

The methods used as pre-treatment to clean the landfill biogas in these systems, such as

Sudbury's, are (Lee et al., 2014):

1. Gas-to-air coolers: lower the temperature of the gas after it is compressed, which reduces moisture to prevent condensation and acid formation in the engine;
2. Gas-to-gas heat exchanger: precool the gas entering the dryer to reduce dryer power demand. The gas leaving the dryer is reheated by the gas-to-gas heat exchanger to prevent water from condensing downstream;
3. Gas dryers: reduce halogens and hydrogen sulfides (H_2S) in the gas. The gas is dried to its dew point (2-3˚C). Halogens and the H_2S are water soluble which means reducing their water content reduces their concertation in the gas. This step also reduces siloxanes;
4. Coalescing filters: remove any remaining water or oil droplets and small solids at 0.4 microns and
5. Condensate drains: collect water removed from the gas. The water may be treated for discharge to a sewer system or in some cases reintroduced into the landfill to stimulate methane production.

Reciprocating engines emit pollutants of nitrogen oxides (NO_x), carbon monoxide (CO) and volatile organic compounds (VOCs) (Darrow et al., 2015). CO_2 is not considered a pollutant, but it contributes to greenhouse gases. The amount of CO_2 emitted is a function of both landfill biogas content and the generator system efficiency (Darrow et al., 2015). When using landfill biogas as a source of fuel the main composition is 45%-60% CH_4 and 40%-60% CO_2 with minimal amounts of nitrogen, oxygen, ammonia, sulfides, hydrogen and nonmethane organic compounds. The bulk of CO_2 emitted from the exhaust gas, comes from the combustion of methane (Broun & Sattler, 2016).

The existing plant in the Sudbury landfill, has been proven to be beneficial, generating significant quantities of electricity from CH_4 within the landfill biogas. However, the biogas contains on average 34% CO_2 and additional CO_2 is produced from CH_4 combustion and released from the exhaust stack. Currently, none of this CO_2 is captured or repurposed in any way. The average CH_4 in the landfill biogas is 55% and has an unidentified balance gas of 11%, which is higher than what is reported in literature.

3.2 Site Specific Data

The landfill is in Sudbury and located at a latitude of 46˚37’32” N and a longitude 80˚47’52” W, and at an elevation of 348.40 m (Government of Canada, 2019c). The reciprocating engine studied in this research generates electricity delivered to the grid at an average of 1.4 megawatts per hour (MWh). The electricity generator combusts the CH_4 from the biogas and the generator releases CO_2 rich off-gas that is released to the atmosphere. The intention is that data collected from this operation will provide a basis for modeling a CO_2 capture system based on enhancing photosynthetic microalgae cultivation and building a pilot plant.

The collected data was used to design a model (Chapter 4) to help consider sparging the CO_2 rich off-gas into on-site bioreactors to stimulate the growth of photosynthetic green microalgae. Cultivation of specific microalgae is of significant interest because other than mitigating CO_2, it can produce high value-added biocompounds, specifically lipids.

3.2.1 Climate Conditions

Canada’s climate is challenging for year-round cultivation of microalgae due to long periods of temperatures well below the 15°C, which is the growth threshold. Large-scale outdoor

microalgal ponds are, therefore, currently found exclusively in warmer climates, as the common solution in colder climates, to create an artificial environment (such as housing bioreactors within buildings), is generally considered uneconomical (Pankratz et al., 2017).

In Sudbury, the lowest average temperature is -13˚C in January and the highest 19˚C in July (Figure 2), with air temperatures generally only favourable to grow microalgae from mid-May to mid-September. Designing a bioreactor that can accommodate and heat the microalgae culture in the colder months will be, therefore, be needed to allow for year-round CO_2 capture and biomass production.

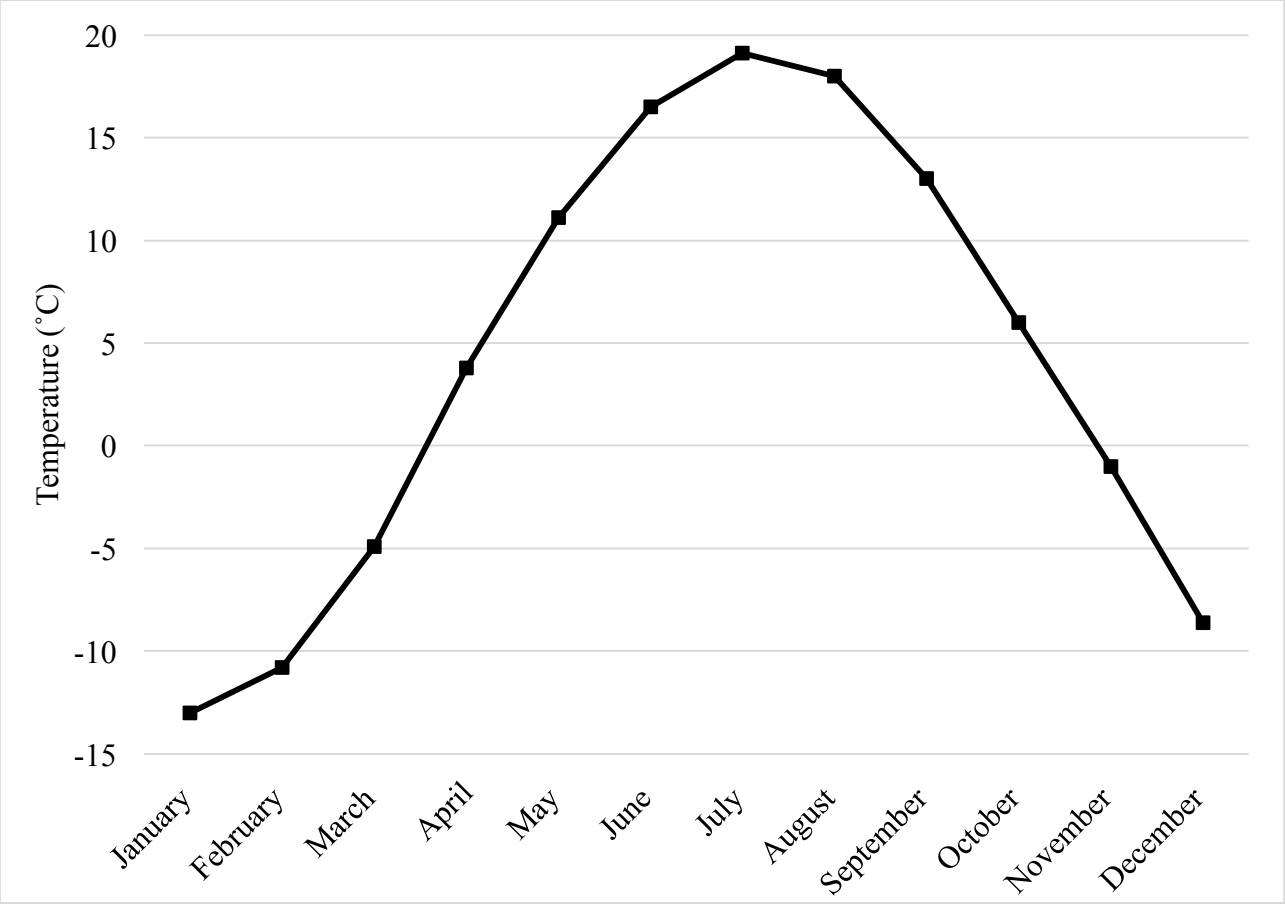

Figure 2: Average monthly temperatures in Sudbury, Ontario (Canada) adapted from (Government of Canada, 2019c)

3.2.2 Landfill biogas composition

The composition of landfill biogas is impacted by time, geographical location, economic conditions, structure and waste management technique used (Guermoud et al., 2009). When a collection system is not in place the biogas is released into the atmosphere and environmental factors, such as precipitation and temperature (Karanjekar et al., 2015), affect the gas rate and the ability for the gas to escape from the landfill through cracks in the soil cover.

At the Sudbury landfill, due to the soil layer they use to cap the landfill daily (Cook & Educator, 2015), temperature is maintained all year inside the waste material. This serves to keep the biogas collection system efficient, as varying ambient temperatures do have a significant impact on the waste. This temperature stability also produces a relatively constant biogas composition, with a year-round average of 55% CH_4 content. A fixed gas analyzer is used to continuously monitor, at standard temperature and pressure, the biogas production before entering the generator and the CH_4, CO_2, and O_2, as well as the balance gas which can contain nitrogen, elemental sulphur, siloxanes and other gases, are recorded daily. The biogas is treated to remove any water vapour, halides, siloxanes and sulphur compounds which are corrosive on metal (Lee et al., 2014) and this treatment room reduces the CH_4 down to an average of 50% (Figure 3).

It can be seen in Figure 3 that there is a section of outlying data from June –September 2019 where the CH_4 fed to the generator after biogas treatment is very high compared to pre-treatment. The equipment used was suspected to not have been calibrated to properly analyze the CH_4 percentage.

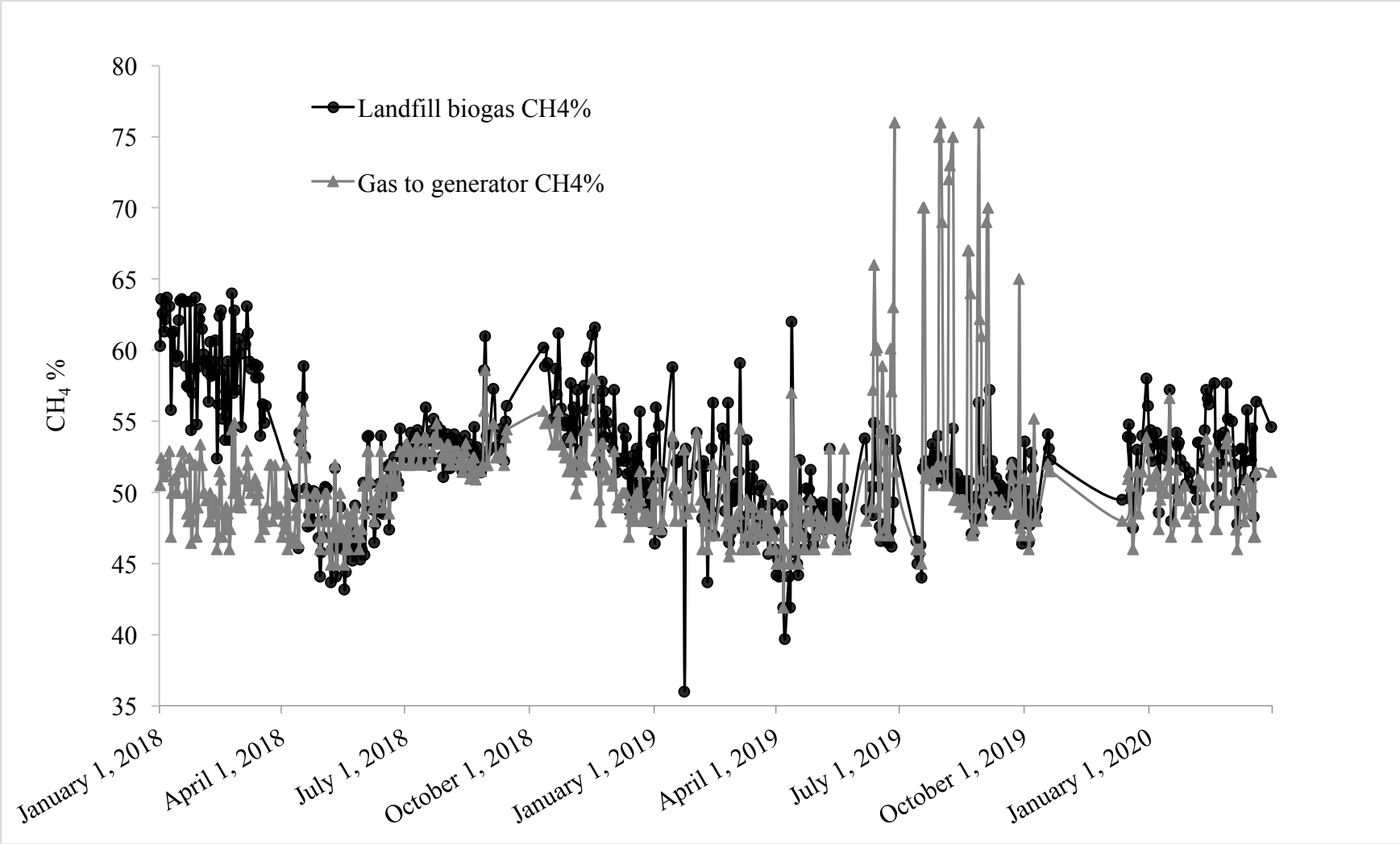

Figure 3: Volume percentage of landfill biogas CH_4 before and after pre-treatment*. The post-pre-treatment gas is what is combusted in the generator engine. Data from January 2018-March 2020.

*Measured at standard temperature and pressure.

Table 9 displays the landfill biogas averages and the average CH_4 percentage of the biogas after it is treated. Data on CO_2, O_2 and balance gas after pre-treatment are not recorded by the landfill. The full daily data can be seen in Appendix A.

Table 9: Average biogas composition* collected from Sudbury Landfill pre-treatment of landfill biogas and after treatment.

Gas Flow (m^3/hr)	**Pre-treatment CH_4 (%)**	**Pre-treatment CO_2 (%)**	**Pre-treatment O_2 (%)**	**Pre-treatment Balance Gas (%)**	**Engine CH_4 After Pre-treatment (%)**
715	55	34	1	11	50

* Measured at standard temperature and pressure

3.2.3 Temperature impacts on gas flow to generator and generator performance

Although temperature did not directly affect biogas collection, it did affect the electricity generator performance. When warm temperatures occur in the summer, the generator becomes very hot and the gas flow to the generator has to be reduced so that the generator will not overheat. Cold temperatures in the winter season do not have this affect, and the generator can operate as usual. Figure 4 depicts the ambient temperature and the volume of biogas flow to the generator, at standard temperature and pressure, and can be seen that as the temperature increases, the biogas flow entering the generator decreases. But as the temperature decreases the biogas flow remains at an average level and does not increase. This shows that the warmer months have an effect on generator production and the amount of off-gas entering the generator has to be reduced to avoid overheating.

Even though the volumetric biogas flow to the generator varies, the composition of the off-gas, and the CO_2 percentage, remains constant, which is important for microalgae production.

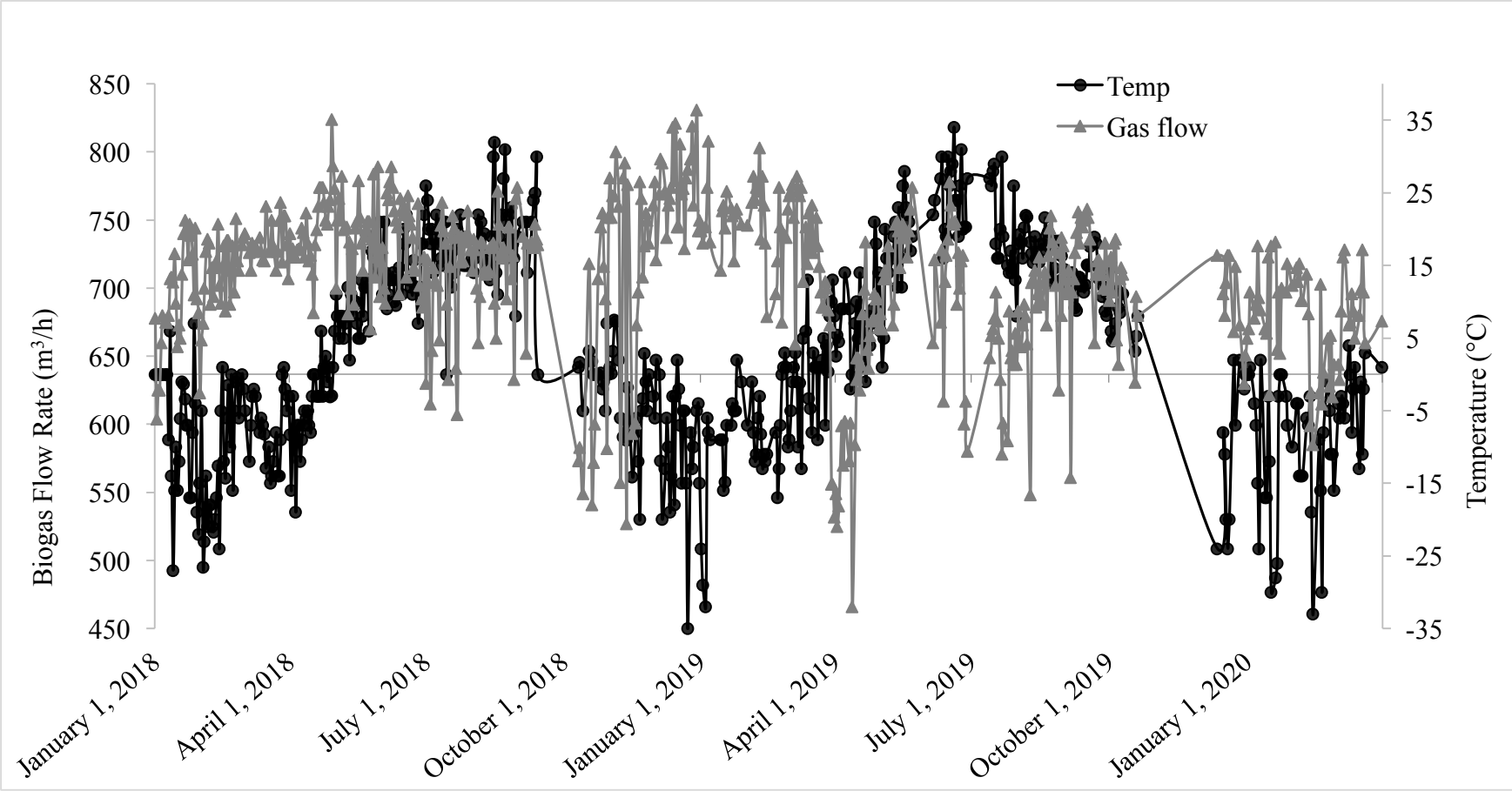

Figure 4: Landfill generator data for ambient temperature and biogas flow rate. Data from January 2018-March 2020, biogas flow rate measurements are converted to normal m^3 hr^{-1}.

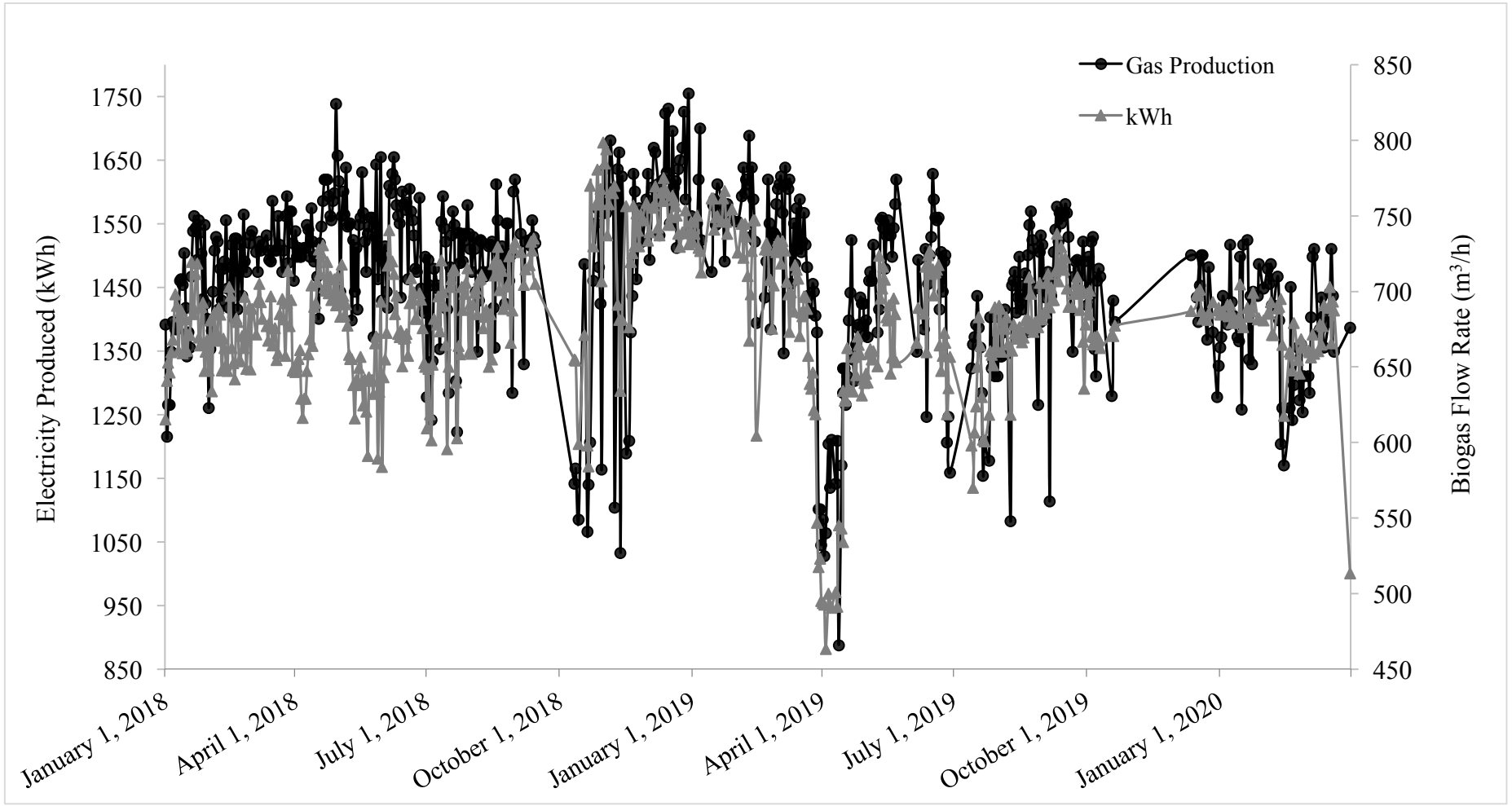

Figure 5: Landfill generator data for the amount of CH_4 rich biogas entering the generator and the associated kWh of electricity produced. Data from January 2018-March 2020, biogas flow rate measurements are converted to normal m^3 hr^{-1}.

Figure 5 shows how the electricity produced (kWh) follows the trend for the amount of landfill biogas entering the generator, converted to normal temperature and pressure. If the amount of biogas to the generator increases, the electricity output also increases. This is a direct correlation that the amount of CH_4 from the biogas entering the generator has an impact on how much electricity is sent to the electricity grid. The details in Figure 4 also show that the level of electricity generation has remained constant over the last two years, with minimal drops in generation and gas volume in late October-early November 2019 and April 2019.

3.3 Off-gas from landfill electricity generator

The generator exhaust off-gas is not monitored and, therefore, a study was undertaken to determine the CO_2 concentration and temperature of the off-gas. Assuming 100% combustion of CH_4, the off-gas will be composed of CO_2, water vapour, oxygen, nitrogen, and carbon monoxide. All volumetric flows are measured at normal m^3 (Nm^3). Using the average biogas flow of 715 Nm^3/hr, a calculation was done to determine the exit off-gas total at 5,556 Nm^3/hr with the quantity of CO_2 in the off-gas being 631 Nm^3/hr. The calculated composition of the off-gas can be seen in Table 10 using the average inlet gas flow rate from the landfill data. The weekly samples taken can be seen in Appendix B. The electricity generator was down from October 19 to December 17 due to mechanical and part issues.

Table 10: Average calculated composition of the off-gas from the electricity generator at the Sudbury landfill

Composition	**Flow Rate (Nm^3/hr)**
Total off-gas	5556
CO	6
CH_4	0
CO_2	631
H_2O	787
O_2	240
N_2	3893

As the heat of combustion for methane is 889 kJ/mol (Bergman & Incropera, 2011), with an average output of 1.4 MWh (5 040 000 kJ/h), the total energy from combustion is 15 099 940 kJ/hr. Calculating the energy loss by the difference of the average output and the total energy combustion, the energy loss is 10 059 940 kJ/h, which results in an efficiency of 33% for the electricity generator. This efficiency agrees with the 30-40% efficiency of other literature work on electricity production by a reciprocating engine, which only utilizes power generation and not combined heat and power. (Darrow et al., 2015; Gupta et al., 2012).

3.3.1 Off-gas sampling

Weekly samples of the electricity generators off-gas were taken at the Sudbury landfill. A UEI Test Instruments C85 CO_2 CO and temperature gas analyzer was used to determine the CO_2 percentage and the temperature of the off-gas, measured at standard temperature and pressure.

Other parameters, such as CO (ppm), O_2 (%), CO/CO_2 ratio, excess air (%), combustion efficiency (%), were also recorded but were not necessary in determining the validity of the CO_2 or the temperature of the electricity generator off-gas for this particular situation. The sampling began with climbing to the top of the electricity generator, staring up the analyzer and letting it "zero" with using ambient temperature. Once the analyzer was ready, the probe was connected and lifted to the top of the exhaust stack, where it was held for 5 minutes to assure the data was remaining at constant values, without varying. Samples were taken for a whole year, March 2019-March 2020, and with these results the average CO_2 percentage of the generator off-gas was 11% and the average temperature of the off-gas was 526˚C. Appendix B details all the information for the weekly data taken.

The consistency of the CO_2 at a high percentage of 11% makes it a promising source of CO_2 for microalgae growth. However, the very high temperature of the off-gas causes issues as this temperature directly to the tanks could damage and kill microalgae. The high temperatures from the off-gas need to be reduced and is a pilot plant design is discussed in Chapter 4.

3.4 Conclusion

The Sudbury landfill has shown positive efforts in reducing the impact of greenhouse gases by repurposing landfill biogas and combusting the CH_4 present in the biogas to produce electricity to the grid. The reciprocating engine used on average generates 1.4 MWh of electricity. The reciprocating engine has an exhaust off-gas which is released and is not monitored. Many engines that use biogas (from landfill, wastewater etc.) for combustion will likely have a similar off-gas as the one in Sudbury. The measurements carried out found an average of 11% CO_2 was present in the off-gas, which was at an average temperature of 526˚C.

The capture and repurposing of this CO_2 from the generator to produce microalgae could be a further environmental and potential economic benefit. It has been determined that the CO_2 percentage is consistent and the off-gas also contains a significant amount of heat. Further work is needed to determine if this heat can be repurposed during the cold winter months to maintain a suitable water temperature for the microalgae. The microalgae produced could be then a year-round source of lipids for biodiesel production and/or other nutraceuticals.

Chapter 4

4 Modelling microalgal capture of generator off-gas CO_2

This chapter examines microalgal capture of CO_2 in generator off-gas, associated potential for the production of biodiesel or bioactive compounds and a conceptual design of an intended pilot plant.

4.1 Background and previous model

The process of capturing anthropogenic CO_2 for use as a carbon source in microalgal cultivation has potential to both mitigate emissions and produce beneficial bioproducts. This carbon capture process is gaining attention compared to other biological options, as microalgae have higher growth rates and CO_2 fixation compared to terrestrial plants and ocean fertilization (Singh & Ahluwalia, 2013). Microalgae can also tolerate higher CO_2 concentrations, have low light intensity requirements, are environmentally sustainable and able to produce high value-added compounds (Singh & Ahluwalia, 2013) such as biofuels, hydrogen and isoprene production, livestock and fish feed, and beneficial health products (nutraceuticals) (Pankratz et al., 2017). Microalgal CO_2 utilization requires two stages: absorption of CO_2 from the gas phase to the liquid medium by mass transfer and subsequent chemical reaction and CO_2 fixation through photosynthesis (Pankratz et al., 2017; Seyed Hosseini et al., 2018).

Off-gases from large-scale industries, such as fossil fuel power generation, cement production, chemical production and iron and steel production (Davison & Thambimuthu, 2009), have been considered for their potential for microalgae carbon capture. Fossil fuel power generation, for example, can product CO_2 concentrations ranging from 3-30%, depending on the fuel source and the design of the plant (Packer, 2009). This concentration range is typical for previously reported

industrial off-gas, including from natural gas power plants, coal fired power plants, steel and iron production, cement production and smelter furnace off gas, are 9%, 10%, 30%, 15-25%, 6-7%, respectively (Bounaceur et al., 2006; Laamanen et al., 2014; Seyed Hosseini et al., 2015).

However, small scale sources, such as landfill biogas fired electricity generators, could also be a target for microalgae production. Stand-alone generators emit high temperature off-gas containing concentrations of CO_2 in the middle of the previously reported large scale emitter range (~12%). The produced CO_2 and waste heat can both be captured for potential microalgae production, as outlined in Figure 6.

Data from a stand-alone electricity generator in Sudbury (Ontario, Canada) has been collected to evaluate the site's potential for microalgae production. To determine if this stand-alone electricity generator is able to support year-round algal growth, a mathematical model has been adapted to determine (1) if the off-gas can provide and maintain a suitable temperature for microalgae cultivation year round, and (2) how much experimental microalgae could be produced onsite in a pilot plant which consists of ten 1 m^3 bioreactors (1 seed tank and 3 sets of biological triplicates). This research will help determine the potential of a large-scale operation utilizing the full off-gas stream.

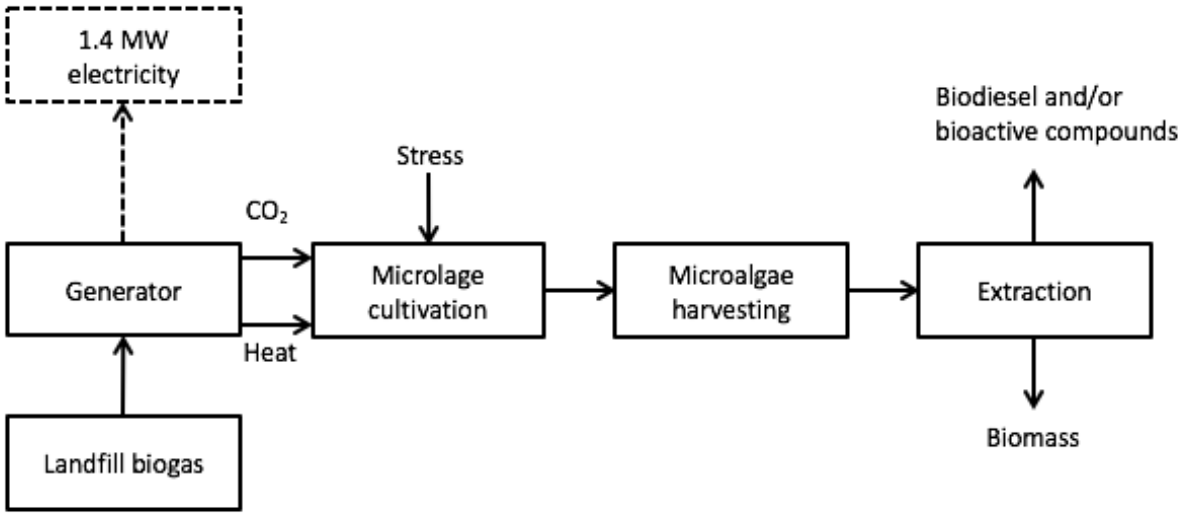

Figure 6: Block diagram of the landfill biogas electricity generator and the proposed microalgae production system

Previously published research on the benefit of capturing nickel smelter furnace off gas (6-7% CO_2) using microalgae showed positive results with respect to emissions reduction. In this research, a novel bioreactor was developed, utilizing a top-lit gas-lift bioreactor design to capture off-gas and increase operational depth from 30 cm open-pond, which is typical of most commercial microalgae systems (based on self-shading and light requirements) to 1 m due to agitation provided by the off-gas. This decreased footprint is important for allowing the construction of such bioreactors near industrial off-gas sources. The agitation technique also allows for excellent gas-liquid contacting, efficient mixing with low stress, high volumetric gas transfer, and reduces microbial growth on the walls due to a light scrubbing action (Znad et al., 2012). Additionally, due to the gas-based agitation, this reactor design requires no mechanical agitation and uses sunlight on the reactor surface as a light source. A further development includes the addition of light tubes, which can guide light deeper into solution inside the bioreactor, eliminating the need for costly internal lighting (Seyed Hosseini et al., 2016).

A gas-lift top-lit bioreactor allows for microalgal cells to have continuous circulation from the dark bottom to the lit top of the bioreactor, which allows intermittent lighting and thereby potentially reducing damage from prolonged exposure to surface light intensities (Seyed Hosseini et al., 2015). Being top-lit the costs of installing, operating and maintaining supplementary lighting are avoided (Seyed Hosseini et al., 2015). Higher lipid productivity has been recognized in top-lit bioreactor which is induced by the light stress as a result of the mixing pattern, compared to other bioreactors (Laamanen et al., 2014; Seyed Hosseini et al., 2015).

An additional concern, commonly overlooked in bioreactor design, is operating temperature. While certain microalgal species have been able to grow at temperatures up to 60˚C, optimal growth is typically 15-26˚C (Seyed Hosseini et al., 2018). The modelled pilot plant system utilizes the direct application of the landfill generator off-gas and the indirect application of exhaust heat from a heat exchanger, aiming to maintain bioreactor temperatures at either 15˚C or 30˚C throughout the entire year.

4.2 Pilot plant model development

The off-gas from the stand-alone electricity generator exits at approximately 5,556 Nm^3/hr (92 600 L/min) at an average of 526˚C and an average of 11% CO_2. Due to the intended pilot plant consisting of ten 1 m^3 tanks, based on previous agitation experiments (Laamanen et al., 2014) it will only need to be fed with 318 L/min of off-gas, or 0.34% of the total off-gas flow.

The application of high temperature off-gas can be damaging to microalgae, as such the off-gas temperature needs to be reduced to a tolerable temperature for it to be directly bubbled into the bioreactor. This temperature reduction, down to 60˚C, which is suitable to bubble through the

bioreactors microalgae culture, can be achieved for the pilot plant through a 4-inch steel pipe with an inside diameter of 0.102 m, an outside diameter of 0.114 m and a length of 18 m. The total off-gas flow, prior to bleeding off the 0.34%, can be put through a jacketed pipe heat exchanger to indirectly capture energy without creating any significant back-pressure on the engine. The quantity of energy that can be removed using the off-gas heat exchanger was examined for the potential use of indirect heating to maintain temperatures throughout the colder winter months.

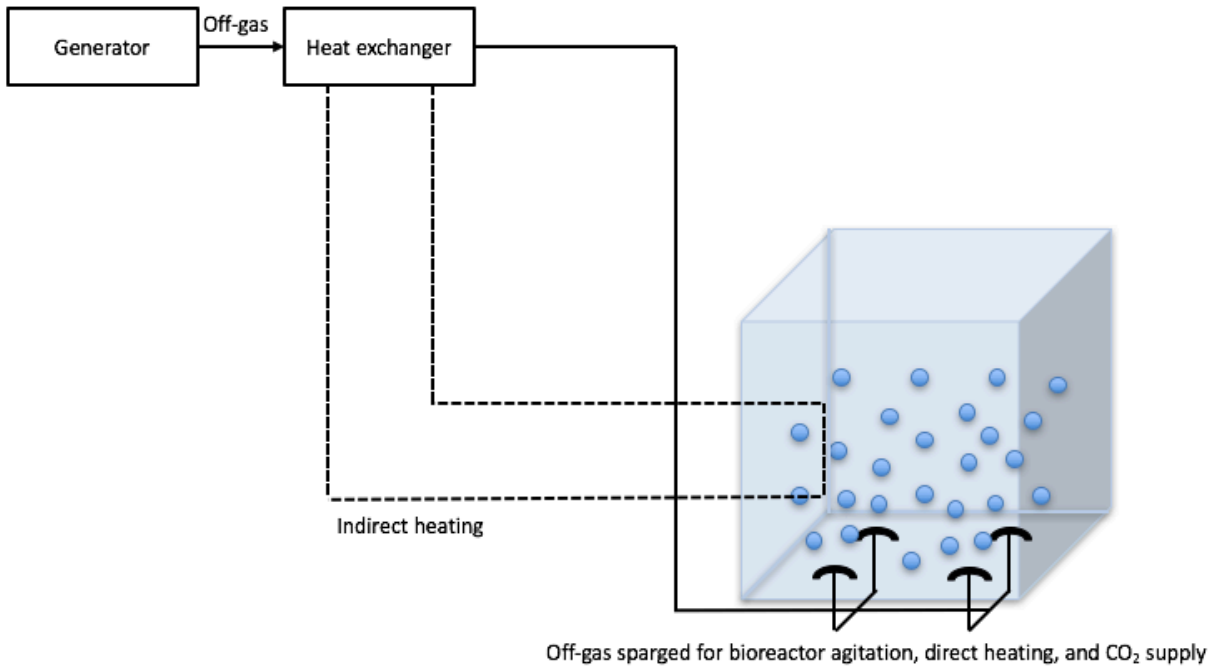

Figure 7: Schematic of the 1 m^3 bioreactor and the off-gas supplying heat and CO_2

The standard, pilot-scale bioreactor used in this model is 1 m^3, based on an open-topped Intermediate Bulk Container (Figure 7), covered with a clear polyethylene plastic, similarly to those used in greenhouses. This will help to reduce contamination, while also reducing the evaporation, by creating 100% humidity and minimizing convective heat loss from wind velocity

(u). The tanks are modelled on top of concrete pads and are insulated with polyurethane on all walls and the bottom.

4.3 Model calculations

The heating model utilizes direct sparging of off-gas from a stand-alone electricity generator, while additionally determining when additional indirect heating is necessary to maintain the bioreactor temperatures at either 15˚C or 30˚C. For this model, the following assumptions are used:

1. Each bioreactor is a batch operation (no water flow in or out);
2. Due to the efficient mixing effect of sparging in off-gas, spatial variations of water temperature are negligible;
3. Constant bubble volume over the height of the system due to small gas transfer;
4. Inertial forces on gas bubbles are negligible compared to buoyancy and drag forces;
5. Gas and water density variations are negligible across the bioreactor;
6. Gas temperature above the water is uniform.

Based on off-gas usage and agitation requirements from Laamanen et al. (2014), the system requires 7.96 L/min/sparger for optimal mixing, as the design includes 4 spargers per 1 m^3, a total of 31.84 L/min/tank is required.

4.3.1 Off-gas

The composition of off-gas from the stand-alone electricity generator was largely unknown, as few published reports have reported either the off-gas composition or other gas characteristics, such as the heat capacity of the gas. As such, the average landfill gas composition was measured and is reported in Table 11. Using these measured values, a stoichiometric combustion calculation was completed to determine the off-gas composition. The volume of CO_2 in the outlet gas was 631 Nm^3/hr.

Table 11: Generator off-gas composition for the inlet gas, inlet air and exit off-gas

Inlet Gas	**Volume (Nm^3/hr)**	**Measured (%)**
Biogas	715	
CH_4	393	55
CO_2	243	34
Balance gas	79	11
Make-up air	4939	
O_2	1037	
N_2	3901	
Exit gas		
Exhaust gas	5556	
CH_4	0	0
CO	6	0 (991 ppm)
CO_2	631	11 (measured with gas analyzer)
H_2O	787	14
O_2	240	5
N_2	3893	70

The heat capacity of the off-gas was calculated using a weighted average of the individual gas components. The heat capacity was determined to be 1267 J/kg·K at 526˚C and is used in the model development below.

4.3.2 Heat transfer model

The heat transfer model uses monthly temperature data for Sudbury (Ontario, Canada) as the ambient temperature for the bioreactor. The model is impacted by the evaporative (q_{evap}), conductive (q_{cond}), convective (q_{conv}), and solar (q_{solar}) heat transfer in addition to the off-gas heat flux ($q_{off\text{-}gas}$) and the heat addition from the heat exchanger (q_{HE}). The overall heat flux (q) of the system can be represented by Equation 9:

$$\mathbf{q = q_{HE} + q_{off-gas} + q_{solar} - q_{evap} - q_{cond} - q_{conv}} \qquad \text{Equation 9}$$

In the equation there are heat addition terms from the heat exchanger, the off-gas and solar heating, while the last three terms are the heat loss from evaporation, conduction through the walls and convection at the surface, respectively. Below are detailed descriptions of these calculations to determine the overall heat flux. Figure 8 depicts the different heat fluxes from the bioreactor, for ease of visualization in the model equations below.

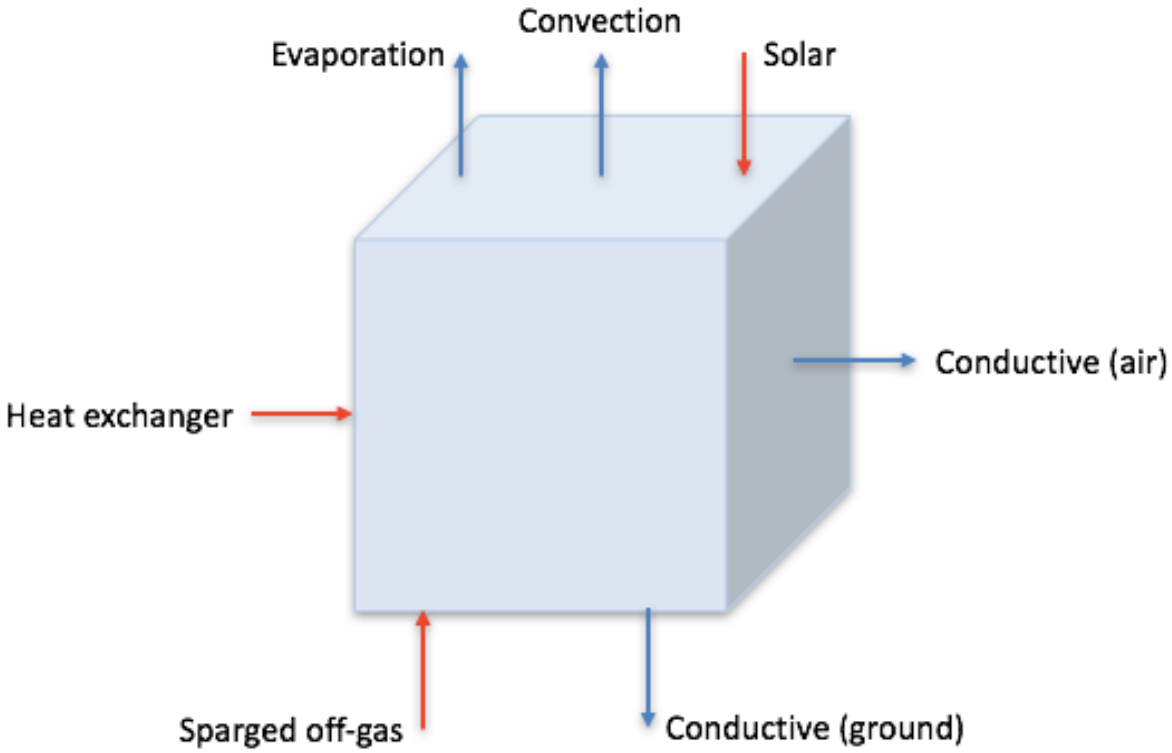

Figure 8: The different heat fluxes influencing the bioreactor

4.3.3 Heat loss due to evaporation (q_{evap})

Evaporative heat loss is predominantly affected by wind velocity (μ) and the difference between the saturated vapor pressure of the water surface above the bioreactor (e_s) and the vapor pressure of the ambient air above the bioreactor (e_G) (Equation 10) (Woolley et al., 2011). The polyethylene cover above the bioreactor helps to reduce evaporation by creating 100% relative humidity (R_h) and eliminating wind velocity (0 m/s).

$$\mathbf{q_{evap} = h_{evap}(e_S - e_G)A} \qquad \text{Equation 10}$$

The heat transfer coefficient (h_{evap}) can be determined using Equation 11 (Woolley et al., 2011):

$$\mathbf{h_{evap} = 0.0360 + 0.0250\mu}$$

Equation 11

While the saturated vapour pressure, e_S (mmHg), and the vapour pressure, e_G (mmHg), can be determined from (Nath & Bolte, 1998; Robert Troxler & Thackston, 1977) as shown in Equations 12 and 13, respectively:

$$\mathbf{e_S = 25.37exp\left(17.62 - \frac{5271}{T_L + 273}\right)}$$ Equation 12

$$\mathbf{e_G = R_h * 25.37exp\left(17.62 - \frac{5271}{T_G + 273}\right)}$$ Equation 13

4.3.4 Heat loss due to convection (q_{conv})

Convective heat loss can be determined using the Bowen ratio (R_{Bowen}), which relates convective heat transfer and evaporative heat transfer (Bowen, 1926), as seen in Equation 14:

$$\mathbf{R_{Bowen} = \frac{q_{conv}}{q_{evap}}}$$ Equation 14

Where the Bowen ratio (R_{Bowen}) can be calculated using Equation 15, using the Bowen coefficient (C_{Bowen}) is 61.3 $Nm^{-2}C^{-1}$ (Bowen, 1926).

$$\mathbf{R_{Bowen} = C_{Bowen} \frac{\rho_G}{\rho_{atm}} \frac{T_L - T_G}{e_S - e_G}}$$ Equation 15

Where ρ_G is the density of the off-gas, ρ_{atm} is the density of the air, and T_L and T_G are the temperatures of the liquid inside the bioreactor and the gas above the bioreactor surface, respectively (Bowen, 1926; Laamanen et al., 2014).

4.3.5 Heat loss due to conduction (q_{cond})

Conductive heat loss is heat transfer through the bioreactors walls and bottom. The walls and bottom are designed to have a 5 cm insulating layer of polyurethane and the insulated system sits on top of a concrete pad. The conductive heat loss is a function of thermal conductivity of polyurethane (k_{ins}), the thickness of the walls (z_{ins}) and the area of the wall (A_{wall}) as well as the temperature of the liquid inside the tank (T_L) and the temperature of air outside the tank (T_{air}) which is seen in Equation 16 (Bergman & Incropera, 2011):

$$\mathbf{q_{cond}} = \frac{\mathbf{k_{ins}}}{\mathbf{z_{ins}}}\mathbf{A_{Wall}}(\mathbf{T_L} - \mathbf{T_{air}}) \qquad \text{Equation 16}$$

4.3.6 Heat addition due to solar radiation (q_{solar})

Solar heat flux is the quantity of solar radiation that raises the temperature of the liquid in the bioreactor. It is a function of absorptivity of the liquid (α_L), reflectivity (ξ) and transmissivity (τ), the solar radiation (S_t) and surface area (A) of the bioreactor, which is represented from Equation 17 (Arora, 2000; Laamanen et al., 2014):

$$\mathbf{q_{solar}} = \boldsymbol{\alpha_L}(\mathbf{1} - \boldsymbol{\xi})\boldsymbol{\tau}\mathbf{S_t}\mathrm{A} \qquad \text{Equation 17}$$

The total solar radiation (H_G) contributes to the temperature of the atmosphere above the bioreactors water surface and it is represented as Equation 18 where the gas hold up (ε) can be determined using Equation 27:

$$\mathbf{H_G} = (\mathbf{1} - \boldsymbol{\alpha_L})(\mathbf{1} - \boldsymbol{\varepsilon})\boldsymbol{\tau}\mathbf{S_t}\mathbf{A} \qquad \text{Equation 18}$$

It is important to note that the light within this model is purely considered with respect to the effect on temperature. This assumption was based on previous research by Bernard et al. (2012) which showed that temperature has a greater influence on microalgal growth than light intensity, as long as a minimum light intensity was met. Solar data measured in Sudbury meet minimum lighting requirements, and as such, the focus of this model is temperature.

Solar heat flux…

4.3.7 Head addition due to generator exhaust off-gas ($q_{off\text{-}gas}$)

The furnace off-gas heat flux impacts the bioreactor temperature by sparging the off-gas from the base of the bioreactor, while also providing continuous mixing of the microalgae and ensuring temperature variations across the bioreactor are small. The bubble size, frequency of bubble formation and bubble ascent velocity are all important parameters in determining the heat input from the off-gas bubbles (Shang et al., 2010), which are explained in this section. Akita and Yoshida (1974) showed that the only significant factors affecting the bubble size were the orifice diameter and the gas velocity through the orifice. For this model it is assumed that the bubbles have a spherical shape and the sizes and departing periods of the bubbles are uniform at low inlet gas flow rate (L. Zhang & Shoji, 2001). Bhavaraju et al. (1978) states that the correlation for gas bubble diameter (D_b) and orifice diameter (D_o) is widely applied due to being able to use the large range of vapor flow rate and can be calculated from Equation 19 (Bhavaraju et al., 1978; Kang et al., 2002):

$$\frac{D_b}{D_o} = 3.23Re^{-0.1}Fr^{0.21} \qquad \text{Equation 19}$$

The Reynolds number (Equation 20) and the Froude number (Equation 21) can be calculated for the bubbles from (Shang et al., 2010):

$$\mathbf{Re} = \frac{\mathbf{4\rho_L Q_o}}{\mathbf{\pi D_o \mu_L}} \qquad \text{Equation 20}$$

and Q_o is the off-gas flow rate applied to each orifice in the sparger (m^3/s) where there are an estimated 2500 orifices per sparger.

$$\mathbf{Fr} = \frac{\mathbf{Q_o}^2}{\mathbf{D_o}^5 \mathbf{g}} \qquad \text{Equation 21}$$

Where μ_L is the dynamic viscosity of the water and Q_o is the volumetric off-gas flow rate per orifice, which can be determined through a simple division of the total gas volume flow rate to the tank ($Q_{off\text{-}gas}$) by the number of orifices per unit area (n) multiplied by the tanks surface area (A) as seen in Equation 22 (Shang et al., 2010):

$$\mathbf{Q_o} = \frac{\mathbf{Q_{off-gas}}}{\mathbf{nA}} \qquad \text{Equation 22}$$

The frequency of bubble formation (f) is determined from dividing the orifice flow rate by the bubble volume which is shown below in Equation 23 (Shang et al., 2010):

$$\mathbf{f} = \frac{\mathbf{6Q_o}}{\mathbf{\pi D_b}^3} \qquad \text{Equation 23}$$

After detachment from the orifice, the bubble reaches a force balance through interactions with the surrounding liquid, the bubble will reach a steady ascent velocity (u_b), assuming negligible inertial forces. The forces exerted on the rising gas bubble are buoyancy (F_b) and drag (F_d). (L. Zhang & Shoji, 2001). Each force is a function of the bubble diameter, liquid (ρ_L)and gas

densities (ρ_G) and can be shown in the following Equations 24 and 25, respectively (L. Zhang & Shoji, 2001):

$$\mathbf{F_b} = \frac{\pi \mathbf{D_b}^3}{6}(\boldsymbol{\rho_L} - \boldsymbol{\rho_G})\mathbf{g} \qquad \text{Equation 24}$$

$$\mathbf{F_d} = \frac{1}{8}\boldsymbol{\rho_L}\pi \mathbf{D_b}^2 \mathbf{C_D}(\mathbf{u_b})^2 \qquad \text{Equation 25}$$

Where the drag force coefficient (C_D) is equal to $15.5/Re^{0.6}$ for 1<Re<1000 or 0.44 for Re>1000 according to Zhang and Shoji (2001). By assuming the gas density is negligible compared to liquid density, the drag force and buoyancy force can be related and the bubble ascent velocity can be determined in Equation 26:

$$\mathbf{u_b} = \sqrt{\frac{4\mathbf{D_b g}}{3\mathbf{C_D}}} \qquad \text{Equation 26}$$

The gas hold up (ϵ) is determined to be the fraction of the gas inside the liquid and can be calculated from Equation 27:

$$\boldsymbol{\varepsilon} = \frac{\mathbf{nf}\pi \mathbf{D_b}}{6\mathbf{u_b}} \qquad \text{Equation 27}$$

By using the above equations of bubble size, frequency, ascent velocity, gas hold up and applying the conservation law, the temperature of the gas bubble can be determined as it rises through a water depth of Z, which can be determined from Equation 28:

$$\frac{\mathbf{dT_b}}{\mathbf{dt}} - \mathbf{u_b}\frac{\mathbf{dT_b}}{\mathbf{dz}} = \frac{\pi \mathbf{D_b}^2 \mathbf{n h_{LG} f}}{\boldsymbol{\rho_G} \mathbf{C_{p,OG}} \boldsymbol{\epsilon} \mathbf{u_b}} (\mathbf{T_L} - \mathbf{T_b}) \qquad \text{Equation 28}$$

The heat flux of the generator off-gas can be determined from Equation 29, where $T_{OG,\ inlet}$ is the temperature of the off-gas at the inlet and T_G is the temperature of the gas above the bioreactor

surface. Based on off-gas usage, 7.96 L/min/sparger is required for adequate agitation of the microalgae and 4 spargers are required per 1 m^2 of surface area (Laamanen et al., 2014).

$$\mathbf{q_{off-gas} = Q_{off-gas} C_{p,OG} \rho_G (T_{OG,inlet} - T_G)} \quad \text{Equation 29}$$

4.3.8 Temperature of gas above surface water in bioreactor

For a covered bioreactor the parameters that will affect the temperature of the gas above the water surface are the water temperatures and the outside air temperatures as well as the solar radiation (Ganguly & Ghosh, 2009; Pieters & Deltour, 1999). In addition, the temperature of the air above the water surface will also be impacted by the heat exchange rate between the atmosphere and the water surface and the energy contribution (E_b) from the gas bubbles with the reach the surface of the water, which can be calculated using Equation 30 and 31:

$$\mathbf{E_b = p_G \frac{\pi {D_b}^3}{6} fnAC_{p,OG}\left(T_{OG,i} - T_G\right)} \quad \text{Equation 30}$$

Where $T_{OG,\,i}$ is the temperature of the off-gas inlet, entering the bioreactor.

$$\mathbf{\frac{dT_G}{dt} = \frac{1}{\rho_L C_{p,G} V_G}\left(\rho_G \frac{\pi {D_b}^3}{6} fnAC_{p,OG}(T_{b0} - T_G) - h_{GL}A(T_G - T_L) - h_{Ga}A(T_G - T_a) + (1 - \alpha_L)(1 - \varepsilon)\tau S_t A\right)} \quad \text{Equation 31}$$

4.3.9 Heat addition due to energy recovered from heat exchanger (q_{HE})

The heat flux from the energy recovery of the heat exchanger is determined by Equation 32:

$$\mathbf{q_{HE} = V\rho_{OG} C_p (T_{out} - T_{in})} \bullet x \quad \text{Equation 32}$$

Where V is the volumetric flow rate, x is the capture efficiency of the heat exchanger which is approximated as 0.6 according to previously published reports on similar heat exchanger designs (Choi et al., 2018; Loken, 2013). The pilot plant uses the heat exchanger to heat the bioreactors during the cold season, with no additional concerns for gas cooling as it is simply discharged to atmosphere. In a scaled up production facility, where all of the off-gas is utilized, the heat exchanger recovers energy and simultaneously reduces the off-gas to a suitable temperature to be bubbled into the bioreactor. This recovered heat can be used to heat the bioreactors during the cold seasons, and for usage year round to facilitate microalgae harvesting and drying, both necessary stages in beneficial bioproduct production.

The previous heat flux calculations were used to determine the quantity of heat that can be added or removed from the bioreactor. The number of tanks that can be supported in any given month are dependent upon the number of bioreactors that can be efficiently agitated and fed with the generator off gas as well as heated to either 15˚C or 30˚C with the off-gas and heat exchanger energy inputs.

4.3.10 Overall heat transfer model

The overall heat transfer model for the bioreactor water temperature is represented by Equation 33:

$$\frac{\mathbf{dT_L}}{\mathbf{dt}} = \frac{\mathbf{1}}{\boldsymbol{\rho}_{\mathbf{L}}\mathbf{(1-\varepsilon)C_{p,L}AZ}}\left(\mathbf{q_{off-gas} + q_{HE} + q_{solar} - q_{evap} - q_{conv} - q_{cond}}\right) \qquad \text{Equation 33}$$

The heat transfer model includes the evaporative and convective heat flux from the bioreactor surface area as well as conduction through the bottom and walls of the bioreactor. This model is

used to determine the energy required to maintain a bioreactor at either 15˚C or 30˚C, representing the low and high end of the typical operating temperature range.

4.4 Simulation Results

Cultivation temperature is a key factor in microalgae production, as it determines the growth rate and the extent of the growing season (Davison, 1991). Northern communities experience low temperatures, well below the cultivation temperatures, for multiple months of the year, making unheated systems unsuitable for large portions of the year. However, repurposing energy from the stand-alone electricity generator, along with the application of off-gas for the mitigation of CO_2, has the potential to sustain year-round microalgae production in Northern communities.

Stand-alone electricity generators have a limitation for the volume of microalgae bioreactors that they can support due to the lower number of total off-gas compared to a large-scale operation, such as a smelter or cement producer. Based on off-gas usage by Laamanen et al. (2014), 7.96 L/min/sparger is required for agitation, where 4 spargers are used per meter squared of surface area for adequate agitation. Based on the volume of off-gas (92 600 L/min), the maximum number of 1 m^3 tanks is 2,908. Which shows that there is significant potential for these systems, but it should be noted that if scaled up to a production facility, bioreactors would also be scaled up to maximize cultivation area and reduce the number of tanks and the associated construction costs. The designed pilot plant consists of ten bioreactor tanks and requires an off-gas flow of 318 L/min, which is 0.34% of the total off-gas.

The results from the pilot plant model were compared for a non-heated bioreactor, a bioreactor maintained at 15˚C and a bioreactor maintained at 30˚C. The generator produces roughly 1.4

MW of electricity to the grid and the 4-inch steel 18 m pipe reduces the small, utilized portion of off-gas from 526˚C to 60˚C to allow for direct application to the microalgae bioreactors. The total off-gas flow enters the heat exchanger and provides a maximum of 666 kW at 60% efficiency. Figure 9 shows the rapid bubble cooling, to the bioreactor operating temperature of 15˚C or 30˚C. Due to using such a small amount of off-gas the temperature regulates very quickly in a 1 m^3 bioreactor.

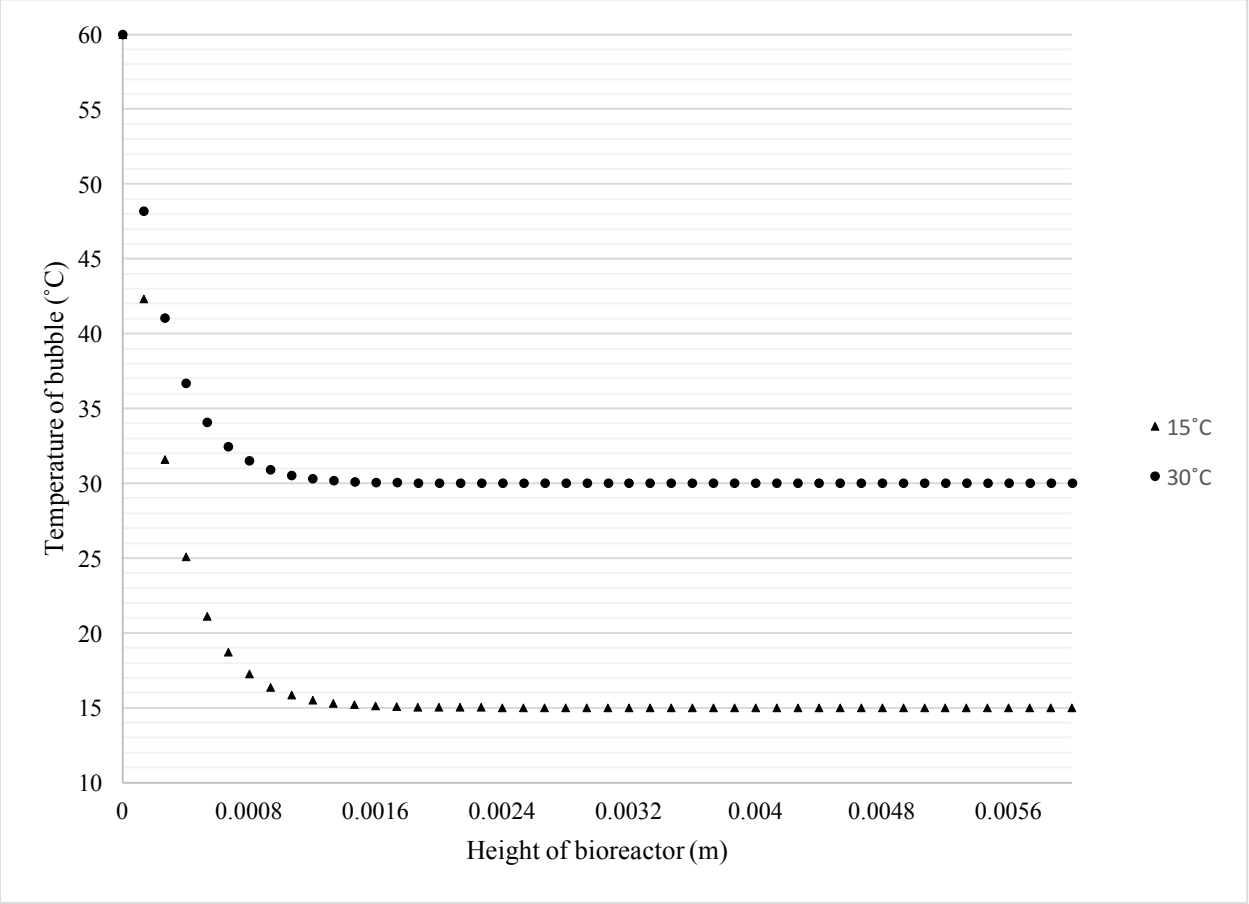

Figure 9: Temperature of the bubble as it rises through bioreactor to reach 15˚C and 30˚C

By sparging in the generator off-gas at 60˚C it provides a constant source of heat, at a rate of 382 W for maintaining a 15˚C operating temperature and 255 W for maintaining a 30˚C operating temperature. This heat addition alone is not enough to match the heat losses and maintain operating temperatures, showing the need for the indirect heating from the heat exchanger. The pilot plant bioreactors were modeled with no heat added to the water, maintained at 15˚C and at 30˚C, which are shown in Tables 12, 13 and 14, respectfully.

Table 12: Unheated bioreactor and temperature of bioreactor water for 1 m^3 tank

Unheated						
Month	Ambient air (˚C)	Heat Transfer Terms (W)				
		q_{evap}	q_{conv}	q_{cond}	$q_{off\text{-}gas}$	q_{solar}
January	-13.0	-12	-27	-27	51	14
February	-10.8	-16	-29	-28	49	24
March	-4.9	-23	-28	-28	44	36
April	3.8	-33	-25	-25	38	46
May	11.1	-43	-22	-22	33	55
June	16.5	-50	-20	-20	29	60
July	19.1	-51	-18	-18	28	60
August	18.0	-44	-17	-17	29	49
September	13.0	-34	-17	-17	33	35
October	6.0	-24	-18	-18	39	22
November	-1.0	-18	-20	-19	44	12
December	-8.6	-14	-23	-23	49	11

The bioreactor is impacted by the climate temperature surrounding it. As can be seen in the results for Figure 10, the typical temperature range for microalgal growth is 15˚C to 30˚C and with no added bubble off-gas heating or heat exchanger the bioreactor would only be able to operate from May to September. With the direct addition of off-gas, and no indirect heat

exchanger addition, the bioreactor can be operated for more of the year, from April to October. There is a need for added heat by a heat exchanger which will keep the temperatures higher than 15˚C and lower than 30˚C for microalgal growth.

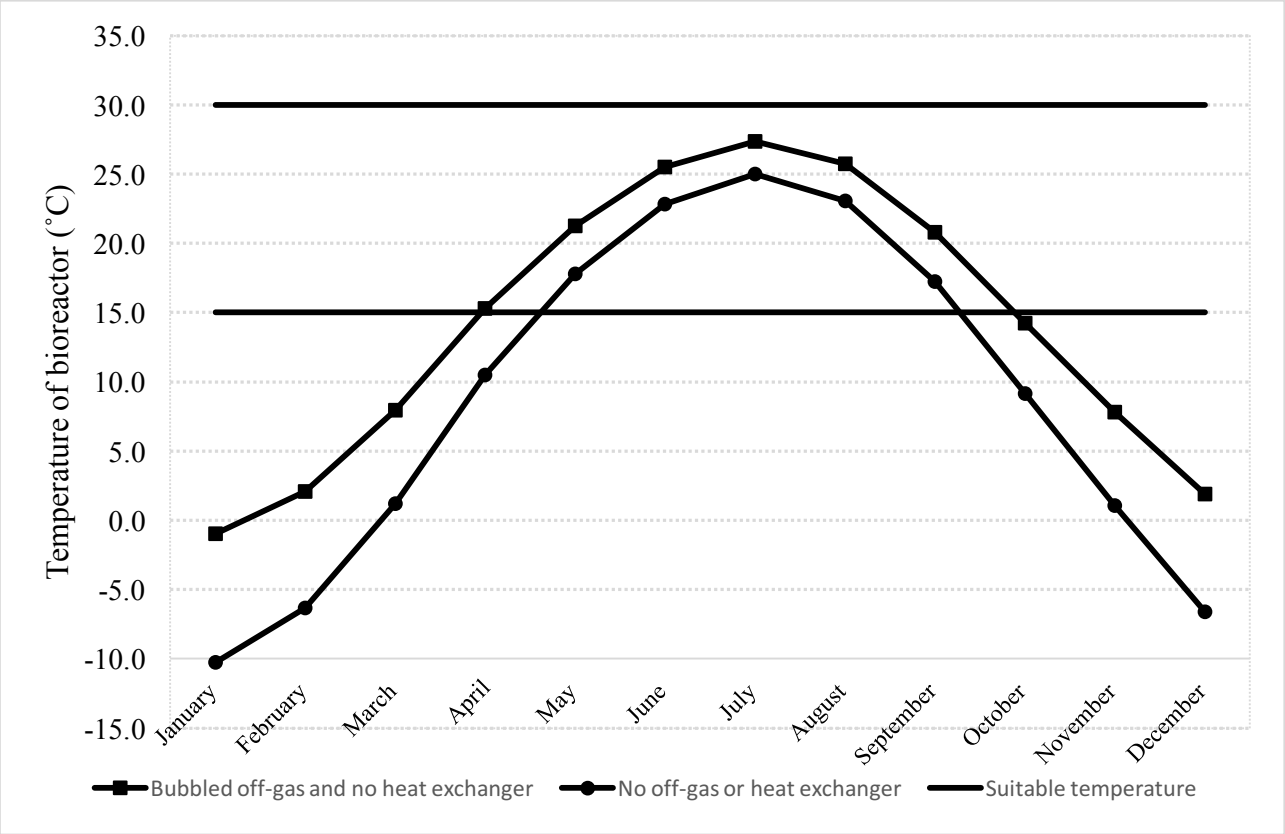

Figure 10: Suitable temperature range compared with temperatures with no off-gas or heat exchanger and bubbled off-gas and no heat exchanger

Table 13: Bioreactor maintained at 15˚C and associated heat fluxes for 1 m^3 bioreactor tank

Bioreactor Temperature at 15˚C											
Month	Ambient T (˚C)	Pond T (˚C)	Heat Transfer Terms (W)							Number of tanks that can be heated	Pilot plant operable
			q_{Evap}	q_{Conv}	q_{Cond}	q_{Solar}	q_{Total}	$q_{off-gas}$	q_{HE} (total)		
January	-13.0	15	-53	-62	-62	14	-163	382	666000	4097	Yes
February	-10.8	15	-51	-57	-57	24	-141	382	666000	4707	Yes
March	-4.9	15	-46	-44	-44	36	-98	382	666000	6805	Yes
April	3.8	15	-32	-25	-25	46	-35	382	666000	18846	Yes
May	11.1	15	-14	-9	-9	55	24	382	666000	>15C	Yes
June	16.5	15	6	3	3	60	73	382	666000	>15C	Yes
July	19.1	15	18	9	9	60	96	382	666000	>15C	Yes
August	18.0	15	13	7	7	49	75	382	666000	>15C	Yes
September	13.0	15	-7	-4	-4	35	19	382	666000	>15C	Yes
October	6.0	15	-27	-20	-20	22	-45	382	666000	14752	Yes
November	-1.0	15	-41	-35	-35	12	-99	382	666000	6735	Yes
December	-8.6	15	-50	-52	-52	11	-143	382	666000	4659	Yes

Table 14: Bioreactor maintained at 30˚C and associated heat fluxes for 1 m^3 bioreactor tank

Bioreactor Temperature at 30˚C											
Month	Ambient T (˚C)	Pond T (˚C)	Heat Transfer Terms (W)							Number of tanks that can be heated	Pilot plant operable
			q_{Evap}	q_{Conv}	q_{Cond}	q_{Solar}	q_{Total}	$q_{off-gas}$	q_{HE} (total)		
January	-13.0	30	-144	-95	-95	14	-319	255	666000	2083	Yes
February	-10.8	30	-142	-90	-90	24	-298	255	666000	2230	Yes
March	-4.9	30	-137	-77	-77	36	-255	255	666000	2612	Yes
April	3.8	30	-123	-58	-58	46	-192	255	666000	3462	Yes
May	11.1	30	-104	-42	-42	55	-133	255	666000	5007	Yes

June	16.5	30	-85	-30	-30	60	-84	255	666000	7922	Yes
July	19.1	30	-73	-24	-24	60	-61	255	666000	10973	Yes
August	18.0	30	-78	-27	-26	49	-82	255	666000	8166	Yes
September	13.0	30	-98	-38	-37	35	-138	255	666000	4826	Yes
October	6.0	30	-118	-53	-53	22	-202	255	666000	3294	Yes
November	-1.0	30	-131	-69	-68	12	-256	255	666000	2602	Yes
December	-8.6	30	-140	-85	-85	11	-300	255	666000	2220	Yes

Table 15: The required amount of heat needed from the heat exchanger for the pilot plant at 15˚C and 30˚C for ten 1 m^3 bioreactor tanks

	Bioreactor Temperature at 15˚ C				**Bioreactor Temperature at 30˚C**			
Month	Number of tanks	q_{Total} (HE and Off-gas) (W)	q_{Needed} (ten tanks) (W)	Portion needed for ten bioreactors (%)	Number of tanks	q_{Total} (HE and Off-gas) (W)	q_{Needed} (ten tanks) (W)	Portion needed for ten bioreactors (%)
January	10	666000	1625	0.24	10	666000	3196	0.48
February	10	666000	1415	0.14	10	666000	2986	0.45
March	10	666000	979	0.15	10	666000	2549	0.38
April	10	666000	353	0.05	10	666000	1923	0.29
May	10	666000	0	0	10	666000	1330	0.20
June	10	666000	0	0	10	666000	840	0.13
July	10	666000	0	0	10	666000	607	0.09
August	10	666000	0	0	10	666000	815	0.12
September	10	666000	0	0	10	666000	1380	0.21
October	10	666000	451	0.07	10	666000	2021	0.30
November	10	666000	989	0.15	10	666000	2559	0.38
December	10	666000	1249	0.21	10	666000	2999	0.45

An unheated bioreactor would not be suitable for producing microalgae year round. The heat exchanger and the off-gas would support heating large numbers of bioreactors but for the design of the pilot plant with ten bioreactor tanks, there is no need to utilize all this off-gas or associated recovered heat. There is evidence that stand-alone electricity generators have the ability to

efficiently heat the bioreactors to 15˚C and 30˚C by only utilizing 0.34% of the total off-gas amount. For the 15˚C bioreactor tanks, ten tanks can be supported all year long with the off-gas and a portion of the heat from the heat exchanger (detailed in Table 15). The heat exchanger can provide 666kW of heat, which maintaining a temperature of 15˚C the highest amount of heat needed from the heat exchanger is in January at 0.24% and lowest is during the warm months of May-September at 0%. This states that the off-gas can heat the tanks efficiently alone from May-September and maintain 15˚C. For the 30˚C pilot plant of ten bioreactor tanks the small portion of off-gas and heat from the heat exchanger can efficiently support 30˚C all year long. Again, not all of the heat exchanger heat needs to be utilized, but a larger percentage to maintain at 30˚C than at 15˚C. The highest amount of heat needed from the heat exchanger is in January at 0.48% and lowest is during July at 0.09%.

4.5 Pilot plant to produce microalgae sourced nutraceuticals or biodiesel

The gas-lift top-lit bioreactor allows for more precise control over algal growth parameters compared to traditional open systems and allows for increased lipid productivity in the biomass. Parameters such as CO_2 content, pH, nutrient delivery, light intensity, light cycle durations, mixing and a lower probability of contamination by other microorganisms all have an impact on lipid production (Hincapie & Stuart, 2015). Microalgae have the ability to produce up to 20-40% and can get as high as 60%-85% of their dry weight as lipids, making them both one of the most efficient biofuel production systems (Rawat, 2013; Sayre, 2010) and providing significant potential for the extraction of secondary metabolites from the lipids, which are a promising source of nutraceuticals (bioactive) compounds of significant commercial value (Goiris et al.,

2012; Senhorinho et al., 2015). Carbon capture efficiency is similar throughout the literature researched and has a reported average of 50% (Keffer & Kleinheinz, 2002; Pires et al., 2012; Weyer et al., 2010). At 10% CO_2 concentration, the efficiency of carbon capture reported by Ramanan et al., was 46%. With these reported averages a carbon capture efficiency of 50% is used in the following calculation for algal production.

A higher CO_2 concentration increases the lipid and biomass productivity in the microalgae biomass (Tang et al., 2011; Eloka-Eboka & Inambao, 2017) , however this results in a decrease in pH of the microalgae (B. Zhao & Su, 2014). Previous work by Laamanen et al. (2017) has shown the potential of producing lipid rich microalgae using nickel smelter off-gas in similar systems. This is facilitated through the cultivation of microalgae prospected from Northern Canada, where specific strains have evolved to tolerate lower pH values (due to their mining-influenced environments (Eibl et al., 2013)), with the potential for high levels of biodiesel or nutraceuticals production.

When algae are grown under stressful condition, by lack of nutrients (such as low nitrogen) or in the presence of supplemental reductants (glycerol), or alterations to light or temperature levels the metabolism of most microalgal species is redirected toward the production and accumulation of energy dense storage compounds such as lipids (Sayre, 2010). Light intensity is required for lipid synthesis (Seyed Hosseini et al., 2018) and by being top lit, the modeled bioreactor delivers a constant light cycle to the microalgae, which has been shown to increase lipid content in the microalgae in addition to the other advantages, including gas-liquid contact, low stress on the microalgae, high CO_2 mass transfer, efficient cycling of microalgae through the light and dark zones to produce higher biomass productivity (Kumar et al., 2011).

Different species of microalgae can offer higher or lower algal biomass, and simultaneously a higher or lower lipid content. Microalgae can have different optimal temperatures for different strains and temperature is much more important than light intensity for growing algal biomass (Bernard & Rémond, 2012). Reviewing published results tabulated by Bernard and Rémond (2012), it can be seen that *Asterionella formosa* grows well at 15˚C. While at 30˚C most microalgae species die, while it is others' optimal temperature and with appropriate strain selection can produce higher growth rates than with any reviewed strain at 15˚C. Table 16 shows the maximum growth rate (μ_T), the higher the value the better specific growth rate as it represents the number of doublings per day for algae. This shows the importance of algal species selection depending on the cultivation conditions.

Table 16: Maximum growth rate of different algal species and impact on temperature on the growth rate (adapted from (Bernard & Rémond, 2012))

Algae Species	**Temperature**	$\boldsymbol{\mu_T}$	**Temperature**	$\boldsymbol{\mu_T}$
Asterionella formosa	15	1.40	30	0
Ceratium furca	15	0.22	30	0.31
Ceratium furcoides	15	0.16	30	0
Ceratium fusus	15	0.16	30	0.23
Cryptomonas marssonii	15	0.80	30	0.03
Dinobryon divergens	15	0.68	30	0
Porphyrium cruentum	15	1.13	30	0
Scenedesmus sp.	15	0.42	30	0.64
Skeletonema costatum	15	0.39	30	0.62
Tychonema bourrellyi	15	0.71	30	0

Ccyclotella. memghinaiana1	15	0.40	30	0
Cyclotella. memghinaiana2	15	0.74	30	0
Dunaliella terioletca1	15	0.67	30	3.22
Dunaliella.terioletca2	15	0.77	30	3.69
Dunaliella terioletca3	15	0.53	30	2.56
Dunaliella terioletca4	15	0.67	30	3.22
Phaeodactylum. tricornutum1	15	1.41	30	0
Phaeodactylum. tricornutum2	15	0.86	30	0

The design considerations in this model are for a pilot plant utilizing ten 1 m^3 tanks and assuming optimal conditions such as algal species, temperature and added nutrients. The stand-alone electricity generator in Sudbury (Ontario, Canada) emits off-gas with an overall average flow rate of 133, 344 Nm^3/day with 11% CO_2 content. A stoichiometric relationship shows that 1.8 kg of captured CO_2 produces 1 kg of dry algal biomass (Chisti, 2007) and with an average carbon capture of 50% of applied carbon rich gas through a microalgae culture (Keffer & Kleinheinz, 2002; Pires et al., 2012; Weyer et al., 2010) the maximum microalgae production can be determined. Using the off-gas application rate of 31.84 L/min/bioreactor, there is enough CO_2 in the off-gas to achieve an algal productivity of 2.7 $kg_{dry\ weight\ microalgae}/m^3$/day. Similar values have been evaluated with 10% CO_2 with *Spirulina* sp. and *Chlorella* sp. with 2.91 $kg_{dry\ weight\ microalage}/m^3$/day and 2.25 $kg_{dry\ weight\ microalage}/m^3$/day, respectively (Ramanan et al., 2010). Similarly (Douskova et al., 2009) reported that with 11% CO_2 off-gas achieved 2.5 $kg_{dry\ weight\ microalgae}/m^3$/day in their bioreactor. While combining this with the lipid content in microalgae, which can commonly range from 20-50% of the dry cellular weight (Sun et al., 2018). Using a

value of 50%, which should be achievable based on appropriate strain selection, the lipid concentration from the microalgae can be 1.39 kg_{lipids}/m^3/day. This value shows significant potential for producing microalgal lipids utilizing small-scale CO_2 sources.

4.5.1 Industrial size tanks

While the ten 1 m^3 tanks were used as a design for the pilot plant-sized system, and as a basis to determine the amount a generator system could support – the use of larger, industrial-scale tanks (20 m (length) x 5 m (width) x 1 m (depth)) was also investigated. The larger tank size of 100 m^3 can produce the same algal productivity as the results reported above, as the conditions remain unaltered in the scaled up tanks. In these larger tanks, each would require 3,184 L/min/tank, where the stand-alone electricity generator will efficiently be able to agitate twenty-nine tanks at this size. For a full-scale operation utilizing twenty-nine 100 m^3 tanks (having a lipid productivity of 1.39 kg_{lipids}/m^3/day as outlined in the previous section), an average day of operation could produce 4,031 kilograms of lipids.

There is an excess of energy from the heat exchanger if operated at 15˚C, compared to the gas requirements for agitation, as such the number of tanks that can be supported is determined exclusively by agitation requirement and twenty-nine tanks can be ran year round. While if the operating temperature is to be 30˚C the heating requirement become limiting and the number of tanks needs to be reduced to twenty-six in December, twenty-five in January, and twenty-seven in February (the rest of the year could support the twenty-nine tank limit).

4.5.2 Use on remaining biomass

After lipid extraction, the remaining biomass, which consists of carbohydrates and proteins, can still have positive uses. These uses include, but are not limited to being animal feed additives, fish feed additives, or land ameliorant (Desjardins et al., 2020). Even if this does not create an additional income stream, it can have a positive impact and avoids any cost of disposal

4.6 Conclusion

This research has shown that using stand-alone electricity generators can efficiently produce microalgae while mitigating CO_2 emissions. The selection of both operating temperature and microalgae species are crucial to achieve a high growth rate and lipid productivity. As such, further investigation is needed to determine the best microalgae species for growth in Sudbury. As Canada has a significant number of remote, small communities that rely on self-generation of electricity as well as growing numbers of generators that run on biogas from landfills and municipal wastewater treatment plants, there is both a need for and an opportunity in mitigating the CO_2 off-gas and utilizing this gas in a beneficial and economic way, through microalgae cultivation.

The design of the bioreactor is efficient in providing adequate CO_2 mass transfer to the microalgae, mixing, proficient light cycles and reducing any contaminants by having a cover. The design is used to stimulate growth in microalgae and increase lipid productivity inside the microalgae. The model is based on a pilot plant that can repurpose the off-gas from the generator.

The overall heat transfer model of the system can be determined by the heat fluxes in and out of the bioreactor system. This includes the additional heat from solar radiation, heat exchanger and off-gas bubbling and heat losses due to evaporation, conduction and convection. The heat transfer model determined that the generator can easily support ten 1 m^3 tanks utilizing 0.34% of the generators off-gas at 15˚C and 30˚C. Such a system will have the potential to produce 2.5 $kg_{dry\ weight\ microalgae}/m^3/day$. An optimization of industrial size tanks can be considered to use twenty-nine (twenty-five year-round based on heating limitations if operating at 30˚C) 100 m^3 tanks. The proposed systems can produce large quantities of microalgae biomass and lipids to produce valuable, economical alternatives such as biodiesel or nutraceuticals, as well as reducing local CO_2 emissions.

Chapter 5

5 Conclusion

This conclusion chapter summarizes the research and findings throughout the thesis and discusses future work.

5.1 Summary of results

Chapter 2 is a literature review that explains the different technologies used to reduce GHG emissions from landfills. Untreated landfill gas and possible treatments by direct use, electricity generation/combined heat and power and alternative fuels are discussed. The use of landfill gas for methane combustion, can produce electricity that can be delivered to the electricity grid. This technology has the greatest reduction of GHG emissions. Although this represents the current best option for emissions reduction, further reductions are possible. The electricity generator combusts methane and releases a CO_2 rich off-gas which can be considered for repurposing as a carbon source for microalgae cultivation. This consideration, of further reducing GHG emissions from the combustion of landfill gas, has led to research in Chapters 3 and 4.

Chapter 3 examines the site-specific climate in Sudbury, ON, and presents data collected from a local landfill. At this site a reciprocating engine is used to combust the methane rich landfill biogas to generate electricity. The existing generator has been proven to be extremely beneficial and economical with delivering on average 1.4 MW of electricity to the grid. The off-gas released from this generator, and similar, systems are not monitored or recorded in literature. Weekly samples were taken to determine the off-gas quantity, CO_2 concentration and temperature using a gas analyzer. The off-gas quantity, CO_2 concentration and temperature of the off-gas were recorded, and the average off-gas flow rate was 6556 Nm^3/hr, with an average CO_2

concentration of 11% and an average temperature of 526˚C. This small-scale generator would produce a similar off-gas to other generators that use landfill biogas, water and wastewater biogas, or diesel generators in remote communities.

While a hurdle to utilizing microalgae cultivation for further reductions is that the Canadian climate is not suitable for year-round microalgae growth, so repurposing the off-gas to heat bioreactor tanks (or large tanks) is a potentially beneficial way of repurposing the current waste heat. Chapter 4 develops a model that uses a novel design, called a top-lit gas-lift bioreactor, which sparges in off-gas to provide constant agitation and a carbon source. The addition of a light tube can deliver sunlight deep into the reactor, eliminating the need for internal lighting. The model uses the direct application off-gas from the generator and the indirect use of exhaust heat from a heat exchanger to maintain bioreactors temperatures at 15˚C or 30˚C.

An overall heat transfer model was developed using data from Chapter 3 and includes the evaporative, conductive and convection heat loss, as well as the added heat from solar radiation, the off-gas being sparged into the bioreactor and heat delivered from the heat exchanger. The heat transfer model was used to determine the number of tanks that can be supported year-round.

The pilot plant consisted of ten 1 m^3 tanks and considering the large amount of off-gas being released, only 0.34% of the total off-gas flow (318 L/min/ for ten tanks) is needed to provide carbon dioxide and adequate agitation. Both the 15˚C and 30˚C bioreactor tanks for the pilot plant can be supported year-round with the off-gas and a portion of the heat from the heat exchanger. To maintain 15˚C the highest heat addition needed from the heat exchanger is in January at 0.24% and lowest is during the warm months of May-September at 0%. To maintain 30˚C the highest heat addition needed from the heat exchanger is in January at 0.48% and lowest

is during July at 0.09%. Supporting the concept of production, as the landfill electricity generator could clearly support a system much larger than the proposed pilot plant.

The repurposing of the generators off-gas is to stimulate the growth of microalgae for lipid production using the 11% CO_2 in the off-gas. The gas-lift top-lit bioreactor increases lipid productivity and can have the ability to produce 50% of lipids per gram dry weight of algal biomass which makes it suitable for biodiesel and nutraceuticals production, both of high commercial value. The pilot plant model used determined that the average flow rate from the generator using 0.34% (453 Nm^3/day) with 11% CO_2 using ten 1 m^3 bioreactors at 15˚C and 30˚C would achieve an algal productivity of 2.7 $kg_{\text{dry weight microalgae}}/m^3$/day with a lipid percentage of 50% the lipid dry weight of the biomass will be 1.39 kg_{lipids}/m^3/day.

Industrial size tanks were considered for scale up in the thesis. It was determined that twenty-nine tanks at 100 m^3 at 15˚C could be supported all year round in the northern climate. An average gas flow of 133,344 Nm^3/day can produce a lipid productivity of 4,031 kg of lipids per day. The number of tanks that can be supported and maintained at 30˚C are a limiting number of twenty-six 100 m^3 tanks for the months of December, twenty-five in January and twenty-seven in February with the remainder of the year supporting twenty-nine tanks.

Based on these results, it is determined that repurposing the electricity generators CO_2 rich off-gas for microalgae production is an economical and beneficial way of reducing GHG emissions being released to the environment. As Canada has a significant number of remote, small communities that rely on self-generation of electricity, as well as growing numbers of generators that run on biogas from landfills and municipal wastewater treatment facilities, there is a large market for a ‘plug and go’ bioreactor system to create nutraceuticals. This will help to mitigate

CO_2 emissions and generate a potential income from the high demand nutraceutical products.

5.2 Future work

The future work for this research is to implement the development of the pilot plants at the landfill to verify the model used in the thesis. Continuous off-gas monitoring will be conducted for a further electricity generator off-gas trend. By implementing the bioreactor tanks, we could determine the actual amount of microalgae produced per 1 m^3 tank in the local climate. This would provide an important development for this bioreactor technology in determining the amount of microalgae that could be produced. This would verify the numbers in the model at a pilot plant scale and would provide a significant step towards developing industrial size tanks.

An analysis would be done to determine if the heat transfer model was correct and investigate any heat loss that was not considered that could happen inside the tanks. This would allow for further development of the heat transfer model to improve the pilot plant for cold climate conditions and production of microalgae.

An investigation in the gas-lift top-lit bioreactor to determine if the microalgae has a higher growth production when using a top-lit source of light or by adding internal light tubes into the bioreactor. If algal production increases, then introducing plastic light tubes the length of the bioreactor into the pilot plant could further develop the novel bioreactor design. This would be an important result to address the assumption made about light requirements, and would provide another model input to increase accuracy. This, similar to the work proposed above, would be best done through the construction of a pilot facility.

The final design consideration is building an industrial scale tank that is considered a ‘plug and go’ system. A microalgae bioreactor production system housed in a transportable modular

(containerized) system that can be sized and attached to an exhaust of generator emissions. Such a technology will allow for small-scale CO_2 emitters, such as small northern community diesel generators, isolated mining camp generators, and biogas generators to beneficially reduce their carbon emissions while producing either biodiesel or high market valued nutraceutical.

References

Abdel-Shafy, H. I., & Mansour, M. S. M. (2018). Solid waste issue: Sources, composition, disposal, recycling, and valorization. *Egyptian Journal of Petroleum*, *27*(4), 1275–1290. https://doi.org/10.1016/j.ejpe.2018.07.003

Aghdam, E. F., Fredenslund, A. M., Chanton, J., Kjeldsen, P., & Scheutz, C. (2018). Determination of gas recovery efficiency at two Danish landfills by performing downwind methane measurements and stable carbon isotopic analysis. *Waste Management*, *73*, 220–229. https://doi.org/10.1016/j.wasman.2017.11.049

Aguilar-Virgen, Q., Taboada-González, P., Ojeda-Benítez, S., & Cruz-Sotelo, S. (2014). Power generation with biogas from municipal solid waste: Prediction of gas generation with in situ parameters. *Renewable and Sustainable Energy Reviews*, *30*, 412–419. https://doi.org/10.1016/j.rser.2013.10.014

Akita, K., & Yoshida, F. (1974). Bubble Size, Interfacial Area, and Liquid-Phase Mass Transfer Coefficient in Bubble Columns. *Industrial & Engineering Chemistry Process Design and Development*, *13*(1), 84–91. https://doi.org/10.1021/i260049a016

Al-Ghussain, L. (2019). Global warming: Review on driving forces and mitigation. *Environmental Progress & Sustainable Energy*, *38*(1), 13–21. https://doi.org/10.1002/ep.13041

Aracil, C., Haro, P., Fuentes-Cano, D., & Gómez-Barea, A. (2018). Implementation of waste-to-energy options in landfill-dominated countries: Economic evaluation and GHG impact. *Waste Management*, *76*, 443–456. https://doi.org/10.1016/j.wasman.2018.03.039

Arora, C., P. (2000). *Refrigeration and Air Conditioning* (Second addition). Tata McGraw-Hill Publishing Company Limited. https://books.google.ca/books?id=JyGeRoZIy80C&pg=PA11-IA102&lpg=PA11-IA102&dq=transmissivity+0.86&source=bl&ots=1nvHZBZ04d&sig=ACfU3U3667ijs2nwi_LCu0DwimMYO3-mpQ&hl=en&sa=X&ved=2ahUKEwj3sqbngeboAhVXbs0KHUzkBVkQ6AEwAnoECAsQLg#v=onepage&q=transmissivity%200.86&f=false

Australian Government. (2019). *Australian Energy Statistics, Table O Australian electricity generation, by fuel type, physical units* (Department of the Environment and Energy).

Ayodele, T. R., Alao, M. A., & Ogunjuyigbe, A. S. O. (2020). Effect of collection efficiency and oxidation factor on greenhouse gas emission and life cycle cost of landfill distributed energy generation. *Sustainable Cities and Society*, *52*, 101821. https://doi.org/10.1016/j.scs.2019.101821

Bade Shrestha, S. O., & Narayanan, G. (2008). Landfill gas with hydrogen addition – A fuel for SI engines. *Fuel*, *87*(17–18), 3616–3626. https://doi.org/10.1016/j.fuel.2008.06.019

Berger, S., Dun, S., Gavrelis, N., Helmick, J., Mann, J., Nickle, R., Perlman, G., Warner, S., Wilhelmi, J., Williams, R., & Zarus, G. (2001). *Landfill Gas Primer: An Overview for Environmental Health Professionals. Chapter 2: Landfill Gas Basics*. Agency for Toxic Substances and Disease Registry.

Bergman, T. L., & Incropera, F. P. (Eds.). (2011). *Fundamentals of heat and mass transfer* (7th ed). Wiley.

Bernard, O., & Rémond, B. (2012). Validation of a simple model accounting for light and temperature effect on microalgal growth. *Bioresource Technology*, *123*, 520–527. https://doi.org/10.1016/j.biortech.2012.07.022

Bhavaraju, S. M., Russel, T. W. F., & Blanch, H. W. (1978). The design of gas sparged devices for viscous liquid systems. *AIChE Journal*, *24*, 454–466.

Bounaceur, R., Lape, N., Roizard, D., Vallieres, C., & Favre, E. (2006). Membrane processes for post-combustion carbon dioxide capture: A parametric study. *Energy*, *31*(14), 2556–2570. https://doi.org/10.1016/j.energy.2005.10.038

Bove, R., & Lunghi, P. (2006). Electric power generation from landfill gas using traditional and innovative technologies. *Energy Conversion and Management*, *47*(11–12), 1391–1401. https://doi.org/10.1016/j.enconman.2005.08.017

Bowen, I. S. (1926). The Ratio of Heat Losses by Conduction and by Evaporation from any Water Surface. *Physical Review*, *27*(6), 779–787. https://doi.org/10.1103/PhysRev.27.779

Brander, M. (2012). *Greenhouse Gases, CO2, CO2e, and Carbon: What Do All These Terms Mean?* 3.

Broun, R., & Sattler, M. (2016). A comparison of greenhouse gas emissions and potential electricity recovery from conventional and bioreactor landfills. *Journal of Cleaner Production*, *112*, 2664–2673. https://doi.org/10.1016/j.jclepro.2015.10.010

Burger, D. B. (2017). *Power generation in Germany – assessment of 2017*. 46.

Chai, X., Tonjes, D. J., & Mahajan, D. (2016). Methane emissions as energy reservoir: Context, scope, causes and mitigation strategies. *Progress in Energy and Combustion Science*, *56*, 33–70. https://doi.org/10.1016/j.pecs.2016.05.001

Chiemchaisri, C., Chiemchaisri, W., Kumar, S., & Hettiaratchi, J. P. A. (2007). Solid waste characteristics and their relationship to gas production in tropical landfill. *Environmental Monitoring and Assessment*, *135*(1–3), 41–48. https://doi.org/10.1007/s10661-007-9706-2

Chisti, Y. (2007). Biodiesel from microalgae. *Biotechnology Advances*, *25*(3), 294–306. https://doi.org/10.1016/j.biotechadv.2007.02.001

Choi, Y., Song, D., Seo, D., & Kim, J. (2018). Analysis of the variable heat exchange efficiency of heat recovery ventilators and the associated heating energy demand. *Energy and Buildings*, *172*, 152–158. https://doi.org/10.1016/j.enbuild.2018.04.066

Colpan, C. O., Dincer, I., & Hamdullahpur, F. (2010). Reducing Greenhouse Gas Emissions from a Landfill Site Using Various Thermal Systems. In I. Dincer, A. Hepbasli, A. Midilli, & T. H. Karakoc (Eds.), *Global Warming* (pp. 161–178). Springer US. https://doi.org/10.1007/978-1-4419-1017-2_8

Cook, S., & Educator, S. W. (2015). *Waste Diversion Plan*. 87.

Cucchiella, F., D'Adamo, I., Gastaldi, M., & Miliacca, M. (2018). A profitability analysis of small-scale plants for biomethane injection into the gas grid. *Journal of Cleaner Production*, *184*, 179–187.

Curley, R. (2018, May 27). *Sanitary Landfill*. Encyclopedia Britannica. https://www.britannica.com/technology/sanitary-landfill

Danthurebandara, M., Passel, S. V., Nelen, D., Tielemans, Y., & Acker, K. V. (2012). *ENVIRONMENTAL AND SOCIO-ECONOMIC IMPACTS OF LANDFILLS*. 13.

Darrow, K., Tidball, R., Wang, J., & Hampson, A. (2015). *Catalog of CHP Technologies: Section 2. Technology Characterization-Reciprocating Internal Combustion Engines*. United States Environmental Protection Agency and the U.S. Department of Energy. https://www.epa.gov/sites/production/files/2015-07/documents/catalog_of_chp_technologies_section_2._technology_characterization_-_reciprocating_internal_combustion_engines.pdf

Davison, I. (1991). Environmental effects on algal photosynthesis: Temperature. *J Phycol*, *27*, 2–28.

Davison, & Thambimuthu. (2009). An overview of technologies and costs of carbon dioxide capture in power generation. *Proceedings of the Institution of Mechanical Engineers, Part A: Journal of Power and Energy*, *223*(3), 201–212. https://doi.org/10.1243/09576509JPE625

Desjardins, S., Laamanen, C. A., Basiliko, N., & Scott, J. A. (2020). Utilization of lipid-extracted biomass (LEB) to improve the economic feasibility of biodiesel production from green microalgae. *Enviornmental Reviews*, *28*(3). https://doi.org/10.1139/er-2020-0004

Douskova, I., Doucha, J., Livansky, K., Machat, J., Novak, P., Umysova, D., Zachleder, V., & Vitova, M. (2009). Simultaneous flue gas bioremediation and reduction of microalgal

biomass production costs. *Applied Microbiology and Biotechnology*, *82*(1), 179–185. https://doi.org/10.1007/s00253-008-1811-9

Dudek, J., Klimek, P., Kolodziejak, G., Niemczewska, J., & Zaleska-Bartosz, J. (2010). *Landfill Gas Energy Technologies*. Oil and Gas Institute in Krakow.

El Zein, A. (2015). The Effect of Greenhouse Gases on Earth's Temperature. *International Journal of Environmental Monitoring and Analysis*, *3*(2), 74. https://doi.org/10.11648/j.ijema.20150302.16

Eloka-Eboka, A. C., & Inambao, F. L. (2017). Effects of CO 2 sequestration on lipid and biomass productivity in microalgal biomass production. *Applied Energy*, *195*, 1100–1111. https://doi.org/10.1016/j.apenergy.2017.03.071

Environment and Climate Change Canada. (2019). *National Inventory Report 1990-2017: Greenhouse Gas Sources and Sinks in Canada. Executive Summary* [Annual]. Pollutant Inventories and Reporting Division. https://www.canada.ca/content/dam/eccc/documents/pdf/climate-change/emissions-inventories-reporting/nir-executive-summary/National%20Inventory%20Report%20Executive%20Summary%202018.pdf

Environmental Protection Agency. (2017). *Landfill Methane Outreach Program: LFG Energy Project Development Handbook*. 98.

Fei, F., Wen, Z., & De Clercq, D. (2019). Spatio-temporal estimation of landfill gas energy potential: A case study in China. *Renewable and Sustainable Energy Reviews*, *103*, 217–226. https://doi.org/10.1016/j.rser.2018.12.036

Froiland Jensen, J. E., & Pipatti, R. (2001). *CH4 EMISSIONS FROM SOLID WASTE DISPOSAL* (Good Practice Guidance and Uncertainty Management in National Greenhouse Gas Inventories). Internal Governmental Panel on Climate Change. https://www.ipcc-nggip.iges.or.jp/public/gp/english/

Ganguly, A., & Ghosh, S. (2009). Model development and experimental validation of a floriculture greenhouse under natural ventilation. *Energy and Buildings*, *41*(5), 521–527. https://doi.org/10.1016/j.enbuild.2008.11.021

Gewald, D., Siokos, K., Karellas, S., & Spliethoff, H. (2012). Waste heat recovery from a landfill gas-fired power plant. *Renewable and Sustainable Energy Reviews*, *16*(4), 1779–1789. https://doi.org/10.1016/j.rser.2012.01.036

Goiris, K., Muylaert, K., Fraeye, I., Foubert, I., De Brabanter, J., & De Cooman, L. (2012). Antioxidant potential of microalgae in relation to their phenolic and carotenoid content. *Journal of Applied Phycology*, *24*(6), 1477–1486.

Goldsmith, C. D., Chanton, J., Abichou, T., Swan, N., Green, R., & Hater, G. (2012). Methane emissions from 20 landfills across the United States using vertical radial plume mapping. *Journal of the Air & Waste Management Association*, *62*(2), 183–197. https://doi.org/10.1080/10473289.2011.639480

Goswami, R., Chattopadhyay, P., Shome, A., Banerjee, S. N., Chakraborty, A. K., Mathew, A. K., & Chaudhury, S. (2016). An overview of physico-chemical mechanisms of biogas production by microbial communities: A step towards sustainable waste management. *3 Biotech*, *6*(1). https://doi.org/10.1007/s13205-016-0395-9

Government of Canada. (2017). *CANADA'S 7TH NATIONAL COMMUNICATION AND 3RD BIENNIAL REPORT*. Environment and Climate Change Canada. http://doi.wiley.com/10.1111/j.1467-9388.1992.tb00046.x

Government of Canada. (2019a). *Canada's Renewable Power Landscape 2017-Energy Market Analysis*. Canada Energy Regulator. https://www.cer-rec.gc.ca/nrg/sttstc/lctrct/rprt/2017cndrnwblpwr/ghgmssn-eng.html?=undefined&wbdisable=false

Government of Canada. (2019b). *Global Warming Potentials*. https://www.canada.ca/en/environment-climate-change/services/climate-change/greenhouse-gas-emissions/quantification-guidance/global-warming-potentials.html

Government of Canada. (2019c, December 4). *Canadian Climate Normals 1981-2010 Station Data*. Climate Normals & Averages. https://climate.weather.gc.ca/climate_normals/results_1981_2010_e.html?stnID=4132&autofwd=1

Government of Ontario. (2019, March 22). *Landfill Standards: A guideline on the regulatory and approval requirements for new/expanding land* [Environment and energy]. Landfill Standards: A Guideline on the Regulatory and Approval Requirements for New/Expanding Land. https://www.ontario.ca/page/landfill-standards-guideline-regulatory-and-approval-requirements-newexpanding-land

Grossule, V., Morello, L., Cossu, R., & Lavagnolo, M. C. (2018). BIOREACTOR LANDFILLS: COMPARISON AND KINETICS OF THE DIFFERENT SYSTEMS. *Detritus*, *In Press* (1), 1. https://doi.org/10.31025/2611-4135/2018.13703

Guermoud, N., Ouadjnia, F., Abdelmalek, F., Taleb, F., & addou, A. (2009). Municipal solid waste in Mostaganem city (Western Algeria). *Waste Management*, *29*(2), 896–902. https://doi.org/10.1016/j.wasman.2008.03.027

Gupta, S., Biruduganti, M., & Sekar, R. (2012). Natural Gas Fired Reciprocating Engines for Power Generation: Concerns and Recent Advances. In *Natural Gas—Extraction to End Use*. InTech. https://doi.org/10.5772/45992

Hincapie, E., & Stuart, B. J. (2015). Design, Construction, and Validation of an Internally Lit Air-Lift Photobioreactor for Growing Algae. *Frontiers in Energy Research*, *2*. https://doi.org/10.3389/fenrg.2014.00065

Holm-Nielsen, J. B., Al Seadi, T., & Oleskowicz-Popiel, P. (2009). The future of anaerobic digestion and biogas utilization. *Bioresource Technology*, *100*(22), 5478–5484. https://doi.org/10.1016/j.biortech.2008.12.046

Hoo, P. Y., Hashim, H., & Ho, W. S. (2018). Opportunities and challenges: Landfill gas to biomethane injection into natural gas distribution grid through pipeline. *Journal of Cleaner Production*, *175*, 409–419. https://doi.org/10.1016/j.jclepro.2017.11.193

Jaramillo, P., & Matthews, H. S. (2005). Landfill-Gas-to-Energy Projects: Analysis of Net Private and Social Benefits. *Environmental Science & Technology*, *39*(19), 7365–7373. https://doi.org/10.1021/es050633j

Kang, Y. T., Nagano, T., & Kashiwagi, T. (2002). Visualization of bubble behavior and bubble diameter correlation for NH3–H2O bubble absorption. *International Journal of Refrigeration*, *25*(1), 127–135. https://doi.org/10.1016/S0140-7007(00)00045-1

Karakurt, I., Aydin, G., & Aydiner, K. (2012). Sources and mitigation of methane emissions by sectors: A critical review. *Renewable Energy*, *39*(1), 40–48. https://doi.org/10.1016/j.renene.2011.09.006

Karanjekar, R. V., Bhatt, A., Altouqui, S., Jangikhatoonabad, N., Durai, V., Sattler, M. L., Hossain, M. D. S., & Chen, V. (2015). Estimating methane emissions from landfills based on rainfall, ambient temperature, and waste composition: The CLEEN model. *Waste Management*, *46*, 389–398. https://doi.org/10.1016/j.wasman.2015.07.030

Kaza, S., Yao, L., Bhada-Tata, P., & Van Woerden, F. (2018). *What a Waste 2.0. A Global Snapshot of Solid Waste Management to 2050*. World Bank Group.

Keffer, J. E., & Kleinheinz, G. T. (2002). Use of Chlorella vulgaris for CO 2 mitigation in a photobioreactor. *Journal of Industrial Microbiology and Biotechnology*, *29*(5), 275–280. https://doi.org/10.1038/sj.jim.7000313

Kumar, K., Dasgupta, C. N., Nayak, B., Lindblad, P., & Das, D. (2011). Development of suitable photobioreactors for CO2 sequestration addressing global warming using green algae and cyanobacteria. *Bioresource Technology*, *102*(8), 4945–4953. https://doi.org/10.1016/j.biortech.2011.01.054

Kweku, D., Bismark, O., Maxwell, A., Desmond, K., Danso, K., Oti-Mensah, E., Quachie, A., & Adormaa, B. (2018). Greenhouse Effect: Greenhouse Gases and Their Impact on Global

Warming. *Journal of Scientific Research and Reports*, *17*(6), 1–9. https://doi.org/10.9734/JSRR/2017/39630

Laamanen, C. A., Shang, H., Ross, G. M., & Scott, J. A. (2014). A model for utilizing industrial off-gas to support microalgae cultivation for biodiesel in cold climates. *Energy Conversion and Management*, *88*, 476–483. https://doi.org/10.1016/j.enconman.2014.08.047

Laamanen, C. A., Shang, H., Ross, G. M., & Scott, J. A. (2017). Smelter off-gas waste heat and carbon dioxide sequestration to promote production of biodiesel. *CIM Journal*, *8*(3), 1–12.

Lee, Lau, P., & Teo, T. (2014). *Sustainable Application of Reciprocating Gas Engines Operating On Alternative Fuels*. 17.

Lee, U., Han, J., & Wang, M. (2017). Evaluation of landfill gas emissions from municipal solid waste landfills for the life-cycle analysis of waste-to-energy pathways. *Journal of Cleaner Production*, *166*, 335–342. https://doi.org/10.1016/j.jclepro.2017.08.016

Leone, J. (2007). *The Effects of Atmospheric Pressure Changes on Landfill Gas Collection Efficiency and Quality*. 56.

Loken, M. (2013). *Recovery of waste heat from pyrometallurgical facilities for use in microalgae production.* [Masters Dissertation]. Laurentian University.

Lombardi, L., Carnevale, E., & Corti, A. (2006). Greenhouse effect reduction and energy recovery from waste landfill. *Energy*, *31*(15), 3208–3219. https://doi.org/10.1016/j.energy.2006.03.034

Lou, X. F., & Nair, J. (2009). The impact of landfilling and composting on greenhouse gas emissions – A review. *Bioresource Technology*, *100*(16), 3792–3798. https://doi.org/10.1016/j.biortech.2008.12.006

Manfredi, S. (2009). *Environmental Assessment of Solid Waste Landfilling in a Life Cycle Perspective (LCA model EASEWASTE)*. Technical University of Denmark.

Manfredi, S., Tonini, D., Christensen, T. H., & Scharff, H. (2009). Landfilling of waste: Accounting of greenhouse gases and global warming contributions. *Waste Management & Research*, *27*(8), 825–836. https://doi.org/10.1177/0734242X09348529

Matsufuji, K. (2007). *Caution for Application of "Fukuoka Method" (Semi-Aerobic Landfill Technology)*. Japanese International Cooperation Agency.

McIntyre, J., Berg, B., Seto, H., & Borchardt, S. (2011). *Comparison of Lifecycle Greenhouse Gas Emissions of Various Electricity Generation Sources*.

Mohsen, R. A., & Abbassi, B. (2020). Prediction of greenhouse gas emissions from Ontario's solid waste landfills using fuzzy logic based model. *Waste Management*, *102*, 743–750. https://doi.org/10.1016/j.wasman.2019.11.035

Murphy, J. D., & McKeogh, E. (2004). Technical, economic and environmental analysis of energy production from municipal solid waste. *Renewable Energy*, *29*(7), 1043–1057. https://doi.org/10.1016/j.renene.2003.12.002

Nath, S. S., & Bolte, J. P. (1998). A water budget model for pond aquaculture. *Aquacultural Engineering*, *18*(3), 175–188. https://doi.org/10.1016/S0144-8609(98)00029-6

Natividad Pérez-Camacho, M., Curry, R., & Cromie, T. (2019). Life cycle environmental impacts of biogas production and utilisation substituting for grid electricity, natural gas grid and transport fuels. *Waste Management*, *95*, 90–101. https://doi.org/10.1016/j.wasman.2019.05.045

Niemczewska, J. (2012). *Characteristics of utilization of biogas technology*. *68*(5), 293–297.

Nwachukwu, A. N., & Diya, A. W. (2013). Estimation of emissions of nonmethane organic compounds from a closed landfill site using a landfill gas emission model. *International Journal of Energy and Environment*, *4*(1), 8.

Nwaokorie, K. J., Bareither, C. A., Mantell, S. C., & Leclaire, D. J. (2018). The influence of moisture enhancement on landfill gas generation in a full-scale landfill. *Waste Management*, *79*, 647–657. https://doi.org/10.1016/j.wasman.2018.08.036

Ontario Power Generation Inc. (2016). *GREENHOUSE GAS EMISSIONS ASSOCIATED WITH VARIOUS METHODS OF POWER GENERATION IN ONTARIO*.

Packer, M. (2009). Algal capture of carbon dioxide; biomass generation as a tool for greenhouse gas mitigation with reference to New Zealand energy strategy and policy. *Energy Policy*, *37*(9), 3428–3437. https://doi.org/10.1016/j.enpol.2008.12.025

Pankratz, S., Oyedun, A. O., Zhang, X., & Kumar, A. (2017). Algae production platforms for Canada's northern climate. *Renewable and Sustainable Energy Reviews*, *80*, 109–120. https://doi.org/10.1016/j.rser.2017.05.220

Paolini, V., Petracchini, F., Segreto, M., Tomassetti, L., Naja, N., & Cecinato, A. (2018). Environmental impact of biogas: A short review of current knowledge. *Journal of Environmental Science and Health, Part A*, *53*(10), 899–906. https://doi.org/10.1080/10934529.2018.1459076

Pierson, R. (2013). *Fact Sheet: Landfill Methane*. https://www.eesi.org/files/FactSheet_Landfill-Methane_042613.pdf

Pieters, J. G., & Deltour, J. M. (1999). *MODELLING SOLAR ENERGY INPUT IN GREENHOUSES*. 12.

Pires, J. C. M., Alvim-Ferraz, M. C. M., Martins, F. G., & Simões, M. (2012). Carbon dioxide capture from flue gases using microalgae: Engineering aspects and biorefinery concept. *Renewable and Sustainable Energy Reviews*, *16*(5), 3043–3053. https://doi.org/10.1016/j.rser.2012.02.055

Purmessur, B., & Surroop, D. (2019). Power generation using landfill gas generated from new cell at the existing landfill site. *Journal of Environmental Chemical Engineering*, *7*(3), 103060. https://doi.org/10.1016/j.jece.2019.103060

Rajaram, V., Siddiqui, F., & Khan, M. (2011). *From Landfill Gas to Energy: Technologies and Challenges*.

Ramanan, R., Kannan, K., Deshkar, A., Yadav, R., & Chakrabarti, T. (2010). Enhanced algal CO2 sequestration through calcite deposition by Chlorella sp. And Spirulina platensis in a mini-raceway pond. *Bioresource Technology*, *101*(8), 2616–2622. https://doi.org/10.1016/j.biortech.2009.10.061

Rawat, I. (2013). Biodiesel from microalgae: A critical evaluation from laboratory to large scale production. *Applied Energy*, 24.

Reinhart, D. R., & Barlaz, M. A. (2010). *Landfill Gas Management: A Roadmap for EREF Directed Research*. 158.

Reinhart, D. R., McCreanor, P., & Townsend, T. (2002). *The bioreactor landfill: Its status and future*. *20*, 172–186.

Robert Troxler, & Thackston, E. (1977). Predicting the Rate of Warming of Rivers below Hydroelectric Installations. *Water Pollution Control Federation*, *49*(8), 1902–1912.

Sayre, R. (2010). Microalgae: The Potential for Carbon Capture. *BioScience*, *60*(9), 722–727. https://doi.org/10.1525/bio.2010.60.9.9

Senhorinho, G. N. A., Ross, G. M., & Scott, J. A. (2015). Cyanobacteria and eukaryotic microalgae as potential sources of antibiotics. *Phycologia*, *54*(3), 271–282. https://doi.org/10.2216/14-092.1

Seyed Hosseini, N., Shang, H., Ross, G. M., & Scott, J. A. (2015). Microalgae cultivation in a novel top-lit gas-lift open bioreactor. *Bioresource Technology*, *192*, 432–440. https://doi.org/10.1016/j.biortech.2015.05.092

Seyed Hosseini, N., Shang, H., Ross, G. M., & Scott, J. A. (2016). Comparative analysis of top-lit bubble column and gas-lift bioreactors for microalgae-sourced biodiesel production. *Energy Conversion and Management*, *130*, 230–239. https://doi.org/10.1016/j.enconman.2016.10.048

Seyed Hosseini, N., Shang, H., & Scott, J. A. (2018). Biosequestration of industrial off-gas CO 2 for enhanced lipid productivity in open microalgae cultivation systems. *Renewable and Sustainable Energy Reviews*, *92*, 458–469. https://doi.org/10.1016/j.rser.2018.04.086

Shang, H., Scott, J. A., Shepherd, S. H., & Ross, G. M. (2010). A dynamic thermal model for heating microalgae incubator ponds using off-gas. *Chemical Engineering Science*, *65*(16), 4591–4597. https://doi.org/10.1016/j.ces.2010.04.042

Singh, U. B., & Ahluwalia, A. S. (2013). Microalgae: A promising tool for carbon sequestration. *Mitigation and Adaptation Strategies for Global Change*, *18*(1), 73–95. https://doi.org/10.1007/s11027-012-9393-3

Singleton, M., Williams, M., Frankowski, C., & Allen, G. (2017). *Sustainable Buildings Canada 33 Longboat Avenue Toronto, Ontario M5A 4C9 mike-singleton@rogers.ca*. 18.

Sun, X.-M., Ren, L.-J., Zhao, Q.-Y., Ji, X.-J., & Huang, H. (2018). Microalgae for the production of lipid and carotenoids: A review with focus on stress regulation and adaptation. *Biotechnology for Biofuels*, *11*(1), 272. https://doi.org/10.1186/s13068-018-1275-9

Tang, D., Han, W., Li, P., Miao, X., & Zhong, J. (2011). CO2 biofixation and fatty acid composition of Scenedesmus obliquus and Chlorella pyrenoidosa in response to different CO2 levels. *Bioresource Technology*, *102*(3), 3071–3076. https://doi.org/10.1016/j.biortech.2010.10.047

Tsatsarelis, T., Karagiannidis, A., Moussiopoulos, N., & Perkoulidis, G. (2006). *TECHNOLOGIES OF LANDFILL GAS MANAGEMENT AND UTILIZATION*. 8.

U.S Department of Energy. (2019, November 1). *Combined Heat and Power Technology Fact Sheet Series* [Energy Efficiency and Renewable Energy]. https://www.energy.gov/sites/prod/files/2016/09/f33/CHP-Recip%20Engines.pdf

USEPA. (1990). *Landfill Air Emissions Estimation Model User's Manual* (EPA-600/8-90-085a; Control Technology Center).

USEPA. (2008). Clean Energy Strategies for Local Governments: 7.4 Landfill Methane Utilization. In *Clean Energy Strategies for Local Governments*. https://www.energy.gov/sites/prod/files/2014/05/f15/7.4_landfill_methane_utilization.pdf

USEPA. (2012). *Global Anthropogenic Non-CO2 Greenhouse Gas Emissions: 1990-2030*. Office of Atmospheric Programs: Climate Change Division. https://www.epa.gov/sites/production/files/2016-08/documents/epa_global_nonco2_projections_dec2012.pdf

USEPA. (2018a). *Inventory of U.S Greenhouse Gas Emissions and Sinks: 1990-2016.*

USEPA. (2018b, October 5). *Basic Information about Landfill Gas*. United States Environmental Protection Agency. https://www.epa.gov/lmop/basic-information-about-landfill-gas

Vu, H. L., Ng, K. T. W., & Richter, A. (2017). Optimization of first order decay gas generation model parameters for landfills located in cold semi-arid climates. *Waste Management*, *69*, 315–324. https://doi.org/10.1016/j.wasman.2017.08.028

Weyer, K. M., Bush, D. R., Darzins, A., & Willson, B. D. (2010). Theoretical Maximum Algal Oil Production. *BioEnergy Research*, *3*(2), 204–213. https://doi.org/10.1007/s12155-009-9046-x

Woolley, J., Harrington, C., & Modera, M. (2011). Swimming pools as heat sinks for air conditioners: Model design and experimental validation for natural thermal behavior of the pool. *Building and Environment*, *46*(1), 187–195. https://doi.org/10.1016/j.buildenv.2010.07.014

World Bank Group. (2019). *Guidance Fact Sheet: Landfill Design*.

Yechiel, A., & Shevah, Y. (2016). Optimization of energy generation using landfill biogas. *Journal of Energy Storage*, *7*, 93–98. https://doi.org/10.1016/j.est.2016.05.002

Zhang, C., Guo, Y., Wang, X., & Chen, S. (2019). Temporal and spatial variation of greenhouse gas emissions from a limited-controlled landfill site. *Environment International*, *127*, 387–394. https://doi.org/10.1016/j.envint.2019.03.052

Zhang, L., & Shoji, M. (2001). Aperiodic bubble formation from a submerged oriÿce. *Chemical Engineering Science*, 11.

Zhao, B., & Su, Y. (2014). Process effect of microalgal-carbon dioxide fixation and biomass production: A review. *Renewable and Sustainable Energy Reviews*, *31*, 121–132. https://doi.org/10.1016/j.rser.2013.11.054

Zhao, R., Xi, B., Liu, Y., Su, J., & Liu, S. (2017). Economic potential of leachate evaporation by using landfill gas: A system dynamics approach. *Resources, Conservation and Recycling*, *124*, 74–84. https://doi.org/10.1016/j.resconrec.2017.04.010

Znad, H., Naderi, G., Ang, H. M., & Tade, M. O. (2012). CO2 Biomitigation and Biofuel Production Using Microalgae: Photobioreactors Developments and Future Directions. In Z. Nawaz (Ed.), *Advances in Chemical Engineering*. InTech. https://doi.org/10.5772/32568

Zulfequar Ahmad Khan, Md. (2017). Causes and Consequences of Greenhouse Effect & Its Catastrophic Problems for Earth. *International Journal of Sustainability Management and Information Technologies*, *3*(4), 34. https://doi.org/10.11648/j.ijsmit.20170304.11

Appendices

Appendix A: Daily data samples from the Sudbury landfill from January 2018-March 2020

Date	Engine CH_4 (%)	Gas Flow (Nm^3/hr)	Intake Air (Nm^3/hr)	Landtec CH_4 (%)	Landtec CO_2 (%)	Landtec O_2 (%)	Landtec Balance gas (%)	Outside Temperature (˚C)
January 1, 2018	50.5	678	5300	60.3	34.9	0.3	4.4	0
January 2, 2018	52.42	604	5180	63.6	36.1	0.1	0.2	0
January 3, 2018	51.95	625	5214	62.6	35.8	0.1	1.5	0
January 4, 2018	51.11	625	5614	61.3	35.4	0	3.3	0
January 5, 2018	51.47	660	5698	62.2	36.8	0.2	1.8	0
January 6, 2018	52	680	5739	63.7	35.3	0.1	0.7	0
January 8, 2018	52.89	675	5877	63.1	36.8	0	0.1	0
January 9, 2018	46.89	675	5679	55.8	34.3	0.3	9.6	0
January 10, 2018	49.97	680	5812	61.2	35.3	0.1	3.4	-9
January 11, 2018	50.92	707	5826	61.3	35.8	0.1	2.8	6
January 12, 2018	50.97	708	5873	59.6	35.2	0.3	4.9	-14
January 13, 2018	49.97	704.5	5620	59.2	34.5	0.4	5.6	-27
January 14, 2018	49.97	725.5	5680	59.6	34.3	0.4	5.6	-16
January 15, 2018	51.45	689	5879	62.1	35	0.2	2.7	-10
January 16, 2018	51.92	657	5675	63.5	35.4	0.2	0.9	-16
January 17, 2018	52.89	673	5821	63.6	36.1	0.1	0.2	-12
January 18, 2018	52.89	663	5818	63.4	36.2	0.2	0.1	-6.1
January 19, 2018	51.47	710	6244	63.4	36.3	0.2	0.1	-1
January 20, 2018	49.97	740	5935	58.9	35.6	0.4	4.9	-1.3
January 21, 2018	48.5	750	5890	57.5	35.4	0.5	7.3	-3.4
January 22, 2018	47.97	742	5987	57.4	34.2	0.3	8.1	-7
January 23, 2018	52.42	721	6085	63.4	36.2	0.1	0.3	-7
January 24, 2018	46.44	747	5662	54.4	33.4	0.5	11.7	-17

January 25, 2018	48	739	5641	57	33.8	0.3	8.9	-17
January 26, 2018	48.94	725	5775	58.7	34.2	0.3	6.8	-8
January 27, 2018	51.95	695	6002	63.7	35.8	0.2	0.3	7
January 28, 2018	46.89	744	5545	54.8	33.4	0.6	11.3	-4
January 29, 2018	48.94	692	5513	58.8	34.3	0.2	6.8	-19
January 30, 2018	51.95	682	5624	62.2	35.4	0.2	2.2	-22
January 31, 2018	53.39	623	5556	62.9	37	0	0.1	-15
February 1, 2018	51.92	662	5667	61.5	35.5	0.4	2.6	-5
February 2, 2018	49.97	674	5498	59.7	34.2	0.4	5.7	-26.6
February 3, 2018	49.97	700	5620	59.3	34.3	0.6	5.5	-23
February 4, 2018	49.47	727	5899	59.1	34.3	0.7	6	-14
February 5, 2018	49.5	736	5736	58.5	34.5	0.4	6.6	-21
February 6, 2018	47.97	733	5616	56.4	33.8	0.6	9.2	-18
February 7, 2018	49.97	688	5743	60.6	34.7	0.2	4.5	-18
February 8, 2018	47.97	715	5706	58.2	33.9	0.4	7.5	-21
February 9, 2018	48.5	694	5490	58.3	33.9	0.5	7.1	-21.7
February 10, 2018	49	715	5723	59.2	34.3	0.5	6	-20
February 11, 2018	49.47	720	5686	60.7	34.9	0.3	4	-17
February 12, 2018	46.02	747	5421	52.4	32.5	0.8	14.2	-12.6
February 13, 2018	46.89	702	5355	56.2	33.2	0.4	10.2	-24
February 14, 2018	51.47	689	5825	62.4	35.3	0.2	2.1	-5
February 15, 2018	50.92	716	5922	62.8	35.8	0.2	1.2	1
February 16, 2018	46.89	731	5563	55.2	33.9	0.5	10.4	-12
February 17, 2018	48.53	683	5437	58.6	34.4	0.3	6.6	-14.3
February 18, 2018	47.44	735	5430	53.7	33.1	0.6	12.7	-6
February 19, 2018	49	735	5749	57.1	34	0.4	8.3	-1.5
February 20, 2018	48.53	688	5680	59.2	34.6	0.2	6	-10

February 21, 2018	46	713	5576	53.7	33.1	0.5	12.7	0
February 22, 2018	47.41	731	5638	54.6	32.9	0.4	12.1	-16
February 23, 2018	54.42	697	5900	64	35.8	0	0.2	-5
February 24, 2018	49.97	751	5800	57	34.3	0.4	8.5	-1
February 25, 2018	54.89	720	6230	62.8	37	0.1	0.2	-0.5
February 26, 2018	49	713	5718	57.2	33.8	0.7	8.3	-6
February 28, 2018	51.45	732	6024	60.8	35.2	0.3	3.7	0
March 1, 2018	49.5	737	5717	59.7	36	0.3	4	-2
March 2, 2018	48.94	740	5887	54.6	34.2	0.5	10.7	-5
March 5, 2018	50.97	726	5676	60.4	34.5	0.2	4.9	-12
March 6, 2018	52.92	713	6172	63.1	35.1	0.2	1.6	-7
March 7, 2018	51.97	733	6273	61.2	35.8	0.3	2.7	-3
March 8, 2018	50.47	727	6012	59.2	34.9	0.4	5.5	-2
March 9, 2018	49.97	731	6000	58.7	34.7	0.4	6.2	-3
March 12, 2018	50.97	737	5913	59	34.3	0.4	6.3	-8
March 13, 2018	49.5	727	5884	58.1	34.2	0.4	7.3	-6
March 14, 2018	50.47	721	5784	58.9	34.4	0.4	6.3	-7
March 15, 2018	49.97	720	5855	58.1	34.3	0.07	6.5	-8.2
March 16, 2018	46.89	760	5788	54	32.8	0.8	12.4	-12.9
March 18, 2018	48.53	727	5809	56.2	33.7	0.7	9.3	-10
March 19, 2018	47.41	727	5698	54.9	33.1	0.6	11.4	-15
March 20, 2018	47.97	750	5758	56.1	33.3	0.5	10.1	-14
March 21, 2018	48.94	731	5889	*	*	*	*	-12
March 23, 2018	51.95	713	6155	*	*	*	*	-8
March 24, 2018	51.95	727	6000	*	*	*	*	-14
March 25, 2018	48	750	4749	*	*	*	*	-14
March 26, 2018	48.94	763	5948	*	*	*	*	-9

March 27, 2018	51.92	719	6210	*	*	*	*	0
March 28, 2018	48.53	753	5930	*	*	*	*	1
March 29, 2018	48.94	753	6059	*	*	*	*	-2
March 30, 2018	49	732	5630	*	*	*	*	-5
March 31, 2018	49	707	5707	*	*	*	*	-3
April 1, 2018	46.89	740	5460	*	*	*	*	-8.3
April 2, 2018	47.97	723	5588	*	*	*	*	-16
April 3, 2018	47.41	729	5574	*	*	*	*	-3
April 4, 2018	51.95	723	5812	*	*	*	*	-8
April 5, 2018	46.02	723	5341	*	*	*	*	-19
April 6, 2018	49.97	728	247	*	*	*	*	-7
April 7, 2018	46.89	729	5390	*	*	*	*	-7
April 8, 2018	46.89	729	5390	*	*	*	*	-12
April 9, 2018	46.44	744	243	*	*	*	*	-9
April 10, 2018	46.89	741	245	*	*	*	*	-7
April 11, 2018	48.39	723	5980	49.7	35.9	2.3	12	-5
April 12, 2018	48.94	755	6067	50.2	35.8	1.5	12.5	-6
April 13, 2018	46.44	733	5683	46.1	33	1.6	19.3	-5
April 14, 2018	53.89	720	6134	54.2	34.5	0.7	10.6	-7
April 15, 2018	52.92	724	6120	53.6	34.1	0.7	11.6	-8
April 16, 2018	54.87	710	6258	56.7	35.6	0.5	7.1	-3
April 17, 2018	55.73	682	6499	58.9	36.8	0.3	3.9	0
April 18, 2018	52.45	732	6385	52.5	34.8	0.7	12	0
April 19, 2018	49.97	743	6300	50.3	34.1	0.8	15.8	-3
April 20, 2018	48	760	6108	47.6	32.8	1	18.6	-3
April 21, 2018	48.94	774	6075	48.4	32.8	1	17.2	-3
April 22, 2018	48.94	774	6200	47.7	32.5	1.1	18.7	6

April 23, 2018	48.94	774	6260	48	32.7	1	18.3	-3
April 24, 2018	49.22	763	6350	50.1	33.6	0.7	15.6	1
April 25, 2018	49.97	750	6310	49.5	33.3	0.9	16.4	2.5
April 26, 2018	49.94	747	6154	50	33.5	0.8	15.7	-1
April 27, 2018	49.94	760	6175	49.8	33.7	0.9	15.6	1
April 28, 2018	48	765	6271.5	46.8	32.6	1.3	19.6	-3.1
April 29, 2018	46.02	824	6160	44.1	31.4	1.4	23.2	-2.9
April 30, 2018	46.89	790	6200	45.8	32.3	1.1	20.8	1
May 1, 2018	46.89	773	6065	46.9	33	1.4	18.7	6
May 2, 2018	48.94	700	5959	48	33.1	1.3	17.7	11
May 3, 2018	49.94	750	6321	50.4	33.1	1.1	15.5	8
May 4, 2018	49.94	766	6261	50.3	33.5	1.1	15.1	5
May 5, 2018	47.97	751	6084	*	*	*	*	8
May 6, 2018	46	782	6110	*	*	*	*	8
May 7, 2018	44.91	743	5717	43.7	31.3	2	22.8	5
May 8, 2018	46.89	744	5685	46	32	1.8	20.2	7
May 9, 2018	48	745	5733	46.8	32	1.7	19.3	8
May 10, 2018	51.95	681	5673	51.7	34.2	1.1	13	12
May 11, 2018	44.91	734	5396	44.1	31.4	2	22.4	2
May 12, 2018	46.89	700	5240	46.2	31.9	1.9	20	11
May 13, 2018	47.44	729	5402	46.5	32	1.9	19.2	8.1
May 14, 2018	49.97	688	5510	49	32.9	21.6	16.5	10
May 15, 2018	46.89	744	5510	46.1	31.6	2.1	20.2	10
May 16, 2018	47.41	749	5510	47	32	1.7	19.3	7
May 17, 2018	44.91	779	5600	43.2	30.4	2.4	24	5
May 18, 2018	46	752	5535	44.4	30.8	2.2	22.6	5
May 19, 2018	48.53	733	5560	*	*	*	*	13

May 20, 2018	46.02	713	5264	*	*	*	*	8
May 21, 2018	46.89	738	5174	*	*	*	*	12
May 22, 2018	47.97	743	5669	47.7	32	1.7	18.6	12
May 23, 2018	48.5	749	5672	45.2	31	2.1	21.7	13
May 24, 2018	47.97	749	5664	46	31.2	2	20.8	6
May 25, 2018	48.94	670	5416	49.1	32.5	1.5	16.9	19
May 26, 2018	47.44	736	5723	46.7	31.8	2	19.6	17
May 27, 2018	46.89	784	5842.6	46.1	31.5	2.1	20.3	16.2
May 28, 2018	46	708	5037	45.9	31.4	2	20.7	17
May 29, 2018	46.89	723	5540	45.3	31	2.1	21.6	14
May 30, 2018	47.41	789	5635	46	31.3	2	20.7	15
May 31, 2018	50.47	694	5126	50.7	33.5	1.3	14.5	21
June 1, 2018	48.53	720	5624	45.6	31.4	2	21	14
June 2, 2018	50.47	730	5764	*	*	*	*	11
June 3, 2018	52.89	700	5900	53.9	35.1	0.7	10.7	21
June 4, 2018	52.89	689	6197	54	35.2	0.7	10.1	14
June 5, 2018	50.92	770	6400	50.6	34.4	0.8	14.2	9
June 6, 2018	49.47	765	6171	49.1	33.9	0.8	16.2	11
June 7, 2018	48.94	778	6248	48.8	33.6	0.9	16.7	13
June 8, 2018	47.97	789	6199	46.5	32.8	1	19.7	13
June 9, 2018	49	774	6027	47.8	32.8	1.1	18.3	14
June 10, 2018	49.5	757	6114	49	33.4	1	16.6	10
June 11, 2018	49.94	750	5922	49.3	34	0.7	16	9.5
June 12, 2018	50.47	745	5911	50.6	34.8	0.8	14.6	13
June 13, 2018	52.89	696	6100	54	35	0.5	10.3	14.7
June 14, 2018	50.47	766	6122	48.5	33.4	0.8	17.3	13
June 15, 2018	48.94	758	5910	48.5	33.5	0.9	17.1	11

June 16, 2018	50.92	754	5922	*	*	*	*	20
June 17, 2018	50.92	759	5942	*	*	*	*	18
June 18, 2018	50.92	708	5874	51.8	34.1	0.08	13	22
June 19, 2018	48.53	768	6012	47.4	33	1	18	13
June 20, 2018	51.92	753	6269	52	34	0.8	12	13
June 21, 2018	50.47	747	6162	49.8	34	1.2	14.2	12
June 22, 2018	50.47	737	6151	50.5	33.9	0.8	14.1	11
June 23, 2018	51.95	715	6006	52.5	34.4	0.7	12.1	15.7
June 24, 2018	50.97	713	6009	51.2	33.9	0.9	14.1	12.1
June 26, 2018	50.47	762	6178	50.7	33.8	0.8	14.6	7
June 27, 2018	52.89	702	6152	54.5	34.3	0.7	10.1	12
June 28, 2018	51.95	692	5969	53.1	34.8	0.6	11.4	18
June 29, 2018	51.95	686	5947	52.4	34.3	0.7	13.1	18
June 30, 2018	52.89	723	5824	*	*	*	*	22
July 1, 2018	52.89	630	5287	*	*	*	*	26
July 2, 2018	53.45	721	5709	*	*	*	*	24
July 3, 2018	52.92	704	5373	52.9	34.4	0.6	11.9	20
July 4, 2018	51.92	615	5330	53.4	34.3	0.7	11.5	18
July 5, 2018	52.89	654	5816	54.2	34.4	0.7	10.3	20
July 6, 2018	51.95	715	6112	52.2	34.2	0.8	13.1	14
July 8, 2018	52.92	704	6062	53	34.1	0.08	12.1	22
July 9, 2018	53.84	702	6224	54	34.5	0.7	10.9	18
July 10, 2018	53.89	662	5950	54.4	35	0.6	10.3	18
July 11, 2018	51.95	746	6273	52.7	34.6	0.6	12.1	16
July 12, 2018	51.95	763	6188	52.3	34.3	0.6	12.8	15
July 13, 2018	52.92	742	6242	53.5	34.7	0.5	11.3	21
July 14, 2018	52.89	733	5943	*	*	*	*	21

July 15, 2018	53.89	688	5220	*	*	*	*	0
July 16, 2018	53.89	633	5707	56	35.6	0.5	7.2	16
July 17, 2018	52.92	716	6330	53.6	35	0.6	10.7	16
July 18, 2018	52.03	737	6310	52.3	35.4	0.6	11.2	12
July 19, 2018	51.95	753	6354	51.9	34.4	0.7	12.6	17
July 20, 2018	51.95	744	6435	52.2	34.6	0.6	12.3	14
July 21, 2018	52.89	641	5706	54.4	35.2	0.5	9.6	19
July 22, 2018	53.89	607	5338	55.2	35.2	0.5	9.1	20
July 23, 2018	53.89	739	5890	54	34.9	0.5	10.6	18
July 24, 2018	54.87	719	5651	54.7	35.3	0.4	9.6	22
July 25, 2018	53.45	738	6103	53.7	35	0.5	10.8	19
July 26, 2018	53.45	720	6090	54.4	35.2	0.5	9.87	15
July 27, 2018	53.45	738	6210	54.4	35.4	0.4	9.8	15
July 28, 2018	52.45	734	6356	52.5	34.7	0.6	12.1	15
July 29, 2018	52.45	757	6267	51.1	34.1	0.7	13.7	15
July 30, 2018	52.92	738	5743	53.8	34.9	0.4	10.9	15
July 31, 2018	52.45	728	5911	52.6	34.43	0.6	12.4	15
August 1, 2018	53.39	713	263	54.1	36.1	0.4	10.4	16
August 2, 2018	53.39	736	267	52.6	34.7	0.5	12.2	14
August 3, 2018	51.95	728	273	51.7	34.3	0.5	13.5	16
August 4, 2018	51.95	700	264	51.8	34.4	0.7	12	17
August 5, 2018	52.45	660	273	53.6	34.9	0.4	11	22
August 6, 2018	52.89	694	285	54.1	35.1	0.4	10.2	18
August 7, 2018	52.89	734	288	52.8	34.6	0.6	12	21
August 8, 2018	52.89	733	284	53.1	34.8	0.6	11.4	17
August 9, 2018	52.89	713	258.8	53.7	35.1	0.4	10.7	19.4
August 10, 2018	51.95	710	267.7	52.6	34.6	0.6	12.7	15.3

August 11, 2018	52.42	712	269.2	52.6	34.7	0.6	12.1	15.6
August 12, 2018	51.45	713	268.9	51.5	34.3	0.6	13.7	15
August 13, 2018	51.45	730	254	53.3	35.3	0.4	11	13
August 14, 2018	52.92	731	262	54	35.3	0.4	10.3	19
August 15, 2018	53.45	733	256	53	34.9	0.4	11.7	30
August 16, 2018	51.92	689	268	52.8	35.3	0.3	11.6	32
August 17, 2018	51.92	663	266	53.4	34.8	0.5	11.3	14
August 18, 2018	50.97	771	288.1	51.3	34.6	0.7	13.7	11
August 19, 2018	51.45	747	288	51.3	34.4	0.7	13.6	19
August 20, 2018	52.45	725	245	53.1	35.8	0.4	10.7	21
August 21, 2018	52.45	722	267	54.6	35.9	0.3	9.2	22
August 22, 2018	50.92	730	271	51.8	34.6	0.6	13	27
August 23, 2018	51.47	724	261	53.2	35.1	0.5	11.2	31
August 24, 2018	51.47	692	265	52.5	34.7	0.5	12.3	16
August 25, 2018	51.47	745	279	52	34.5	0.6	12.9	18
August 26, 2018	51.47	745	277	51.4	34.4	0.6	13.2	22
August 27, 2018	51.92	707	274	52.5	34.9	0.5	12.1	23
August 28, 2018	55.73	724	265	58.6	36.3	0.3	4.8	18
August 29, 2018	58.59	633	279	61	36.7	0.4	1.8	16
August 30, 2018	51.92	766	287	54	37.5	0.4	8.1	8
August 31, 2018	51.92	774	278	52.9	35	0.5	11	19
September 4, 2018	54.87	738	283	57.3	36.2	0.3	6.2	21
September 6, 2018	52.45	652	257	53.2	34.6	0.5	11.7	21
September 7, 2018	52.45	733	281	53.2	35.1	0.5	11.2	14
September 10, 2018	52.92	734	277	54.5	35.4	0.4	9.7	21
September 11, 2018	52.42	730	282	53.9	35.2	0.5	11.5	24
September 12, 2018	51.92	747	274	52.2	34.8	0.6	12.4	25

September 13, 2018	53.89	736	274	55	35.9	0.3	8.8	30
September 14, 2018	54.42	732	263	56.1	36	0.3	7.6	0
October 11, 2018	55.73	573	233	60.2	38.4	0.3	1.1	1
October 12, 2018	54.87	583	230	58.9	38	0.2	2.9	1.7
October 14, 2018	54.89	549	5081	59.1	37.5	0.4	3	-5
October 18, 2018	53.39	718	207	55.2	36.4	0.5	7.9	3.2
October 20, 2018	54.89	541	4907	58.7	37.5	0.5	4	1.8
October 21, 2018	53.39	572	5068	56.9	37.2	0.4	6.1	0
October 22, 2018	55.73	600	271	61.2	38.3	0.2	0.3	0
October 24, 2018	53.45	707	266	55.9	36.7	0.5	6.9	0
October 26, 2018	52.89	745	276	55.2	36.6	0.7	7.5	0.2
October 27, 2018	52.45	755	6612	54.7	36.3	0.7	8.1	-2
October 28, 2018	52.45	716	6589	54.9	36.5	0.6	7.4	-1
October 29, 2018	51.47	692	240	53.8	36.2	0.7	9.3	-5
October 30, 2018	51.47	582	240	53.5	35.6	0.9	10	7
October 31, 2018	53.89	752	302	57.7	37.2	0.4	4.7	0
November 1, 2018	51.47	781	299	54.6	36.1	0.6	8.7	1
November 2, 2018	51.47	752	287	56	36.8	0.6	6.6	0.1
November 3, 2018	52.17	768	0	54.3	36	0.8	9	3.2
November 4, 2018	49.94	768	0	51.7	34.4	1	12.7	7.5
November 5, 2018	50.92	800	314	57.2	36.4	0.5	5.9	7.3
November 7, 2018	52.92	760	277					2
November 8, 2018	51.45	557	210	53	35.6	0.9	10.5	-6
November 10, 2018	54.39	781	0	57.5	36.8	0.6	5.1	-8.6
November 11, 2018	51.95	792	0	55.8	36.1	0.7	7.4	-6.2
November 12, 2018	54.39	527	0	59.2	37	0.4	3.4	-9.1
November 13, 2018	54.89	776	285	59.5	36.5	0.6	3.3	-1.8

November 16, 2018	57.98	593	242.2	61.1	38.5	0.3	0.1	-14.1
November 18, 2018	57.93	601	247.3	61.6	37.8	0.5	0.2	-8
November 19, 2018	52.92	673	256	56.6	36.7	0.6	6.1	-6
November 20, 2018	51.92	697	262	54.9	36.1	0.8	8.2	-12
November 21, 2018	49.5	778	273	51.9	35.3	1	11.8	-20
November 22, 2018	47.97	766	267	51.4	34.4	1	13.2	-5
November 23, 2018	53.45	708	277	57.8	36.6	0.4	5.1	-3.3
November 24, 2018	53.45	731	0	57.1	36.6	0.6	5.2	2.9
November 25, 2018	51.45	755	0	53.9	36.3	0.8	9.7	-1
November 26, 2018	51.95	750	280	55.7	36.4	0.7	7.5	-5
November 27, 2018	50.92	733	274	54.9	36	0.8	8.4	0
November 30, 2018	50.97	761	277	53.8	35.4	0.8	10	-3
December 1, 2018	50.47	778	0	53.1	35.1	0.9	11.2	-6
December 2, 2018	52.89	721	0	57.2	36.4	0.6	5.6	2
December 4, 2018	48.94	769	267	51.4	34.3	1.1	13.2	0
December 5, 2018	49.5	795	286	52.4	34.8	1	11.8	-11.9
December 6, 2018	49	792	278	52.2	34.6	1	12.2	-20
December 8, 2018	49.97	771	0	52.4	34.4	1.1	12.3	-13
December 9, 2018	49.97	737	0	54.5	35	0.9	9.5	-6
December 10, 2018	49.97	761	269	52.2	34.3	1.1	12.3	-10
December 11, 2018	49.97	766	280	53.9	35	0.9	10.2	-19
December 12, 2018	48.94	774	278	51.3	34.1	1.2	132.4	-14
December 13, 2018	46.89	818	279	48.7	32.9	1.5	16.9	-3
December 14, 2018	48.53	779	277	51.4	34	1.3	132.3	-18
December 15, 2018	48	821	0	49.5	33.3	1.4	15.6	-3
December 16, 2018	49.47	745	0	52.6	34.2	1.1	11.9	2
December 17, 2018	49.47	745	278	52.1	34.5	1.1	12.3	-2

December 18, 2018	48	806	271	49.4	33.3	1.4	16.4	-7
December 19, 2018	49.97	769	277	53.1	34.8	1	11.1	-15
December 20, 2018	49	773	275	52	34.7	1.1	12.2	-5
December 21, 2018	51.47	729	273	55.7	35.9	0.7	7.7	-5
December 22, 2018	49.47	781	0	51.4	34.6	1.1	12.9	-15
December 23, 2018	48	787	0	50.6	33.9	1.1	14.5	-35
December 25, 2018	48.5	795	0	50	33.5	1.1	15.2	-8
December 26, 2018	48	819	0	48.8	33.1	1.6	16.6	-13
December 27, 2018	48.5	761	273	50.7	33.9	0.9	14.5	-10
December 29, 2018	48	831	0	47.9	32.8	1.3	18.1	-5
December 30, 2018	49.97	742	0	53.5	34.9	0.9	10.7	-4
December 31, 2018	50.47	750	277	53.8	35	0.8	10.4	-15
January 1, 2019	47.44	742	0	46.4	33.4	1.6	19.5	-24
January 2, 2019	51.95	733	275	56	35.4	0.4	8.2	-29
January 4, 2019	51.47	745	276	54.7	35.6	0.6	9.1	-32
January 5, 2019	49.5	774	0	51	34.2	1.1	13.7	-6
January 6, 2019	47.44	808	0	47.2	32.6	1.5	18.6	-8
January 7, 2019	48	734	257	51.4	33.9	0.9	13.8	-9
January 14, 2019	54	713	273	58.8	36.1	0.4	4.7	-9
January 15, 2019	50.5	757	274	53.4	34.6	0.8	11.2	-9
January 16, 2019	48	761	261	49.8	33.6	1.4	15.2	-16
January 17, 2019	49.5	744	264	52.1	34.3	0.6	13	-14.8
January 18, 2019	50	771	279	52.3	34.3	1	12.4	-7
January 21, 2019	48	759	271	52.3	34.4	0.8	12.5	-7
January 22, 2019	49.5	753	265	52.6	34.2	0.8	12.4	-4
January 23, 2019	53	720	279	36	0.6	6.6	0	-5
January 24, 2019	50.5	755	273	53.1	34.7	1	11.2	-5

January 25, 2019	48.5	758	261	50.3	33.9	1.3	14.5	2
January 28, 2019	49	747	252	51.2	34	1	13.8	-1
February 1, 2019	54.2	746	241	54.2	35.1	0.8	9.9	-7
February 4, 2019	49.5	763	271	51.9	34.1	1.1	12.9	-1
February 5, 2019	46	782	263	48.2	32.6	1.4	17.8	-8
February 6, 2019	49	765	268	52.2	34	0.9	12.9	-12
February 7, 2019	48	774	270	51.8	33.8	1	13.4	-11
February 8, 2019	48.5	771	262	49.3	33	1.5	16.2	-6
February 9, 2019	46	803	0	43.7	30.8	1.9	23.4	-3
February 10, 2019	47	736	0	49.5	32.5	1.5	16.3	-8.2
February 11, 2019	47	782	262	48.8	32.2	1.5	17.5	-13
February 12, 2019	50	761	265	53.1	33.9	1	12	-11
February 13, 2019	52	733	276	56.3	35.7	0.7	7.3	-12
February 14, 2019	47	679	212	47	30.5	3.6	18.9	-11
February 20, 2019	51.5	696	261	54.5	35	1.4	9.1	-8
February 21, 2019	51	720	264	54	35.1	1.6	9.3	-17
February 22, 2019	47	774	265	48.7	32.6	1.9	16.8	-13
February 23, 2019	48	745	0	49.6	32.8	1.8	15.8	-7
February 24, 2019	53	675	0	56.3	35.6	1.4	6.7	0
February 25, 2019	45.5	739	739	46.5	32.2	1.9	19.4	1
February 26, 2019	46	739	239	47.1	32.2	1.8	18.9	3
February 27, 2019	48	737	255	50.3	33.1	1.4	15.2	1
February 28, 2019	47.5	758	758	49.4	32.7	1.5	16.4	-10
March 1, 2019	48	768	256	49.5	32.7	1.7	16.1	-9
March 2, 2019	48	771	0	50.6	33.2	1.6	14.8	-5
March 3, 2019	48.5	776	0	49.7	33.2	1.6	15.7	-1
March 4, 2019	48.5	752	267	51.5	33.5	1.5	13.5	1

March 5, 2019	54.5	659	259	59.1	36.2	0.9	3.8	3
March 6, 2019	46	782	259	48.3	33	1.6	17.1	-1
March 7, 2019	46	771	252	47.5	32.1	1.8	18.6	-10
March 8, 2019	46	768	0	48.2	32.2	1.8	17.8	-1.2
March 9, 2019	47	774	0	46.5	31.8	1.9	19.6	-13
March 10, 2019	49.5	705	0	53.7	34.3	1.4	10.9	5
March 12, 2019	47	745	250	48.6	32.5	1.7	17.2	6
March 13, 2019	46	718	250	50.2	33.2	1.4	15.2	13
March 14, 2019	49	755	261	51	33.5	1.5	14	-3.3
March 15, 2019	49	728	258	51.9	33.9	1.5	12.7	-4.7
March 16, 2019	46	761	0	46.7	31.5	2.3	19	-8
March 17, 2019	47.5	726	0	48.5	32.2	2	17.2	3
March 18, 2019	47.5	733	248	48.5	32.4	1.8	17.3	1
March 19, 2019	47	752	249	48.1	32.2	1.8	17.9	1
March 20, 2019	48.5	731	253	50.1	32.9	1.7	15.2	-9
March 21, 2019	48.5	716	250	50.5	33.1	1.8	14.6	1
March 22, 2019	48.5	697	234	49.1	33	1.9	16	1
March 23, 2019	47	686	0	47.9	32.3	2	17.6	2
March 24, 2019	47.5	686	0	47.5	32.5	1.9	17.9	5
March 25, 2019	48	705	232	47.7	32.3	1.9	18.1	-7
March 26, 2019	50.2	700	219	45.7	31.7	2	20.6	4
March 27, 2019	46	684	224	47.8	32.4	1.7	18.1	0.4
March 28, 2019	48	673	196	49.2	34.3	1.2	15.3	8
March 29, 2019	47	556	184	47.4	33.5	1.5	17.6	10
March 30, 2019	47	556	179.4	47.3	33.4	1.5	17.8	13
March 31, 2019	46	532	170.3	46	33.1	1.6	18.9	8
April 1, 2019	45	549	172	44.2	32.7	1.7	21.4	2.5

April 2, 2019	45	525	166	45.3	33.4	1.5	19.8	5.4
April 3, 2019	45	540	167	44.1	33.6	1.6	20.7	4.5
April 5, 2019	48	599	201	49.1	34.9	2	13.9	9
April 6, 2019	41.9	570	0	41.9	32	2.1	23.4	9
April 7, 2019	46	602	0	39.7	31.4	2.2	26.6	14
April 10, 2019	45	573	173	44.1	31.9	2.1	21.9	9
April 11, 2019	45	601	166	41.9	31.1	2.2	24.9	-2
April 12, 2019	57	466	192	62	37	0.8	0.2	0
April 14, 2019	46	585	0	45.8	30.5	3.2	20.4	7
April 15, 2019	47.5	649	209	46.8	31.1	3.1	18.5	10
April 15, 2019	52.1	633	209	47.5	31.5	2.9	18.1	1
April 16, 2019	47.3	649	204	45	30.4	3.1	21.5	5
April 17, 2019	45	625	211	44.2	30.9	2.7	22.2	14
April 18, 2019	49.5	644	229	52.3	34.3	1.4	12	6
April 19, 2019	47	681	0	48	32.5	2.1	17.8	1
April 20, 2019	47	699	0	47.1	32.4	2.1	18.4	8
April 21, 2019	46	734	0	46	31.5	2.5	22.1	-1
April 22, 2019	46	655	226	46.9	31.5	2	19.6	5
April 23, 2019	48.5	641	222	50.3	33.1	1.6	15	8
April 24, 2019	48	665	227	49.4	32.5	1.8	16.2	4
April 25, 2019	48	676	236	50.2	33.1	1.6	15.1	7
April 26, 2019	49.5	678	241	51.6	33.6	1.6	13.2	9
April 27, 2019	48	696	0	49.4	32.7	1.9	16.1	21
April 28, 2019	46	692	0	46.3	31.4	2.3	20	18
April 29, 2019	46	692	224	46.8	31.4	2.1	19.7	7
April 30, 2019	47	671	225	48.4	31.9	1.9	17.8	14
May 1, 2019	48.5	681	233	48.7	32.6	1.7	15.6	6

May 2, 2019	47.5	670	226	48.7	32	1.9	17.4	1
May 3, 2019	48	707	235	49.1	32.5	1.8	16.6	5
May 4, 2019	48	713	0	49	32.1	1.9	17	20
May 5, 2019	48	707	0	49.3	32.4	1.8	16.3	16
May 6, 2019	46.5	731	241	47.4	31.8	2	18.8	14
May 9, 2019	47.5	673	229	49.1	31.7	2.2	18	16
May 10, 2019	53.1	688	250	53.1	34	0.9	12	19
May 11, 2019	48	747	0	48.1	32.5	1.5	17.9	21
May 12, 2019	48	749	0	49	32.8	1.4	16.9	12
May 13, 2019	47.5	742	253	48.8	32.8	1.4	17	23
May 14, 2019	47.5	715	248	49.2	32.7	1.2	16.9	16
May 15, 2019	47.5	737	250	48.6	32.4	1.3	17.7	12
May 16, 2019	46	747	245	47.3	32.4	1.4	18.9	26
May 17, 2019	47.5	741	250	48.3	33	1.3	17.1	28
May 18, 2019	46	737	0	46.5	32.3	1.5	19.7	23
May 19, 2019	47	723	0	49	32.3	1.3	19.4	22
May 20, 2019	48	742	0	50.3	33.3	1.1	14.8	21
May 21, 2019	53.1	758	246	46.2	31.8	1.5	20.5	17
May 22, 2019	46	774	245	46.6	31.9	1.4	20.1	19
June 5, 2019	52	660	243	53.8	34.8	0.5	10.8	22
June 6, 2019	48	721	250	48.8	32.1	1	18.1	24
June 10, 2019	49	675	240	50.4	32.1	0.7	16.8	27
June 11, 2019	57.2	728	251	48.4	32	1.1	18.5	30
June 12, 2019	66	617	236	54.9	34.1	0	11	16
June 13, 2019	60	705	258	51.8	33	0.6	14.6	20
June 14, 2019	60.2	724	256	51.6	33	0.7	14.7	19
June 15, 2019	49	736	0	50.4	32.4	0.8	15.8	30

June 16, 2019	47	778	0	47.6	31.7	1	19.8	26
June 17, 2019	54.3	761	257	46.6	31.4	1.1	20.9	28
June 18, 2019	58.9	749	267	47.2	31.3	1	20.5	29
June 19, 2019	54.2	747	257	47.8	31.6	0.9	19.7	34
June 20, 2019	47.5	749	255	47.5	31.7	1	19.8	24
June 21, 2019	53	688	235	54.3	34.2	0.1	11.4	24
June 22, 2019	47	726	0	46.5	31	1.7	20.8	19
June 23, 2019	47	700	0	46.6	30.8	1.7	20.5	26
June 24, 2019	60.1	720	246	47.4	31.4	1.7	19.5	31
June 25, 2019	57.1	724	244	46.2	30.9	1.9	21	20
June 26, 2019	63	600	209	49.3	32.1	1.1	17.5	20.3
June 27, 2019	76	617	234	53.7	33	0.6	12.7	20.3
June 28, 2019	51.5	580	0	53	32	0.8	14	27
July 13, 2019	46	649	0	46.6	30.8	1.8	20.7	27
July 14, 2019	46	665	0	45	30	2.1	22.8	26
July 15, 2019	46	670	221	45.7	30.5	1.9	21.9	28
July 16, 2019	46	678	224	46.3	30.6	1.8	21.3	29
July 17, 2019	45	697	224	44	29.6	2.3	24.1	18
July 18, 2019	70	676	246	51.7	32.5	0.7	15.1	16
July 19, 2019	70	663	246	51.6	32.4	0.7	15.3	16
July 20, 2019	51	633	0	52.2	32.4	0.7	14.8	20
July 21, 2019	51.5	578	0	52	32.3	0.8	14.9	30
July 22, 2019	51	601	0	52.1	32.8	0.7	14.6	19
July 25, 2019	51.5	588	0	53.4	33.3	0.7	12.5	15
July 26, 2019	50.5	683	0	50.8	31.9	0.9	16.3	14
July 27, 2019	51.5	649	5408	52.6	32.4	0.9	14	17
July 28, 2019	51.5	654	5494	52.6	32.6	0.8	13.4	14

July 29, 2019	52	644	252	54	33.1	0.7	12.2	26
July 30, 2019	75	667	254	52	32.1	0.9	15	13
July 31, 2019	76	644	240	51.1	32.1	1	15.8	8
August 1, 2019	69	683	248	51.1	32.2	0.9	15.8	18
August 2, 2019	52	657	249	52	32.1	0.7	15	19.3
August 3, 2019	50.5	657	0	50.9	32	1	16	18.2
August 4, 2019	50.5	673	0	50.9	32.1	1	16	16
August 5, 2019	50.5	688	0	51.2	32.3	1	15.6	20.2
August 6, 2019	72	679	250	52.2	32.7	0.8	14.3	21.9
August 7, 2019	73	659	246	51.5	32.4	0.8	15.3	21.7
August 9, 2019	75	548	209	54.5	33.6	0.5	11.4	18.2
August 10, 2019	49.5	704	0	50.8	32	1	16.2	16.6
August 11, 2019	49.5	707	0	50.4	32	1	16.6	15.4
August 12, 2019	49.5	713	0	51.3	32.1	0.9	15.5	19
August 13, 2019	49.5	686	0	50.7	32	1	16.4	16
August 14, 2019	49	696	0	49.7	31.7	1.1	17.5	16.2
August 15, 2019	49.5	723	0	50.2	31.9	1.1	16.8	15.5
August 16, 2019	49.5	692	0	50.6	32	1	16.4	17.9
August 17, 2019	49.5	688	0	50.8	31.9	1	16.4	17.2
August 18, 2019	49	704	0	49.7	31.5	1	17.6	17.9
August 19, 2019	48.5	712	252	49	31.6	1.2	18.2	21.6
August 20, 2019	67	673	239	49.8	31.9	1	17.3	19.1
August 21, 2019	67	724	259	50.8	32	0.9	16.3	19.6
August 22, 2019	64	744	262	49.1	31.7	1.2	18	17.5
August 23, 2019	47.1	753	257	47.1	30.9	1.4	20.6	13.4
August 24, 2019	47	734	0	47.1	31	1.3	21	12.5
August 25, 2019	47.5	728	0	48.1	31	1.2	19.6	14.6

August 26, 2019	49	702	0	49.7	31.4	1.1	17.8	18.4
August 28, 2019	76	625	243	56.3	34.1	0.1	9.5	18.4
August 29, 2019	62.2	726	726	49	31.7	1	18.3	17.4
August 30, 2019	61	737	248	48.2	31.5	1.2	19.1	16.3
August 30, 2019	51	680	251	53	34.1	0.4	12.5	13
August 31, 2019	48	731	0	49.5	32.6	0.7	17.5	13
September 1, 2019	50	707	0	50.6	32.6	0.6	15.3	14.5
September 2, 2019	50	696	0	51.4	32.9	0.6	14.9	14
September 3, 2019	69	700	250	51	32.7	0.6	15.7	13.4
September 4, 2019	70	713	253	50	32.6	0.7	16.7	12.5
September 5, 2019	50.5	561	219	57.2	34.5	0.2	8.1	12
September 6, 2019	50.5	697	254	51.6	32.8	0.7	14.9	14
September 7, 2019	50.5	707	0	52.2	33.3	0.7	13.9	12.7
September 8, 2019	49.5	726	0	49.9	32.3	0.9	16.9	9.2
September 9, 2019	49.5	741	255	50.2	32.5	0.8	16.5	8.8
September 10, 2019	49.5	756	256	51	32.5	0.7	15.8	13.4
September 11, 2019	48.5	733	258	48.7	32.1	0.9	17.3	13.4
September 12, 2019	48.5	752	261	49	31.9	1	18.1	12.2
September 13, 2019	49	745	265	50.5	32.2	0.9	16.4	12.2
September 14, 2019	49.5	750	0	50.3	32.5	1	16.5	11.3
September 15, 2019	48.5	752	0	49.3	32	1	17.7	12.3
September 16, 2019	48.5	758	263	49.6	32	0.9	17.5	15.1
September 17, 2019	48.5	752	261	49.2	32.2	1.1	17.5	14.9
September 18, 2019	48.5	736	257	50.2	32.1	0.8	16.9	17.6
September 21, 2019	52	660	0	51.1	31.1	0.5	12.1	18.9
September 22, 2019	51	710	0	52.1	32.4	0.6	15	18.1
September 23, 2019	50	720	260	51.5	32.9	0.6	15	14.9

September 24, 2019	48.5	721	253	49.7	32.2	0.8	17.3	13.2
September 25, 2019	50	715	258	51.4	32.9	0.6	15.1	13.9
September 26, 2019	49	710	248	50.6	32.7	0.8	15.9	10.7
September 27, 2019	65	700	245	49.9	32.5	1	16.6	12.1
September 28, 2019	47.5	733	0	47.7	31.5	1.2	19.3	8.7
September 29, 2019	47	720	0	46.4	31.2	1.3	21.1	8.1
September 30, 2019	48.5	699	245	49.4	31.8	0.9	17.9	11.1
October 1, 2019	51	691	258	53.6	33.5	0.2	12.7	14.5
October 2, 2019	48	723	250	49.1	31.8	1.1	18	6
October 3, 2019	48	697	244	50.1	32.2	0.9	16.8	4.6
October 4, 2019	46	733	240	46.5	31	1.4	21.1	5
October 5, 2019	47	736	5561	47.7	31.5	1.2	19.6	7
October 6, 2019	51	662	5502	52.8	32.9	0.6	13.7	11.7
October 7, 2019	50	644	228	51.7	32.7	0.9	14.9	9.2
October 8, 2019	55.2	707	232	48.6	31.7	1.2	18.5	8.5
October 9, 2019	48	715	236	48.3	31.6	1.2	18.9	11.2
October 10, 2019	48	710	239	48.8	31.9	1.1	18.2	11.1
October 18, 2019	52	631	233	54.1	33.5	0.6	11.8	3.2
October 19, 2019	51.5	694	0	53.1	33.1	0.8	12.9	5.3
October 20, 2019	51.5	680	0	52.3	32.9	0.7	14	8
December 12, 2019	48	724	243	49.5	31.7	1.2	17.6	-24
December 16, 2019	50.93	696	252	53.9	33.4	0.6	12.1	-8
December 17, 2019	51.45	680	244	54.8	33.6	0.4	11.2	-11
December 18, 2019	50.47	704	248	53.8	33.3	0.6	12.2	-20
December 19, 2019	48	724	243	49.5	31.7	1.2	17.6	-24
December 20, 2019	46.02	724	240	47.5	31.1	1.2	20.2	-20
December 23, 2019	51.47	668	247	53	33	0.6	13.4	2

December 24, 2019	48.5	716	246	50.1	31.9	0.8	17.2	-7
December 27, 2019	51.45	673	246	54	33.3	0.6	12.1	2
December 30, 2019	53.89	630	247	58	39.4	0.3	7.3	-2
December 31, 2019	52.92	651	246	56.1	34.1	0.4	9.4	0
January 1, 2020	50.92	663	244	53.6	33.2	0.7	12.5	0
January 2, 2020	50.92	670	246	54.4	33.6	0.6	11.4	0
January 3, 2020	50.47	697	248	52.2	32.9	0.8	14.1	1
January 6, 2020	51.45	678	24	54.2	33.3	0.5	12	-4
January 7, 2020	50.92	688	247	53.4	33.1	0.7	12.8	-7
January 8, 2020	47.41	731	244	48.6	31.6	1.1	18.7	-15
January 9, 2020	49.5	693	244	52.4	32.2	0.8	14.5	-24
January 10, 2020	50.47	684	248	53.4	32.9	0.5	13.2	2
January 13, 2020	49.97	670	239	52.9	32.5	0.7	13.9	-17
January 14, 2020	50.92	667	242	53.6	32.5	0.6	13.3	-17
January 15, 2020	51.92	723	257	52.2	32.5	0.8	14.5	-3
January 16, 2020	56.62	622	244	57.2	33.8	0.2	7.7	-12
January 17, 2020	46.89	731	238	48	31.2	1.2	19.6	-30
January 20, 2020	47.97	734	247	50.2	32.1	0.9	16.8	-28
January 21, 2020	51.59	655	241	54.2	33	0.4	12.4	-26
January 22, 2020	49.97	697	255	53.3	32.6	0.7	13.4	-3
January 23, 2020	49.47	652	239	53.5	32.6	0.5	13.4	0
January 24, 2020	49.47	700	353	52.3	32.2	0.7	14.7	0
January 27, 2020	50.47	697	249	51.8	32.7	0.8	14.7	-3
January 28, 2020	48.53	718	245	50.6	31.1	0.9	16.4	-7
January 31, 2020	48.94	702	245	51.4	32	0.8	15.8	-10
February 3, 2020	48	715	248	50.3	32	0.9	16.8	-4
February 4, 2020	48	705	249	50.4	32.3	0.9	16.5	-4

February 5, 2020	46.89	718	244	49.5	31.9	1	17.6	-14
February 6, 2020	50.92	691	246	53.5	33.1	0.8	12.8	-14
February 7, 2020	50.92	691	246	53.5	33.1	0.8	12.8	-14
February 10, 2020	48.94	710	253	52.1	32.3	0.9	14.7	-6
February 11, 2020	50.47	681	251	54.4	33.1	0.5	12	-7
February 12, 2020	53.78	599	229	57.2	34	0.3	850	-3
February 13, 2020	52.45	623	235	56.6	33.8	0.4	9.2	-19
February 14, 2020	51.95	585	219	56.2	33.6	0.3	9.9	-33
February 18, 2020	52.89	623	240	57.7	33.8	0.3	8.2	-9
February 19, 2020	47.44	703	237	49.1	31.6	1	18.3	-16
February 20, 2020	47.44	615	201	50.4	31.9	0.8	16.9	-30
February 21, 2020	49.5	638	236	54	33	0.5	12.5	-8
February 24, 2020	49.5	663	234	52	32.5	0.9	14.6	-1
February 25, 2020	51.47	628	232	54.2	32.7	0.6	12.5	-5
February 26, 2020	49.5	665	240	53.1	32.5	0.9	13.5	-11
February 27, 2020	53.45	620	239	57.7	34.2	0.3	7.8	-11
February 28, 2020	53.89	644	235	55.2	33.6	0.6	10	-16
March 2, 2020	51.47	644	235	55	34.1	0.2	10.7	-4
March 3, 2020	49.5	633	235	52.9	33.2	0.4	13.5	-6
March 4, 2020	49.5	683	237	52	33	0.05	14.6	-3
March 5, 2020	47.39	723	242	50	32.3	0.5	17.2	-4
March 6, 2020	46.01	728	236	47.8	31.6	0.7	19.9	-6
March 9, 2020	49.97	673	240	53.1	32.8	0.3	13.8	4
March 10, 2020	49.5	675	244	53	32.8	0.4	13.8	0
March 11, 2020	47.97	696	237	50.9	32.1	0.5	16.5	-8
March 12, 2020	49	683	242	52.2	32.6	0.4	14.5	-2
March 13, 2020	50.97	663	245	55.8	33.9	0.2	10.1	1

March 16, 2020	48.53	680	239	52.3	32	0.3	15.3	-13
March 17, 2020	50.39	699	253	54.5	32	0.4	12.1	-1
March 18, 2020	46.89	728	238	48.3	32	0.6	19.8	-11
March 19, 2020	46.89	697	243	51.2	32	0.5	16.3	-2
March 20, 2020	51.45	660	250	56.4	33.9	0.1	9.6	3
March 31, 2020	51.45	676	250	54.6	33.1	0.3	12	1

Appendix B: Landfill off-gas sampling throughout March 2019-March 2020 with a calibrated gas analyzer

Date	CO_2 percentage in off-gas (%)	Off-gas Temperature (˚C)	Outside Temperature (˚C)
March 29 2019	12	539	10
April 16 2019	10.7	535	5
April 26 2019	11.3	519	9
May 3rd 2019	11.6	527	5
May 17 2019	10.2	522	28
June 6 2019	11.5	520	24
June 14 2019	11.6	514	19
June 21 2019	10.8	522	24
June 28 2019	11.6	528	27
July 19 2019	11.4	529	16
July 26 2019	11.4	532	14
August 2 2019	8.6	527	19.3
August 9 2019	12.4	529	18.2
August 16 2019	11.2	524	17.9
August 26 2019	12	528	18.4
August 29 2019	11.6	517	17.4
Sept 4 2019	11.8	522	12.5
Sept 6 2019	11.9	530	14
Sept 11 2019	12	526	13.4
Sept 24 2019	10.5	522	13.2
Oct 4 2019	12.4	530	5
Oct 8 2019	11.9	528	8.5
Oct 18 2019	11.8	522	3.2
Dec 17 2019	12.1	526	-11
Jan 10 2020	11.1	528	2
Jan 16 2020	11.7	529	-12
Jan 17 2020	11.9	541	-30
Jan 24 2020	12.6	524	0
Feb 7 2020	11.8	520	-14
Feb 13 2020	11.8	526	-19
Feb 28 2020	10.5	523	-16
March 2 2020	11.6	518	-4